Published for SISSA by Springer

Received: February 8, 2016
Revised: June 20, 2016
Accepted: July 27, 2016
Published: August 23, 2016

Short-distance QCD corrections to $K^0\bar{K}^0$ mixing at next-to-leading order in Left-Right models

Véronique Bernard,[a] **Sébastien Descotes-Genon**[b] **and Luiz Vale Silva**[a,b]

[a] *Groupe de Physique Théorique, Institut de Physique Nucléaire, UMR 8608, CNRS, Univ. Paris-Sud, Université Paris-Saclay, 91406 Orsay Cedex, France*

[b] *Laboratoire de Physique Théorique, UMR 8627, CNRS, Univ. Paris-Sud, Université Paris-Saclay, 91405 Orsay Cedex, France*

E-mail: bernard@ipno.in2p3.fr, sebastien.descotes-genon@th.u-psud.fr, luiz.vale@th.u-psud.fr

Abstract: Left-Right (LR) models are extensions of the Standard Model where left-right symmetry is restored at high energies, and which are strongly constrained by kaon mixing described in the framework of the $|\Delta S| = 2$ effective Hamiltonian. We consider the short-distance QCD corrections to this Hamiltonian both in the Standard Model (SM) and in LR models. The leading logarithms occurring in these short-distance corrections can be resummed within a rigourous Effective Field Theory (EFT) approach integrating out heavy degrees of freedom progressively, or using an approximate simpler method of regions identifying the ranges of loop momentum generating large logarithms in the relevant two-loop diagrams. We compare the two approaches in the SM at next-to-leading order, finding a very good agreement when one scale dominates the problem, but only a fair agreement in the presence of a large logarithm at leading order. We compute the short-distance QCD corrections for LR models at next-to-leading order using the method of regions, and we compare the results with the EFT approach for the WW' box with two charm quarks (together with additional diagrams forming a gauge-invariant combination), where a large logarithm occurs already at leading order. We conclude by providing next-to-leading-order estimates for cc, ct and tt boxes in LR models.

Keywords: Beyond Standard Model, CP violation, Kaon Physics, Perturbative QCD

ArXiv ePrint: 1512.00543

doi:10.1007/JHEP08(2016)128

JHEP08(2016)128

Contents

1 Short-distance QCD corrections in the Standard Model **2**
- 1.1 Generalities on the EFT computation 2
- 1.2 EFT computation: specific issues 4
- 1.3 Method of regions at leading order 6
- 1.4 Method of regions at next-to-leading order 10

2 QCD corrections for Left-Right models **11**
- 2.1 Contributions to kaon mixing in Left-Right models 11
- 2.2 Method of regions 14

3 NLO computation of $\bar{\eta}_{cc}^{LR}$ in the EFT approach **17**
- 3.1 Operator basis in the effective four-quark theory 18
  - 3.1.1 Physical operators 18
  - 3.1.2 Evanescent operators 20
- 3.2 Matching at the high scale 23
- 3.3 RG evolution from the high scale down to $\mu = m_c$ 24
- 3.4 Matching between the four- and the three-quark effective theories 25
  - 3.4.1 Expression in the four-quark theory 25
  - 3.4.2 Matching onto the effective three-quark theory 27
  - 3.4.3 Estimate of NNLO corrections 28
- 3.5 Short-distance corrections in EFT 29

4 Discussion of the results **32**
- 4.1 Short-range contributions for the cc box 33
- 4.2 Short-range contributions for the ct and tt boxes 33
- 4.3 Short range contribution from neutral and charged Higgs exchange 34

5 Conclusion **34**

A $|\Delta S| = 2$ effective Hamiltonian in the SM **36**
- A.1 Minimal operator basis 36
- A.2 Matching at the high scale 37
- A.3 RG evolution of the Wilson coefficients from the high scale down to $\mu = m_c$ 38
- A.4 Matching at $\mu = m_c$ 39
- A.5 RG evolution of the Wilson coefficients from $\mu = m_c$ down to the low scale 40

B SM case at NLO with the method of regions **40**

C Operators and anomalous dimensions **43**
- C.1 $|\Delta S| = 1$ operators 43
- C.2 $|\Delta S| = 2$ operators 45

JHEP08(2016)128

D LR case at NLO with the method of regions **46**
D.1 Contributions with $\log \beta$ 46
D.2 Contributions without $\log \beta$ 48

E Result for the individual diagrams **49**
E.1 Diagrams D_i 49
E.1.1 Contributions of the diagrams L_i 52
E.1.2 Insertion of E_i 55

JHEP08(2016)128

A natural extension of the Standard Model (SM) is provided by Left-Right (LR) symmetric models, which explain the left-handed structure of the SM through the existence of a larger gauge group $SU_C(3) \times SU_L(2) \times SU_R(2) \times U_Y(1)$, broken first at a scale μ_R of the order of the TeV (inducing a difference between left and right sectors) followed by an electroweak symmetry breaking occurring at a scale μ_W [1–5]. This extension induces the presence of heavy spin-1 W' and Z' bosons predominantly coupling to right-handed fermions, introducing a new CKM-like matrix for right-handed quarks, as well as charged and neutral heavy Higgs bosons with an interesting pattern of flavour-changing currents [6, 7]. Such a framework has been revived in the recent years for its potential collider implications when parity restoration in the LHC energy reach is considered [8, 9].

Many different mechanisms can be invoked to trigger the breakdown of the left-right symmetry. Historically, LR models (LRM) were first considered with doublets in order to break the left-right symmetry spontaneously. Later the focus was set on triplet models, due to their ability to generate both Dirac and Majorana masses for neutrinos and thus introducing a see-saw mechanism [10, 11]. LR models provide also interesting candidates for a Z' boson as currently hinted at by $b \to s\ell\ell$ observables [12–14]. Stringent constraints come from electroweak precision observables [15] and from direct searches at LHC [16–20], pushing the limit for LR models to several TeV. Studies in the framework of flavour physics suggest also that the structure for the right-handed CKM-like matrix should be quite different from the left-handed one, far from the manifest or pseudo-manifest scenarios [21–25].

In this setting, a particularly important indirect constraint comes from kaon-meson mixing, favouring a mass scale for the new scalar particles of a few TeV or beyond [26–30]. This comes from the very accurate measurement of kaon mixing together with the possibility of generating kaon mixing in the LR model by exchanging at tree level a heavy neutral Higgs boson with flavour-changing neutral couplings. As usual in flavour physics, such a process involves dynamics occurring at several different scales: the heavy degrees of freedom W' of mass of order $\mathcal{O}(\mu_R)$, the degrees of freedom occurring at the electroweak symmetry breaking μ_W, and the dynamics at low energies (around the charm quark mass or below). The first range is addressed directly in the LR model whereas the last energy domain is tackled by lattice QCD computations, which now provide accurate kaon mixing

matrix elements for the operators in the SM and beyond [31]. The two domains can be bridged thanks to the effective Hamiltonian approach, which also provides an elegant framework to take into account higher-order QCD corrections [32].

Indeed, short-distance QCD corrections prove to have an important impact on the computation of kaon mixing in the Standard Model, easily increasing or decreasing the contributions from the different diagrams to the amplitude by 50%. This large impact stems from the multi-scale nature of the problem, leading to the presence of large logarithms (for instance $\alpha_s \cdot \log(m_c^2/M_W^2)$). This requires a resummation of the leading logarithms, which can be obtained by applying an Effective Field Theory (EFT) approach to the problem. One considers a tower of effective Hamiltonians where heavy degrees of freedom are integrated out progressively and which can be matched onto each other. The renormalisation group equations provide the resummation of the large logarithms in a natural way, which requires dedicated computations of two-loop diagrams [33–39].

In the early days of these computations, an alternative method was proposed in refs. [40–42], attempting at catching the main effects of large logarithms by considering the relevant regions of momentum integration in the diagrams. This method of regions was applied to resum the leading logarithms both in the SM [42] and LR models [43, 44], with a much more limited amount of computation, since most of the method relies on anomalous dimensions already known.

The aim of the present paper is to reconsider the evaluation of short-distance QCD corrections needed to evaluate neutral-meson mixing (and in particular kaon meson mixing) precisely in the case of LR models. In section 1, we recall a few elements of the two methods in the SM case at Leading Order (LO), before illustrating how the method of regions of refs. [42–44] could be extended to Next-to-Leading Order (NLO) and comparing the results with the EFT case. In section 2, we discuss the additional contributions arising in LR models and we compute short-distance QCD corrections at NLO using the method of regions. In section 3, we use the EFT approach to compute these corrections in the case of the cc box with W and W' exchanges (together with additional diagrams to get a gauge-invariant contributions), where a large logarithm occurs already at leading order. Our final results for the short-distance corrections in LRM are gathered in section 4. We provide our conclusions in section 5. Several appendices are devoted to more technical aspects of the computation.

1 Short-distance QCD corrections in the Standard Model

1.1 Generalities on the EFT computation

The analysis of kaon mixing is customarily performed in the framework of the effective Hamiltonian, separating short and long distances in the following way [32]

$$H = \frac{G_F^2}{4\pi^2} M_W^2 \left[\lambda_c^{LL} \lambda_c^{LL} \eta_{cc} S^{LL}(x_c) + \lambda_t^{LL} \lambda_t^{LL} \eta_{tt} S^{LL}(x_t) + 2\lambda_t^{LL} \lambda_c^{LL} \eta_{ct} S^{LL}(x_c, x_t) \right] b(\mu_h) Q_V + h.c., \tag{1.1}$$

where the local $|\Delta S| = 2$ operator involved is

$$Q_V = (\bar{s}^\alpha \gamma_\mu P_L d^\alpha)(\bar{s}^\beta \gamma^\mu P_L d^\beta) = \frac{1}{4}(\bar{s}d)_{V-A}(\bar{s}d)_{V-A}\,. \tag{1.2}$$

This result involves the short-distance QCD corrections $\eta_{cc}, \eta_{tt}, \eta_{ct}$ (note that in the literature these corrections are also called η_1, η_2, η_3, respectively). S^{LL} are related to the usual Inami-Lim functions depending on the quark masses through $x_i = m_i^2/M_W^2$ (see eq. (B.1)) and $\lambda_i^{LL} = V_{is}^{CKM}(V_{id}^{CKM})^*$ combines two CKM matrix elements. The derivation of this result relies on the GIM mechanism to eliminate the λ_u^{LL} terms.

The matrix element $\langle \bar{K}^0|H|K^0\rangle$ can be computed knowing $\langle \bar{K}^0|Q_V|K\rangle$ from lattice QCD simulations at a low hadronic scale μ_h of a few GeV [31] and $b(\mu_h)$ is a function which combines with $\langle \bar{K}^0|Q_V|K^0\rangle$ to form a renormalisation-group invariant quantity. This function contains the scale dependence of the Wilson coefficient due to its running down to the hadronic scale. Note that in the literature this function is sometimes absorbed into the definition of the QCD correction factor:

$$\bar{\eta} = \eta\, b(\mu_h), \tag{1.3}$$

which is thus scale and renormalisation-scheme dependent. In the discussion of LR models we will deal with the scale-dependent $\bar{\eta}$ factors, as it proves easier to deal with the latter in the case of several $|\Delta S| = 2$ local operators mixing among each other. In the absence of the resummation of short-distance QCD corrections we would have $\eta_{ct} = \eta_{cc} = \eta_{tt} = 1$. This clearly also holds for the scale-dependent terms $\bar{\eta}$.

The determination of the short-distance QCD contributions requires a detailed analysis of the effective Hamiltonian in the SM, performed in ref. [38]. After integrating out the top quark and the W boson we are left with an effective five-flavour Hamiltonian of the form

$$H = -\frac{G_F}{\sqrt{2}}\lambda_i^{LL}\lambda_j^{LL}\sum_k C_k Q_k - \frac{G_F^2}{2}\lambda_i^{LL}\lambda_j^{LL}\sum_l \widetilde{C}_l \widetilde{Q}_l. \tag{1.4}$$

The Q_k, $\widetilde{Q}_l$ are local $|\Delta S| = 1$ and $|\Delta S| = 2$ operators and the C_k, $\widetilde{C}_l$ are the corresponding Wilson coefficients. The $|\Delta S| = 1$ operators Q_k are necessary since they contribute to the $|\Delta S| = 2$ transition amplitude through four-point functions with two operator insertions. The $|\Delta S| = 2$ operators $\widetilde{Q}_k$ can be obtained by shrinking the top-top box to a point. Yet the $\widetilde{Q}_k$'s are also needed for the light-quark contributions, since diagrams with two operator insertions are in general divergent and require counterterms proportional to $|\Delta S| = 2$ operators.

The detailed structure of the effective Hamiltonian has been worked out in ref. [38]. We summarize the different steps of the calculation here following closely this reference:

i) Find the minimal operator basis in eq. (1.4) to describe the physics of $|\Delta S| = 2$ transition and closing under renormalization.

ii) Consider the full SM Green function $\widetilde{G}$ describing the transition of interest (at the leading order of $m_c/M_{t,W}$, one can neglect the external momenta) and match to the one obtained in the effective theory to obtain the Wilson coefficients C_k and $\widetilde{C}_l$ at the high scale $\mu = \mu_{tW} = \mathcal{O}(M_W, m_t)$.

JHEP08(2016)128

iii) Determine the RG evolution of the Wilson coefficients from the high scale $\mu = \mu_{tW}$ down to the low scale $\mu = \mu_c = \mathcal{O}(m_c)$. This must be obtained by considering the general RG equation for Green functions with double insertions and its solution. The RG equation involves an anomalous dimension tensor in addition to the familiar anomalous dimension matrices, requiring the calculation of two-loop diagrams.

iv) If needed, perform the matching onto theories with fewer flavours when crossing a threshold, in particular the charm quark mass.

The computation requires the choice of a regularisation scheme for the ultraviolet divergences arising in the theory (typically, the NDR-$\overline{MS}$ scheme) and for the infrared divergences (usually by keeping small masses for the external quarks). Also, the simplification of operators in D dimensions requires the introduction of evanescent operators, which can contribute to the physical quantities once inserted in loops.

Since in the case of the LRM we will follow the same lines and in order for the paper to be self-contained we recall the main elements of the SM analysis of the $|\Delta S| = 2$ Lagrangian performed in ref. [38] in appendix A, borrowing heavily from that reference. We will just summarise a few important features for the determination of the short-distance corrections η at the order of leading and next-to-leading logarithms in the next section.

1.2 EFT computation: specific issues

In the case of the tt box [34], the Wilson coefficient can be obtained easily by integrating out both the W boson and the t quark at a high scale $\mu_{tW} = \mathcal{O}(m_t, M_W)$ (the initial conditions of the Wilson coefficients are determined by integrating out the top quark and the W boson simultaneously, thus neglecting the evolution between the scales μ_t and μ_W, see ref. [38] for further discussion). The corresponding effective Hamiltonian consists of a single operator Q_V multiplied by a Wilson coefficient obtained by matching at μ_{tW}. The coefficient is then run down to μ_h. The analytic expression for η_{tt} can be found in appendix B.

The cc box [36] has the additional complication that the charm quark cannot be integrated out at the same time as the W boson. One first integrates out the W boson, leading to a $|\Delta S| = 1$ effective Hamiltonian of the form

$$H^c = \frac{4G_F}{\sqrt{2}} \sum_{U,V=u,c} V_{Us}^{CKM} \left(V_{Vd}^{CKM}\right)^* \left(C_+ O_+^{UV} + C_- O_-^{UV}\right), \tag{1.5}$$

involving the $|\Delta S| = 1$ operators which do not mix into each other under QCD when penguin operators are not present

$$O_\pm^{UV} = \frac{O_1^{UV} \pm O_2^{UV}}{2}, \tag{1.6}$$

with

$$O_1^{UV} = \frac{1}{4}(\bar{s}^\alpha U^\alpha)_{V-A}(\bar{V}^\beta d^\beta)_{V-A}, \qquad O_2^{UV} = \frac{1}{4}(\bar{s}^\alpha U^\beta)_{V-A}(\bar{V}^\beta d^\alpha)_{V-A}, \tag{1.7}$$

JHEP08(2016)128

where α, β are colour indices. $|\Delta S| = 2$ transitions occur through bilocal operators of the form $\int d^4y\, T[H_c(x)H_c(y)]$ yielding a sum of four bilocal operators O_{ij} (with $i, j = \pm$):

$$H^{cc} = 2G_F^2\lambda_c^2 \sum_{i,j=\pm} C_i C_j O_{ij}, \tag{1.8}$$

$$\begin{aligned} O_{ij}(x) = -2i \int d^4y\, T[&O_i^{cc}(x)O_j^{cc}(y) + O_i^{uu}(x)O_j^{uu}(y) \\ &- O_i^{cu}(x)O_j^{uc}(y) - O_i^{uc}(x)O_j^{cu}(y)]. \end{aligned} \tag{1.9}$$

The Wilson coefficients of the operators O_{ij} (equal to the product C_iC_j) must be evolved from $\mu_W = \mathcal{O}(M_W)$ down to μ_c, before matching onto a theory without charm containing the single operator Q_V, see eq. (1.2) (at NLO, the matching must be performed at $\mathcal{O}(\alpha_s)$). The resulting coefficient must be evolved down to μ_h. Note that in some renormalisation schemes one could have to add a set of penguin operators in eq. (1.5) (for more detail see ref. [35]).

Finally, the top-charm contribution η_{ct} requires a more involved analysis of the renormalisation group structure of the theory [38]. The first step consists in integrating out the t and W quarks, adding to the $|\Delta S| = 1$ Hamiltonian eq. (1.5) a set of penguin operators. The resulting expression is

$$H^{ct} = 2G_F^2\lambda_c\lambda_t \left[\sum_{i=\pm,\, j=1,\ldots,6} C_i C_j O_{ij} + C_7 Q_7 \right], \tag{1.10}$$

$$O_{ij}(x) = -2i \int d^4y\, T[2O_i^{uu}(x)O_j^{uu}(y) - O_i^{cu}(x)O_j^{uc}(y) - O_i^{uc}(x)O_j^{cu}(y)], \tag{1.11}$$

for $j = 1, 2$, with a similar result for bilocal operators involving penguins $j = 3, \ldots, 6$, and an additional $|\Delta S| = 2$ operator

$$Q_7 = \frac{m_c^2}{g^2\mu^{2\epsilon}} \frac{1}{4} (\bar{s}d)_{V-A} (\bar{s}d)_{V-A}\,, \tag{1.12}$$

which is required as the bilocal operators O_{ij} exhibit an ultraviolet divergence which has to be regularised by a local counterterm (this problem does not occur for the cc box as the divergences cancel due to the GIM mechanism). This results into the logarithmic contribution $-x_c \log x_c$ to the corresponding Inami-Lim function contained in $S^{LL}(x_c, x_t)$, not present in the cc case. This means that there is a mixing between the bilocal operators O_{ij} and the local operator $(\bar{s}d)_{V-A}(\bar{s}d)_{V-A}$ at leading order, even before taking QCD corrections into account. This undesirable feature can be avoided by introducing the $1/g^2$ normalisation factor for Q_7, so that this mixing is treated on the same footing as QCD radiative corrections and a common RGE framework can be applied to discuss the mixing of all the operators [32, 33]. This theory can be evolved down to the charm quark mass, where it is matched onto a theory without charm, containing the single operator Q_V once again, to be evolved down to μ_h. Neglecting any effects of the five-flavour theory and switching off the penguin operators whose contribution has been found to be of the order of 1% allows one to write a relatively simple expression for η_{ct} [38].

JHEP08(2016)128

In the SM case, the short-distance QCD correction is known at next-to-leading order (NLO) for the dominant top-quark contribution, $\eta_{tt} = 0.5765 \pm 0.0065$ [34, 38]. Since ϵ_K is the relevant observable for kaon mixing and arises by considering the imaginary part of the $|\Delta S| = 2$ matrix element, the small imaginary part of λ_t^{LL} means that the top-top contribution can be of similar size to the charm-top and charm-charm contributions. This led to an evaluation of these contributions at NNLO, leading to a significant positive shift compared to NLO for $\eta_{cc} = 1.87 \pm 0.76$ [46] and a 7% increase for $\eta_{ct} = 0.496 \pm 0.047$ [45] (η_{tt} remaining almost unchanged). This illustrates the importance of higher orders in the evaluation of the short-distance QCD corrections.

1.3 Method of regions at leading order

Historically, the first determination of $K^0\bar{K}^0$ mixing in the SM did not take into account the short-distance QCD corrections [47]. A method to determine these corrections by resumming the leading logarithms was then developed in the case of the charm quark [40, 41], the inclusion of the top quark being studied in ref. [42]. It was further used to calculate the mixing in Left-Right symmetric models [43, 44]. In the following this method will be called "method of regions" (MR) for reasons that will become clear soon.

Contrarily to more recent works which use the EFT approach presented in section 1.1, this method aims at catching the main features in an approximate way. Let us summarise briefly the underlying idea, basically amounting to resum the leading logarithms with the help of renormalisation group equations. We consider first the calculation of the $\mathcal{O}(\alpha_s)$ corrections to the one-loop c quarks contribution to the Green function with the insertion of four weak currents (cc box). This was done in refs. [34, 36], taking into account the GIM mechanism and leading to

$$\langle H^{cc}(\mu)\rangle = \langle H^{cc}(\mu)\rangle^{(0)} + \frac{\alpha_s(\mu)}{4\pi}\langle H^{cc}(\mu)\rangle^{(1)} + \mathcal{O}(\alpha_s^2)\,, \tag{1.13}$$

where $\langle H\rangle^{(n)}$ denotes the value of the matrix element between K^0 and $\bar{K}^0$ external states at $O(\alpha_s^n)$. We have

$$\begin{aligned}
\langle H^{cc}(\mu)\rangle^{(0)} &= \frac{G_F^2}{4\pi^2}\lambda_c^2 m_c^2(\mu)\langle Q_V(\mu)\rangle^{(0)}\,,\\
\langle H^{cc}(\mu)\rangle^{(1)} &= \frac{3G_F^2}{2\pi^2}\lambda_c^2 m_c^2(\mu)\langle Q_V(\mu)\rangle^{(0)}\left[-C_F\log\left(\frac{m_c^2}{\mu^2}\right)\right.\\
&\qquad\left. + \frac{N-1}{2N}\left(2\log\left(\frac{m_c^2}{M_W^2}\right) - \log\left(\frac{m_c^2}{\mu^2}\right)\right)\right] + \cdots
\end{aligned} \tag{1.14}$$

where N denotes the number of colours and the ellipsis contains constant terms proportional to $\langle Q_V(\mu)\rangle^{(0)}$ and contributions from unphysical operators that are not relevant here. Indeed, in the leading-logarithm approximation one only keeps track of the logarithms in eq. (1.14) and resums them to all orders in perturbation theory.

Instead of performing the whole calculation, it was rather proposed in refs. [40–42] to analyse all the possible ways of dressing the box diagrams with gluons. The one-loop momentum k of the original graph is kept fixed, and one has to identify the region for

JHEP08(2016)128

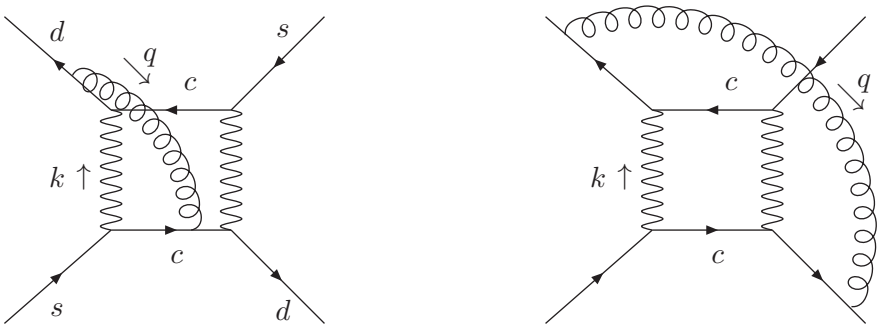

Figure 1. Typical SM cc box diagram leading to the contributions $\log(m_c^2/M_W^2)$ (four possibilities for gluon exchanges in total, left) and $\log(m_c^2/\mu_h^2)$ (two possibilities in total, right) in the computation of short-distance QCD corrections to kaon mixing.

the gluon momentum q leading to a logarithmic behaviour. These logarithms are then resummed at fixed k and finally the integration over k is performed. Let us illustrate this procedure in the case of the $\alpha_s \cdot \log(m_c^2/M_W^2)$ contribution in eq. (1.14).

Vysostskiĭ showed that the integration over q^2 in the range $[k^2, M_W^2]$ in the left diagram in figure 1 leads to a term $\log(k^2/M_W^2)$, responsible for the second logarithm (for $k^2 = \mathcal{O}(m_c^2)$) in eq. (1.14). Cutting this graph along the two internal quark lines yields the set of multiplicatively renormalised operators contributing to each half of the diagram, giving rise to the bilocal operators O_{ij} introduced in eq. (1.9). Using RGE over the relevant range of momentum for q^2 provides the resummation of logarithms as required

$$\frac{1}{2}\left(\frac{\alpha_s(k^2)}{\alpha_s(M_W^2)}\right)^{8/\beta_0} - \left(\frac{\alpha_s(k^2)}{\alpha_s(M_W^2)}\right)^{2/\beta_0} + \frac{3}{2}\left(\frac{\alpha_s(k^2)}{\alpha_s(M_W^2)}\right)^{-4/\beta_0} = \sum_{i,j=\pm} t_{ij}\left(\frac{\alpha_s(k^2)}{\alpha_s(M_W^2)}\right)^{d_{ij}}, \tag{1.15}$$

where the exponents $d_{ij} = \gamma_{ij}^{(0)}/(2\beta_0)$ come from the anomalous dimensions γ_{ij} of the bilocal operators O_{ij} involved (corresponding to the sum of the anomalous dimensions for the individual $|\Delta S| = 1$ operators), $\beta_0 = (11N - 2f)/3$ is the first term in the expansion of the usual renormalisation group function that governs the evolution of the QCD coupling constant (with f the number of active flavours), and

$$t_{ij} = \frac{1}{4}(1 + i + j + N\ ij)\,, \qquad i, j = \pm\,, \tag{1.16}$$

is a factor arising from the matching of the bilocal operators O_{ij} onto the $|\Delta S| = 2$ local operator, leading to the same integral but with different coefficients due to the different projectors involved.

After having introduced the resummation of large logarithms coming from the operator evolution, we still have to perform the remaining integration over the momentum k, typically

$$\int d^4k\ f(k^2)\left(\frac{\alpha_s(k^2)}{\alpha_s(M_W^2)}\right)^{\gamma}, \tag{1.17}$$

($\gamma = 0$ corresponds to the original loop integral without radiative corrections), which is treated in two different ways depending on the behaviour of the one-loop integral. If it has

JHEP08(2016)128

a power law behaviour dominated by a single mass scale m i.e. ($a \neq 0$)

$$\int d^4k\, f(k^2) \sim (m^2)^a\,, \tag{1.18}$$

we can replace the integral as follows

$$\int d^4k\ f(k^2)\left(\frac{\alpha_s(k^2)}{\alpha_s(\mu^2)}\right)^\gamma \sim (m^2)^a\left(\frac{\alpha_s(m^2)}{\alpha_s(\mu^2)}\right)^\gamma. \tag{1.19}$$

This is our case in eq. (1.14) since $\langle H^c(\mu_W)\rangle^{(0)} \propto m_c^2$, and we obtain a sum of contributions to the Wilson coefficient of the form

$$m_c^2\left(\frac{\alpha_s(m_c^2)}{\alpha_s(M_W^2)}\right)^{d_{ij}}. \tag{1.20}$$

If we expand it at leading order in $\alpha_s \log(m_c^2/M_W^2)$ using the evolution of α_s between two scales

$$\alpha_s(m_1) = \frac{\alpha_s(m_2)}{1-\beta_0\frac{\alpha_s(m_2)}{2\pi}\log\left(\frac{m_2}{m_1}\right)}\,, \tag{1.21}$$

we obtain

$$\frac{\alpha_s}{4\pi}\log\left(\frac{m_c^2}{M_W^2}\right)\sum_{i,j=\pm}\frac{\gamma_{ij}^{(0)}}{2}t_{ij}\,, \qquad \sum_{i,j=\pm}\frac{\gamma_{ij}^{(0)}}{2}t_{ij} = 12\frac{N-1}{2N}\,, \tag{1.22}$$

showing that the resummed expression eq. (1.20) indeed reproduces the large logarithm in eq. (1.14).

The resummations leading to the two other logarithms in eq. (1.14) is performed in a similar way. The last logarithm comes from a diagram where the gluon is attached to two external quarks of same flavour, see the right diagram in figure 1. The relevant range of integration of q^2 is $[\mu_h^2, k^2]$, where μ_h is the low hadronic scale. The relevant anomalous dimension is then the one attached to the $|\Delta S| = 2$ local operator. Once again, the remaining integration over k^2 can be simplified by noticing that only the scale $k^2 = \mathcal{O}(m_c^2)$ is relevant (for more detail, see refs. [42, 43]). The first logarithm in eq. (1.14) comes from the evolution of the charm quark mass from the m_c scale down to μ_h. Finally, we take also into account the diagrams with a gluon with both ends attached to the same internal quark line, leading to a renormalisation of the corresponding quark masses m_q (to be evaluated at the scale $\mu = m_q$). In the SM, taking into account the GIM mechanism, all the box diagrams with internal quark lines of the same flavour exhibit such a power law behaviour for which the procedure eq. (1.19) holds.

In the case of the top-charm box, matters are a bit more complicated. Indeed the corresponding original integral has not a simple power law behaviour, but instead a logarithmic behaviour as stated before, i.e. $\int_{m_1^2}^{m_2^2} dk^2 f(k^2) = \log(m_2^2/m_1^2)$. In this case one defines the LO averaging weight $R(\gamma, m_1, m_2)$ such that

$$(\log(m_2^2/m_1^2))^{-1}\int_{m_1^2}^{m_2^2}\frac{dk^2}{k^2}\left(\frac{\alpha_s(k^2)}{\alpha_s(\mu^2)}\right)^\gamma = R(\gamma, m_1, m_2)\left(\frac{\alpha_s(m_1^2)}{\alpha_s(\mu^2)}\right)^\gamma. \tag{1.23}$$

JHEP08(2016)128

The method of regions amounts thus to computing the Wilson coefficients at the lower scale m_1^2 and to multiply them by the appropriate factors R.

One should in principle also consider contributions coming from the graphs where one or both W bosons are replaced by Goldstone bosons. Actually, the sum of those diagrams (WW, WG, GG) is independent of the gauge chosen for the electroweak bosons, and the discussion can be performed in the unitarity gauge where only the WW diagram should be considered.

An additional comment is in order concerning the anomalous dimensions and the number of active flavours. In the EFT approach one performs a matching onto an effective Hamiltonian valid between two scales determined by the number of flavours involved, integrating out a quark flavour each time the scale gets lower than the corresponding quark threshold. One then runs the Wilson coefficient from one scale to the other. In Vysostskiĭ's original procedure, it is assumed that the t and b quarks do no appear in large logarithms so that f could be chosen as 3 or 4, arguing that the difference between the numerical values of β_0 (involved in the running of the operators) for $f = 5$ and $f = 4$ would anyway be very small [42]. Thus only two scales have to be considered, μ_c and the low scale μ_h at which the matrix element of the relevant operator is computed. In a similar vein, in the case of the presence of the logarithm in $\langle H^c(\mu_h)\rangle^{(0)}$ Vysostskiĭ did not distinguish the anomalous dimension of the $|\Delta S| = 2$ local operator between the scale μ_c and μ_W and below μ_c. A later reference [48] showed how to include the effect of these thresholds.

In ref. [43], the same method was reexpressed in a slightly different language. Expressed in the SM case, it amounts to considering the bilocal operators eqs. (1.9) and (1.11), running them from the high scale μ_W^2 to a scale k^2, and multiplying the evolution factors given by the RGE with the evolution factor coming from the local $|\Delta S| = 2$ operator from the scale k^2 down to μ_h^2. This provides the two contributions to large logarithms from the diagrams displayed in figure 1. The integration with respect to k^2 is then performed by the procedure outlined in eqs. (1.19) and (1.23).

The LO values of the short-distance QCD corrections in the SM for the kaon system using this method are given in table 1 and compared with the values obtained from a systematic EFT approach [38]. We included the flavour thresholds neglected by Vysostskiĭ. We do not provide η_{cc} as it turns out that its expression is identical in both approaches up to NLO, see eq. (XII.31) in ref. [32] for example, for the expression in the EFT approach. The numerical results are obtained using the same inputs as in ref. [38], namely $m_t(m_t) = 167\,\text{GeV}$, $m_c(m_c) = \mu_c = 1.3\,\text{GeV}$, $M_W = 80\,\text{GeV}$, $\Lambda^{(4)} = 0.310\,\text{GeV}$. The matchings onto the effective theories are performed at $\mu_b = 4.8\,\text{GeV}$, whereas the high scale μ_W is chosen differently depending on the box considered: $\mu_W = 130\,\text{GeV}$ when a t quark is involved in order to take care of the fact that in the EFT approach the top quark and the W boson are integrated out at the same time (hence μ_W is an average of the two masses), whereas $\mu_W = M_W$ when only c and u quarks are involved and only the W boson has to be integrated out in the diagram. As can be seen in table 1, the method of regions works very well at leading order.

JHEP08(2016)128

	η_{tt}	η_{ct}
MR	$0.591 - 0.010 = 0.581$	$0.345 - 0.011 = 0.334$
EFT	$0.612 - 0.038 = 0.574$	$0.368 + 0.099 = 0.467$

Table 1. Comparison of the SM short-distance QCD corrections using the method of regions (MR) and a systematic EFT approach. The first number corresponds to the LO (resummation of $(\alpha_s \log(m_c/\mu))^n$) and the second to the NLO (resummation of $\alpha_s(\alpha_s \log(m_c/\mu))^n$). Note that in the case of η_{ct} the LO in the four-quark theory corresponds to a resummation of $(\alpha_s \log(m_c/M_W))^n \log(m_c/M_W)$ and the NLO to $(\alpha_s \log(m_c/M_W))^n$. Flavour thresholds are taken into account. Both approaches lead to an identical result in the case of η_{cc}, not shown here.

1.4 Method of regions at next-to-leading order

We will now extend the method of regions to determine the short-range corrections η at NLO taking advantage that the anomalous dimensions of all (most of) the operators involved have been determined for the SM (LRM[1]) [39]. Following closely what is done in the EFT approach one uses the renormalisation group equations for the Wilson coefficients to determine them at $\mathcal{O}(\alpha_s)$ (requiring to know both matching and anomalous dimensions at this order). Second one should calculate the $\mathcal{O}(\alpha_s)$ corrections to the operators involved. Indeed considering both kinds of corrections is mandatory in order to get a scheme-independent result.

We can check that extending the method of regions at NLO is appropriate by applying it to the SM case first. We use the result of ref. [36] for the calculation of the $\mathcal{O}(\alpha_s)$ corrections of the $|\Delta S| = 2$ local operator Q_V appearing in the effective four- and three-quark theories for the computation of η_{cc}. The expressions of η_{tt} and η_{ct} at NLO are given in appendix B and are obtained by including the same diagrams and integration ranges as in the LO case, but considering the additional $\mathcal{O}(\alpha_s)$ corrections for the matching and evolution and modifying the averaging procedure to take them into account. The numerical results are gathered in table 1.

In the case of η_{cc} (which is identical in the EFT MR approaches), let us just stress the importance of the $\mathcal{O}(\alpha_s)$ corrections β_{ij}, $(i, j = \pm)$ coming from the matching of the product of operators $O_\pm$ onto the $|\Delta S| = 2$ local operators. We obtain, using the same input as before except by setting $\mu_W = M_W$:

$$\eta_{cc} = 0.89 + (0.62 - 0.19) \qquad (\text{EFT})\,, \tag{1.24}$$

where the first number corresponds to the LO result (in ref. [32], the LO result corresponds to a calculation with the LO value of α_s leading to $\eta_{cc} = 0.74$), the second and third numbers are the NLO contributions, the former coming from β_{ij} and the latter corresponding to the remaining contributions. The matching at μ_W is also important: neglecting the scheme-invariant quantity $\alpha_s(\mu_W)(B_i + B_j - J_{ij})$ (where $B_\pm$ comes from the matching of the SM to

[1]Some additional anomalous dimensions needed for the LRM will be discussed in the EFT approach, section 3.

JHEP08(2016)128

$O_\pm$ operators at μ_W and J comes from the anomalous dimension matrix of these operators) would lead to a 7% increase coming almost entirely from the B_i terms.

In table 1 the NLO contributions obtained with the method of regions are compared to the EFT approach. The agreement is quite good for the short-distance corrections with two same quarks in the loop, which do not involve any large logarithm in the calculation without QCD corrections. A small discrepancy is obtained in the case of η_{tt} which can be traced back to the fact that the top quark is not integrated out at the same time as the W boson contrarily to the EFT case. The MR method is much less accurate at NLO for η_{ct}, where large logarithms are present and the top quark is not treated on the same footing as the W though both are heavy degrees of freedom: our way of extending Vysostskiĭ's method yields a result with a 30% discrepancy.

2 QCD corrections for Left-Right models

2.1 Contributions to kaon mixing in Left-Right models

The LRM generates corrections for kaon mixing compared to the SM case. We will exploit the hierarchy between the left-right and electroweak symmetry breaking scales, reflected by the hierarchy of masses between W and W' bosons (as well as heavy Higgs bosons), and we keep only the first correction in $\beta = (M_W/M_{W'})^2$ (and assuming $\omega = (M_{W'}/M_H)^2 = \mathcal{O}(1)$).

The problem differs from the SM on several points due to the different structure of W' couplings. First, the GIM mechanism cannot be invoked since the two different CKM-like matrices are involved (one for left-handed quarks, the other one for right-handed quarks). Second, the effective theory at the low scale involves two different $|\Delta S| = 2$ operators which are not multiplicatively renormalised. Third, the WW' box together with the contributions from Goldstone bosons is not gauge invariant (in contrast with the SM case), which means that additional diagrams involving heavy neutral Higgs exchanges together with a W and a W' must be considered [49–51], shown in the first row of figure 2. Additional diagrams are given in the second row of the same figure. Note that we do not consider diagrams suppressed by powers of β.

We will give the results for the method of regions in the t'Hooft-Feynman gauge for the gauge bosons (the complete result being in principle gauge invariant, even though individual contributions are not [50, 52]). The contributions from the gauge bosons and their associated Goldstone bosons at the scale μ_W, diagram 2(a), are given by refs. [7, 43, 49, 50, 53]

$$A^{(\text{box})} = \frac{G_F^2 M_W^2}{4\pi^2} 2\beta h^2 \langle Q_2^{LR} \rangle \times \sum_{UV=c,t} \lambda_U^{LR} \lambda_V^{RL} \sqrt{x_U x_V} [(4 + x_U x_V \beta) I_1(x_U, x_V, \beta) - (1+\beta) I_2(x_U, x_V, \beta)] \,, \tag{2.1}$$

where the $|\Delta S| = 2$ scalar operator $Q_2^{LR} = (\bar{s}^\alpha P_L d^\alpha)(\bar{s}^\beta P_R d^\beta)$ appears. The quark masses enter as $x_i = (m_i/M_W)^2$, and are evaluated at the scale m_i for heavy quarks (we set $m_u = m_d = m_s = 0$). $\lambda_i^{PQ} = (V_{id}^P)^* V_{is}^Q$ collects the product of CKM-like matrices, the

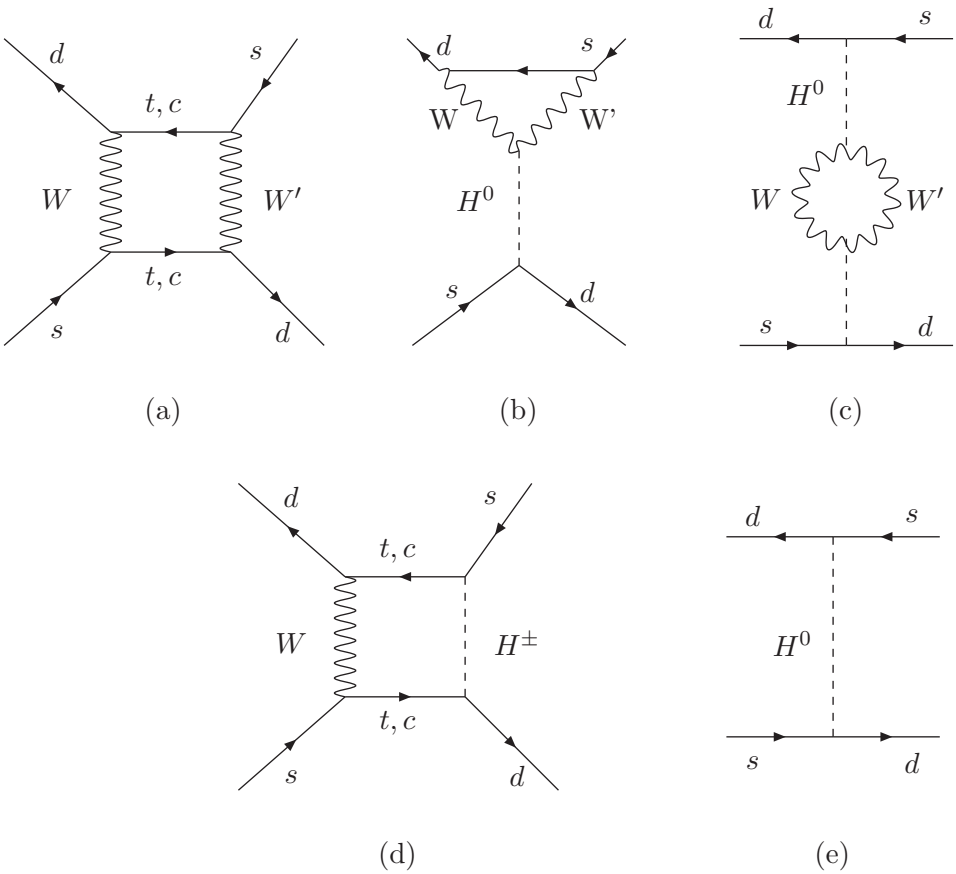

Figure 2. Diagrams for kaon mixing in Left-Right models: the sum of the first row (a)+(b)+(c) is gauge invariant, whereas the second row corresponds to additional diagrams of interest. We do not show the diagrams where one or several gauge bosons are replaced by the corresponding Goldstone bosons. Diagrams with u-quarks in the loop are suppressed by powers of m_u and are thus not considered.

couplings from $\mathrm{SU}(2)_L$ and $\mathrm{SU}(2)_R$ gauge groups appear through $h = g_R/g_L$, and I_1 and I_2 are modified Inami-Lim functions which can be expanded at leading order in β:

$$I_1 = \frac{x_U \log x_U}{(1-x_U)(x_U - x_V)} + (U \leftrightarrow V) + \mathcal{O}(\beta),$$
$$I_2 = \frac{x_U^2 \log x_U}{(1-x_U)(x_U - x_V)} + (U \leftrightarrow V) - \log\beta + \mathcal{O}(\beta)\,. \tag{2.2}$$

In the t'Hooft-Feynman gauge, one can identify the various contributions to eq. (2.1) coming from WW' (term proportional to $I_1(x_U, x_V, \beta)$), GG' (term $\propto x_U x_V \beta \cdot I_1(x_U, x_V, \beta)$, of higher order in β), GW' (term $\propto I_2(x_U, x_V, \beta)$) and WG' (term $\propto \beta \cdot I_2(x_U, x_V, \beta)$, of higher order).

We rewrite the transition amplitude eq. (2.1) in a different form and keep the leading term in x_c:

$$A^{(\mathrm{box})} = \frac{G_F^2 M_W^2}{4\pi^2} 2\beta h^2 \langle Q_2^{LR}\rangle \tag{2.3}$$
$$\times \left(\lambda_c^{LR}\lambda_c^{RL} S^{(\mathrm{box})}(x_c) + \lambda_t^{LR}\lambda_t^{RL} S^{(\mathrm{box})}(x_t) + (\lambda_c^{LR}\lambda_t^{RL} + \lambda_t^{LR}\lambda_c^{RL}) S^{(\mathrm{box})}(x_c, x_t)\right),$$

JHEP08(2016)128

at one-loop order in the absence of QCD corrections and at leading order in β, with

$$S^{(\mathrm{box})}(x_c, x_t) = \sqrt{x_c x_t}\left[\frac{x_t-4}{x_t-1}\log(x_t)+\log(\beta)\right]+\mathcal{O}(\beta, x_c^{3/2})\,, \tag{2.4}$$

$$S^{(\mathrm{box})}(x_t) = x_t\left(\frac{x_t^2-2x_t+4}{(x_t-1)^2}\log(x_t)+\frac{x_t-4}{x_t-1}+\log(\beta)\right)+\mathcal{O}(\beta)\,, \tag{2.5}$$

$$S^{(\mathrm{box})}(x_c) = x_c\,(4\log(x_c)+4+\log(\beta))+\mathcal{O}(\beta, x_c^2)\,. \tag{2.6}$$

We notice that a large $\log(x_c)$ arises for the cc box, whereas ct and tt boxes are dominated by the single scale m_t. The extra $\log(\beta)$ present in these equations comes from the I_2 function which is due to boxes with one Goldstone boson G exchanged in the t'Hooft-Feynman gauge.

The contributions from the vertex correction 2(b) and self-energy diagrams 2(c) read

$$\begin{aligned} A^{(\mathrm{vert})} &= -32\beta\omega h^2\frac{G_F^2M_W^2}{4\pi^2}\langle Q_2^{LR}\rangle S_V(\beta,\omega)\sum_{U,V=c,t}\lambda_U^{LR}\lambda_V^{RL}\sqrt{x_U x_V}\,,\\ A^{(\mathrm{self})} &= -2\beta\omega h^2\frac{G_F^2M_W^2}{4\pi^2}\langle Q_2^{LR}\rangle S_S(\beta,\omega)\sum_{U,V=c,t}\lambda_U^{LR}\lambda_V^{RL}\sqrt{x_U x_V}\,, \end{aligned} \tag{2.7}$$

with the two functions [30, 50, 51]

$$S_S(\beta,\omega) = \left[\frac{\omega^2+1}{\omega}[I_a(0)-I_a(M_H^2)]+\left(\frac{\omega-1}{\omega}\right)^2\frac{M_W^2}{\beta}I_b(M_H^2)\right]+\mathcal{O}(\beta)\,, \tag{2.8}$$

$$S_V(\beta,\omega) = [I_a(0)-I_a(M_H^2)]+\mathcal{O}(\beta^{1/2})\,. \tag{2.9}$$

We only kept the leading power of β in the above expressions, so that for $m_i, M_W \ll M_{W'}$ and an arbitrary $M_{W'}/M_H$

$$I_a(0)-I_a(M_H^2) \simeq -1+(1-\omega)\log\left|\frac{1-\omega}{\omega}\right|+\mathcal{O}(\beta)\,, \tag{2.10}$$

$$I_b(M_H^2) \simeq \frac{\beta}{M_W^2}\left[\omega+\omega^2\log\left|\frac{1-\omega}{\omega}\right|\right]+\mathcal{O}(\beta^2)\,. \tag{2.11}$$

As can be seen no logarithms in β are generated by these diagrams in the t'Hooft-Feynman gauge.

Another contribution must be considered, the one represented in figure 2(e). In these models, heavy neutral Higgs bosons can exhibit flavour-changing neutral couplings generating $|\Delta S| = 2$ transitions at tree level. The corresponding transition has the form

$$A^{(H^0)} = -\frac{4G_F}{\sqrt{2}}u\beta\omega\langle Q_2^{LR}\rangle\sum_{i,j=c,t}\lambda_i^{LR}\lambda_j^{RL}\sqrt{x_i(\mu_H)x_j(\mu_H)}\,, \tag{2.12}$$

with $u=(1+r^2)^2/(1-r^2)^2$ and $r=|\kappa_1/\kappa_2|$ the ratio of Higgs vacuum expectation values triggering electroweak symmetry breaking.

JHEP08(2016)128

Finally, we have contributions coming from the box with a W boson and a heavy charged Higgs (of a mass similar to the neutral Higgs boson considered above), figure 2(d):

$$A^{(H^\pm \text{ box})} = \frac{G_F^2 M_W^2}{4\pi^2}\langle Q_2^{LR}\rangle \sum_{U,V=c,t} \lambda_U^{LR}\lambda_V^{RL} S_{LR}^H(x_U, x_V, \beta\omega)\,, \tag{2.13}$$

with

$$S_{LR}^H(x_U, x_V, \beta\omega) = 2\omega\beta u\sqrt{x_U x_V}[x_U x_V I_1(x_U, x_V, \beta\omega) - I_2(x_U, x_V, \beta\omega)]\,, \tag{2.14}$$

the first term coming from boxes with a Goldstone boson (relevant only for tt boxes) and the second term from boxes with a W boson in the t'Hooft-Feynman gauge.

We remark that in the above expressions, there are no contributions from u-quarks as they always come multiplied by $m_u = 0$. We should notice that in principle, another set of diagrams is necessary to obtain gauge invariance, namely the diagrams figure 2(b) and (c) where W' is replaced by a heavy charged Higgs. However, as noticed in ref. [51], these contributions are suppressed by powers of $M_W/M_{H^\pm}$ compared to the diagrams considered here.

In the above expressions, we assumed that the breakdown of the left-right symmetry is triggered only by non-vanishing vacuum expectation values of scalar fields charged under $\mathrm{SU}(2)_R$ (the structure remains similar, but the prefactor is modified in the case of non-vanishing v.e.v. for scalar fields charged under $\mathrm{SU}(2)_L$ and further effects due to the mixing among the various scalars must be taken into account [54]).

2.2 Method of regions

Short-distance QCD corrections, denoted $\bar{\eta}_{UV}$, will correct the previous expressions. We are now in a position to compute these corrections at NLO since the anomalous dimensions needed for the calculation have been determined in ref. [39] and are summarised in appendix C for completeness.

Ref. [43] considered the LO case, following the same steps as in section 1.3, with the following modifications: when considering a WW' box, the bilocal operators involve one left-handed and one right-handed $|\Delta S| = 1$ operators (O_l^{VLL} and O_r^{VRR}), which are matched onto the LRM at different scales (μ_W versus μ_R), and the matching has to be performed onto two $|\Delta S| = 2$ local operators rather than a single one. Note that in ref. [43] the two additional diagrams involving heavy neutral Higgs exchanges together with W and W' bosons, diagrams 2(b) and 2(c), have been neglected arguing that in the t'Hooft-Feynman gauge their contributions are small for large enough neutral Higgs masses.

We adapt ref. [43] to include the NLO contributions, even though the treatment of the energy range between μ_W and $\mu_{W',H}$ is not appropriate when these scales are very different (which is the situation in practice) since all the heavy particles (W, W', H) are integrated out simultaneously. Note that $\alpha_s(\mu_W) \sim 0.1$ so that the contributions $\alpha_s(\mu_W)\log(\beta)/\pi$ are of the order of 20 to 30% for typical values of $M_{W'}$ between 1 TeV and 10 TeV. We thus expect an uncertainty of this order on our results, which we will take into account in our final error budget. This is in fact sufficient at the present time considering the level of accuracy needed for phenomenological applications.

JHEP08(2016)128

The expression for $\bar{\eta}_{UV}$ at NLO within the method of regions without flavour thresholds (it is rather trivial to take these thresholds into account, but the expressions are somewhat lengthy and will not be given here though we took them into account in our numerical calculation) are easily derived. One gets

$$A^{(\mathrm{box})} = \frac{G_F^2 M_W^2}{4\pi^2} 2\beta h^2 \sum_{a=1,2} \langle Q_a^{LR} \rangle \times \sum_{UV=c,t} \lambda_U^{LR} \lambda_V^{RL} \sqrt{x_U x_V} \left[4\bar{\eta}_{a,UV}^{(W'1)} I_1(x_U, x_V, \beta) - \bar{\eta}_{a,UV}^{(W'2)} I_2(x_U, x_V, \beta) \right] , \tag{2.15}$$

with the two $|\Delta S| = 2$ local operators

$$Q_1^{LR} = (\bar{s}^\alpha \gamma_\mu P_L d^\alpha)(\bar{s}^\beta \gamma^\mu P_R d^\beta) , \qquad Q_2^{LR} = (\bar{s}^\alpha P_L d^\alpha)(\bar{s}^\beta P_R d^\beta) . \tag{2.16}$$

In order to express the short-distance QCD correction $\bar{\eta}_{a,UV}^{(W'1)}$ (U and V denote the quarks in the loop with $m_U \leq m_V$), we start by defining

$$\begin{aligned} \xi_{a,UV}^{(W'1)}[R] = & \sum_{r,l=\pm,i=1,2} \left(\frac{\alpha_s(m_V)}{\alpha_s(\mu_h)} \right)^{-d_l - d_r + d_i + d_m} \left(\frac{\alpha_s(m_U)}{\alpha_s(\mu_h)} \right)^{-d_m} \left(\frac{\alpha_s(\mu_W)}{\alpha_s(\mu_h)} \right)^{d_l} \left(\frac{\alpha_s(\mu_R)}{\alpha_s(\mu_h)} \right)^{d_r} \\ & \times \left[\left(1 + \frac{\alpha_s(\mu_h)}{4\pi} \hat{K} \right) \hat{W} \right]_{ai} \\ & \times R^{NLO} \Bigg(- d_l - d_r + d_i + 2d_m, \\ & \left[\hat{W}^{-1} \left(1 - \frac{\alpha_s(\mu_W)}{4\pi} [J_l - B_l] - \frac{\alpha_s(\mu_R)}{4\pi} [J_r - B_r] + \frac{\alpha_s(m_U) + \alpha_s(m_V)}{4\pi} J_m \right) \begin{pmatrix} \tau_1^{rl} \\ \tau_2^{rl} \end{pmatrix} \right]_i , \\ & \left[\hat{W}^{-1} \left(-\hat{K} + J_l + J_r - 2J_m \right) \begin{pmatrix} \tau_1^{rl} \\ \tau_2^{rl} \end{pmatrix} \right]_i , m_V, \mu_W \Bigg) , \end{aligned} \tag{2.17}$$

with $d_{l,r}$ determined from the anomalous dimensions of the $|\Delta S| = 1$ current-current operators, d_i from the corresponding $|\Delta S| = 2$ local operator, d_m from the evolution of the masses, $J_{l,r,i,m}$ the corresponding terms from the anomalous dimension matrix at NLO and $\hat{W}$ a diagonalisation matrix (see appendix C for a definition of all these quantities). Finally the values of the Wilson coefficients coming from the matching between the bilocal operators O_{rl} and the local $|\Delta S| = 2$ operators are

$$\tau_1^{rl} = \tau_{rl}/4 , \qquad \tau_2^{rl} = 1/4 , \qquad \tau_{rl} = -(r + l + Nrl)/2 . \tag{2.18}$$

For $\bar{\eta}_{a,ct}^{(W'1)}$ and $\bar{\eta}_{a,tt}^{(W'1)}$, there are no large logarithms in the contribution from I_1 in equation (2.4)–(2.5), the integral is dominated by $k^2 = \mathcal{O}(m_V^2)$ and we have

$$\bar{\eta}_{a,ct}^{(W'1)} = \xi_{a,ct}^{(W'1)} \left[R^{NLO} \to R_1^{NLO} \right] , \qquad \bar{\eta}_{a,tt}^{(W'1)} = \xi_{a,tt}^{(W'1)} \left[R^{NLO} \to R_1^{NLO} \right] \tag{2.19}$$

where R^{NLO} should be replaced by R_1^{NLO} defined in eq. (B.12).

JHEP08(2016)128

$\bar{\eta}_{cc}^{(W'1)}$ should in principle be obtained by taking $\xi_{a,ct}^{(W'1)}$ and replacing R^{NLO} by $R_{\log}^{NLO}$ given in equation (B.10). However, eq. (2.17) resums the $\log\left(\frac{m_c}{M_W}\right)\left(\alpha_s \log\left(\frac{m_c}{M_W}\right)\right)^n$ terms (counted as LO), plus some of the terms as $\left(\alpha_s \log\left(\frac{m_c}{M_W}\right)\right)^n$ (counted as NLO). Since $I_1 = \log x_c + 1 + \mathcal{O}(x_c)$ provides contributions both at LO ($\log x_c$, with an average $R_{\log}^{NLO}$) and NLO (1, with an average R_1^{NLO}), we should separate the two contributions. This procedure[2] yields the modified expression

$$\bar{\eta}_{a,cc}^{(W'1)} = \frac{1}{1+\log x_c}\left(\xi_{a,cc}^{(W'1)}\log(x_c) + \sum_{r,l=\pm,i=1,2}\left(\frac{\alpha_s(m_c)}{\alpha_s(\mu_h)}\right)^{-d_l-d_r+d_i} \times \left(\frac{\alpha_s(\mu_W)}{\alpha_s(\mu_h)}\right)^{d_l}\left(\frac{\alpha_s(\mu_R)}{\alpha_s(\mu_h)}\right)^{d_r}\hat{W}_{ai}\left[\hat{W}^{-1}\begin{pmatrix}\tau_1^{rl}\\ \tau_2^{rl}\end{pmatrix}\right]_i\right). \tag{2.20}$$

Similar expressions are obtained for the other short-distance QCD corrections given above, which are gathered in appendix D. They collect the short-distance QCD corrections $\bar{\eta}_{UV}$ for the other diagrams:

$$\begin{aligned}
A^{(H^0)} &= -\frac{4G_F}{\sqrt{2}}u\beta\omega\sum_{a=1,2}\langle Q_a^{LR}\rangle\sum_{UV=c,t}\bar{\eta}_{a,UV}^{(H)}\lambda_U^{LR}\lambda_V^{RL}\sqrt{x_U x_V}\,, \\
A^{(\text{vert})} &= -32\beta\omega h^2\frac{G_F^2M_W^2}{4\pi^2}\sum_{a=1,2}\langle Q_a^{LR}\rangle\sum_{UV=c,t}\bar{\eta}_{a,UV}^{(H)}\lambda_U^{LR}\lambda_V^{RL}\sqrt{x_U x_V}S_V(\beta,\omega)\,, \\
A^{(\text{self})} &= -2\beta\omega h^2\frac{G_F^2M_W^2}{4\pi^2}\sum_{a=1,2}\langle Q_a^{LR}\rangle\sum_{UV=c,t}\bar{\eta}_{a,UV}^{(H)}\lambda_U^{LR}\lambda_V^{RL}\sqrt{x_U x_V}S_S(\beta,\omega)\,, \\
A^{(H^\pm\,\text{box})} &= \frac{G_F^2M_W^2}{4\pi^2}\sum_{a=1,2}\langle Q_a^{LR}\rangle\times\sum_{U,V=c,t}\lambda_U^{LR}\lambda_V^{RL} \\
&\quad\times 2\beta\omega u\sqrt{x_U x_V}\left[\bar{\eta}_{a,UV}^{(H1)}x_U x_V I_1(x_U,x_V,\beta\omega) - \bar{\eta}_{a,UV}^{(H2)}I_2(x_U,x_V,\beta\omega)\right],
\end{aligned} \tag{2.21}$$

where we followed ref. [43] to attribute the same scaling to the three contributions related to neutral Higgs exchanges (the momenta relevant for the method of regions are smaller than the high scales $M_{W,W',H}$).

The results for $\bar{\eta}_{2,UV} \equiv \bar{\eta}_{UV}$ are shown in table 2 with the following inputs: $m_t(m_t) = \mu_t = 170\,\text{GeV}$, $m_c(m_c) = \mu_c = 1.3\,\text{GeV}$, $M_W = \mu_W = 80.385\,\text{GeV}$, $\mu_b = 4.8\,\text{GeV}$, $M_{W'} = 1\,\text{TeV}$, $\omega = 0.1$ and $\Lambda^{(4)} = 0.325\,\text{GeV}$. They include the flavour thresholds. The LO results are in fairly good agreement with the calculation of ref. [30]. The short-distance corrections $\bar{\eta}_{1,UV}$ are at least an order of magnitude smaller than $\bar{\eta}_{2,UV}$ and will not be considered further, in agreement with refs. [29, 30].

Two contributions $(W'2)$ and $(H2)$ contain $\log\beta$, which can be considered either large or small depending on the hierarchy of the gauge bosons (for the above input values, we have the intermediate case $\log\beta \simeq -5$). In table 2 and in appendix D, we provide the expressions without resumming this logarithm ("small $\log\beta$ approach"). One may

[2] A similar separation can be performed in the SM case for η_{ct}, as explained in appendix B.

JHEP08(2016)128

	$\bar{\eta}_{tt}$	$\bar{\eta}_{ct}$	$\bar{\eta}_{cc}$
$(W'1)$	$4.65 + 0.99 = 5.64$	$2.42 + 0.27 = 2.69$	$1.46 + 0.16 - 0.28 = 1.34$
$(W'2)$	$4.66 + 0.98 = 5.64$	$2.42 + 0.27 = 2.69$	$1.26 + 0.01 = 1.27$
(H^0), (vert), (self)	$4.66 + 0.98 = 5.64$	$2.42 + 0.27 = 2.69$	$1.26 + 0.02 = 1.28$
$(H1)$	$4.66 + 1.00 = 5.66$	-	-
$(H2)$	$4.66 + 0.98 = 5.64$	$2.42 + 0.27 = 2.69$	$1.26 + 0.02 = 1.28$

Table 2. Short-distance QCD corrections at NLO for the LR contributions to kaon mixing with the method of regions. Flavour thresholds are taken into account. The $\bar{\eta}$ are calculated at the hadronisation scale $\mu_h = 1\,\text{GeV}$ with the parameters given in the text. The first (second) number corresponds to the LO (NLO, respectively) result. α_s is always evaluated up to NLO. In the case of $\bar{\eta}_{cc}$ the next-to-leading order is split into the NLO corrections to $\log(x_c)$ (second number) and the NLO contribution to the non-logarithmic piece (third number). We do not indicate the value for $(H1)$ when it corresponds to a higher order term in x_c in the effective Hamiltonian.

	$\bar{\eta}_{tt}$	$\bar{\eta}_{ct}$	$\bar{\eta}_{cc}$
$(W'1)$	$4.68 + 0.96 = 5.64$	$2.43 + 0.26 = 2.69$	$1.55 + 0.16 - 0.31 = 1.40$
$(W'2)$	$4.86 + 7.32 - 5.26 = 6.92$	$2.52 + 1.91 - 1.51 = 2.92$	$1.31 - 0.02 = 1.29$
$(H1)$	$4.66 + 0.99 = 5.65$	-	-
$(H2)$, $\omega = 0.1$	$4.86 + 4.11 - 2.65 = 6.33$	$2.53 + 1.17 - 0.86 = 2.83$	$1.31 - 0.02 = 1.29$
$(H2)$, $\omega = 0.8$	$4.84 + 6.70 - 4.76 = 6.79$	$2.52 + 1.77 - 1.40 = 2.89$	$1.31 - 0.03 = 1.28$

Table 3. Same results as in table 2 using the $\log(\beta)$ approach. Note that in this case $(H2)$ is sensitive to the value of ω.

however be worried that for significant hierarchies between the left and right gauge sectors, a resummation would be needed also for $\log\beta$ (even though this term would come with a suppressing factor $\alpha_s(\mu_W)$). Treating it in a similar way to $\log x_c$, we obtain the results for the "large $\log\beta$ approach" gathered in table 3 and in appendix D. The results, obtained for the same input values as in table 2, indicate a typical 10%-20% variation compared to the previous case for tt (and a smaller variation for ct and cc). We also show the mild dependence of the result on M_H.

Up to now we have given the short-range contributions diagrams by diagrams without assessing the uncertainties. We will come back to these short-range contributions and their uncertainty in section 3.5.

3 NLO computation of $\bar{\eta}_{cc}^{LR}$ in the EFT approach

In section 1, we have shown that the method of regions gives results in good agreement with those obtained using EFT in the SM (cc and tt boxes), when we start from diagrams exhibiting no large logarithms at leading order. The agreement is less satisfying in the case of the ct box where a large logarithm occurs and where the heavy degrees of freedom

JHEP08(2016)128

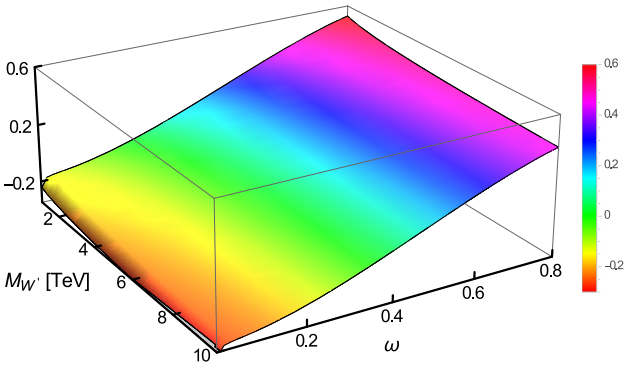

Figure 3. $(S^{LR} - \log(x_c))/\log(x_c)$ as a function of typical values of $M_{W'}$ and ω.

(t and W) are not treated in the same way. Moving to the LRM, one may thus worry that the WW' box with two charm quarks (exhibiting large $\log(x_c)$ contributions) might not be computed accurately within the MR due to the presence of a large logarithm. We will thus determine the corrections also in the EFT framework. In this setting, it is more natural to discuss the short-distance QCD corrections to the gauge-invariant sum of the diagrams 2(a), (b) and (c) involving two c quarks:

$$A_{cc}^{LR} = \frac{G_F^2 M_W^2}{4\pi^2} 2\beta h^2 \langle Q_2^{LR}\rangle \lambda_c^{LR} \lambda_c^{RL} 4 x_c S^{LR}(x_c, \beta, \omega)\,, \tag{3.1}$$

with

$$S^{LR}(x_c, \beta, \omega) = 1 + \log(x_c) + \frac{1}{4}\log(\beta) + \frac{1}{4}F(\omega)\,, \tag{3.2}$$

$$F(\omega) = 18\,\omega - (1 + 16\,\omega - 17\omega^2)\log\big|(1-\omega)/\omega\big|\,. \tag{3.3}$$

We will calculate $\bar{\eta}_{cc}^{(LR)}$ within the EFT approach, following the cases of the cc [36] and ct boxes [38] in the SM. Since we have also computed the short-distance QCD corrections for the LRM using the method of regions in section 2 we will be able to compare both results.

The EFT computation will allow us to determine the mixing between the $|\Delta S| = 1$ and $|\Delta S| = 2$ operators in the four-quark theory, as well as the $\mathcal{O}(\alpha_s)$ contributions to the $|\Delta S| = 2$ operator in the effective four- and three-quark theories. In fact the latter contributions appear at NNLO thus beyond the order at which we work. The comparison between the two methods and the consideration of higher orders (part of NNLO contributions, variation of the scales) will provide an estimate of the remaining uncertainties that we will discuss at the end of our evaluation. This piece of information will be used also when discussing the uncertainties of the short-distance QCD corrections in the ct and tt case in the LRM.

3.1 Operator basis in the effective four-quark theory

3.1.1 Physical operators

Before entering the calculation within the EFT framework, it is worth studying eq. (3.2) more closely. In figure 3, the quantity $(S^{LR}(x_c, \beta, \omega) - \log(x_c))/\log(x_c)$ is shown as a

JHEP08(2016)128

function of $M_{W'}$ and ω for phenomenologically relevant values of these two quantities. In most of this region, the $\log(x_c)$ term is significantly dominant over the rest of $S^{LR}(x_c, \beta, \omega)$. On the other hand, as discussed in section 2.2 the $\alpha_s \log(\beta)/\pi$ contributions can reach 20 to 30%. We will thus ignore the resummation of these terms occurring between μ_H and μ_W, so that we can match directly the LRM onto an EFT at μ_W (to be varied somewhat between M_H and M_W) in order to focus on the resummation of $\log(x_c)$ terms from μ_W to μ_c. In this case, the counting is similar to the one for η_{ct} in the SM: one resums the $\log(x_c)\,(\alpha_s \log(x_c))^n$ terms at LO, and the $(\alpha_s \log(x_c))^n$ ones at NLO. Consequently in our EFT approach the $\alpha_s \log(\beta)$ terms will only appear at NNLO (in contrast with the MR case where a partial resummation of these terms has been performed).

We thus integrate out both W and W' simultaneously and consider the complete set of diagrams necessary for gauge invariance shown in figure 2(a), (b), (c). This leads to the following effective Hamiltonian [55]

$$H^{cc} = 8 G_F^2 \beta h^2 \lambda_c^{LR} \lambda_c^{RL} \left[\sum_{i,j=\pm} C_{ij}(\mu) O_{ij}(\mu) + C_1^r(\mu) Q_1(\mu) + C_2^r(\mu) Q_2(\mu) + \cdots \right] \tag{3.4}$$

where we have considered only the lowest-dimension operators necessary to perform a consistent matching and RGE. This situation is similar to the case of the ct box in the SM, as recalled in appendix A. The operators O_{ij} correspond to one insertion of $\gamma_\mu\, P_L \otimes \gamma^\mu\, P_L$ and one of $\gamma_\nu P_R \otimes \gamma^\nu P_R$ (these operators suffice to describe the sum of the diagrams figure 2 (a), (b), (c), since contributions from other operator structures, in particular scalar ones, correspond to higher-order operators [50]). The last two terms on the right-hand side are required to absorb one-loop divergences, with the local dimension-eight $|\Delta S| = 2$ operators Q_a defined as

$$Q_1 = \frac{m_c^2}{g^2 \mu^{2\epsilon}} (\bar{s} \gamma_\mu P_L d)(\bar{s} \gamma^\mu P_R d)\,, \qquad Q_2 = \frac{m_c^2}{g^2 \mu^{2\epsilon}} (\bar{s} P_L d)(\bar{s} P_R d)\,. \tag{3.5}$$

According to the usual convention [32, 38], two inverse powers of the strong coupling constant have been introduced compared to $Q_{1,2}^{LR}$ in order to avoid mixing of the operators already at $\mathcal{O}(\alpha_s^0)$. The Wilson coefficients C_{ij} are given by $C_{ij}(\mu) = C_i(\mu) C_j(\mu)$ i.e., the product of $|\Delta S| = 1$ Wilson coefficients [36, 55, 56], whereas $C_a^r(\mu_W)$ can be determined from a matching at the scale μ_W. The ellipsis in eq. (3.4) denotes the contribution of penguin operators which we will neglect in the following. The $|\Delta S| = 1$ ones are proportional to λ_i^{XY} and one can distinguish two different types: the ones which come with $X = Y$ and those with $X \neq Y$. In the former case the GIM cancellation operates in the same way as in the Standard Model [35], and the only penguin operators which survive are proportional to λ_t^{XX} thus contributing only to η_{ct}^{LR}. In the latter case GIM cannot be used anymore and one could in principle have contributions from penguin operators for any of the η's. However the QCD penguin contributions do not contribute at the order we are working while the Higgs ones will be suppressed by powers of β which, as already stated, we consistently drop. This same latter reason suppresses the $|\Delta S| = 2$ Higgs penguin contributions.

Following ref. [36], we will work in the $\overline{MS}$ scheme, with an anticommuting γ_5 (NDR scheme) in $D = 4 - 2\epsilon$ dimensions, and we use an arbitrary QCD R_ξ gauge. We keep

JHEP08(2016)128

non-vanishing strange and down quark masses to regularise infrared singularities (this regularisation leads to the appearance of unphysical operators which however do not affect the outcome of the computation [36]). By analogy with the SM case, we can indicate explicitly the renormalisation matrices Z needed here

$$H^{cc} = 8G_F^2 \beta h^2 \lambda_c^{LR} \lambda_c^{RL} \times \left[\sum_{i,j=\pm} C_i C_j \underbrace{\left(\sum_{i',j'=\pm} Z^{-1}_{ii'} Z^{-1}_{jj'} O^{\text{bare}}_{i'j'} + \sum_{k=1,2} Z^{-1}_{ij,k} Q^{\text{bare}}_k \right)}_{\equiv O_{ij}} + \sum_{k,l=1,2} C^r_k Z^{-1}_{kl} Q^{\text{bare}}_l \right]. \tag{3.6}$$

The matrices Z^{-1} are known from $|\Delta S| = 1$ and $|\Delta S| = 2$ operator mixings, whereas the mixing tensor $Z^{-1}_{ij,k}$ corresponding to the mixing between the two kinds of operators must be determined.

As discussed in particular in refs. [37, 57, 58] and briefly mentioned in appendix A, we need to consider also a type of unphysical operators which appear in dimensional regularisation and are necessary to renormalise the theory: these are the so-called evanescent operators, which appear in the ellipsis in eq. (3.4) and will be discussed now.

3.1.2 Evanescent operators

Evanescent operators appear in the discussion of the RGE evolution of the effective Hamiltonian. These operators occur in the definition of the Dirac algebra in D dimensions: they vanish for $D = 4$ dimensions, but they appear as counterterms to physical operators multiplied by $1/\epsilon$. In principle, at each order of perturbation theory, new sets of evanescent operators are required, arising in the computation of radiative corrections to the physical and evanescent operators already present in the theory. In the context of the RGE for the effective Hamiltonian, the evanescent operators play a role in two different issues: first, the matrix elements of evanescent operators can affect the matching equation allowing one to determine the Wilson coefficients in the effective theory [57], and second, the presence of evanescent operators in counterterms for physical operators (and the other way around) means that both set of operators may mix under renormalisation [58]. In refs. [57, 58] it was shown that a finite renormalisation of the evanescent operators could make their matrix elements vanish and that evanescent operators could not mix into physical ones at the level of the anomalous dimension matrix γ, so that evanescent operators do not contribute to the Wilson coefficients through matching or evolution. On the other hand, the renormalisation matrix Z of evanescent operators do contribute to the computation of the anomalous dimension matrix γ for physical operators, and thus must be taken into account to renormalise the effective theory and to determine its running.

In our case, we will need the following evanescent operators $E_i[O]$ when we consider

JHEP08(2016)128

QCD corrections for the bilocal operators

$$\begin{aligned}
\gamma_\nu\gamma_\mu P_R\otimes\gamma^\nu\gamma^\mu P_L &= (4+a_5\epsilon)P_R\otimes P_L + E_5[O]\,,\\
\gamma_\rho\gamma_\nu\gamma_\mu P_R\otimes\gamma^\rho\gamma^\nu\gamma^\mu P_L &= (4+a_3\epsilon)\gamma_\mu P_R\otimes\gamma^\mu P_L + E_3[O]\,,\\
\gamma_\alpha\gamma_\rho\gamma_\nu\gamma_\mu P_R\otimes\gamma^\alpha\gamma^\rho\gamma^\nu\gamma^\mu P_L &= ((4+a_5\epsilon)^2+b\epsilon)P_R\otimes P_L + E_7[O]\,,\\
\big(\bar s^\alpha P_L d^\beta\big)\big(\bar s^\beta P_R d^\alpha\big) + 1/2Q_1^{LR} &= E_1[O]\,,\\
\big(\bar s^\alpha\gamma_\mu\gamma_\nu P_L d^\beta\big)\big(\bar s^\beta\gamma^\mu\gamma^\nu P_R d^\alpha\big) + (4+a_5\epsilon)/2Q_1^{LR} &= E_6[O]\,.
\end{aligned}\tag{3.7}$$

In the equations for $E_{1,6}$ α and β are colour indices. Note that the quark fields have been written explicitly only for these two evanescent operators which involve both colour singlet and anti-singlet operators. In all other cases the operators are colour singlets and each choice of colour structure and external quark fields define a particular evanescent operator. Most of these definitions can be found in ref. [39]. As discussed in ref. [37], the definition of these evanescent operators is not unique (as illustrated by the presence of arbitrary constants a_i) and one has to ensure that one uses the same definitions in all steps of the calculation, so that the physical observables are independent of this choice. The definition of $E_7[O]$ has been chosen in relation with that of $E_5[O]$, introducing a coefficient b in addition to the coefficient a_5 introduced for the latter. This is a consistent choice for the two evanescent operators since $E_7[O]$ may be seen as the evanescent operator coming from an evanescent operator (for instance, when inserting $E_5[O]$ in loop diagrams). It was shown in ref. [37] that such a consistent scheme led the anomalous dimensions to be independent of b.

A few more evanescent operators will be relevant in the four-quark theory when we dress the $|\Delta S| = 2$ operators $Q_{1,2}$ with gluons. These are written in a similar way as the previous ones up to a factor m_c^2/g^2 multiplying the Dirac structure (see the end of section 1.1). For instance one has for $\hat E_5[Q]$ and $\hat E_1[Q]$:

$$\begin{aligned}
\frac{m_c^2}{g^2}\big(\gamma_\nu\gamma_\mu P_R\otimes\gamma^\nu\gamma^\mu P_L\big) &= \frac{m_c^2}{g^2}(4+\bar a_5\epsilon)P_R\otimes P_L + \hat E_5[Q]\,,\\
\frac{m_c^2}{g^2}\big(\bar s^\alpha P_L d^\beta\big)\big(\bar s^\beta P_R d^\alpha\big) + 1/2Q_1 &= \hat E_1[Q]\,,
\end{aligned}\tag{3.8}$$

and similarly for the other combinations considered in eq. (3.7). The parameter associated with the ϵ term is denoted with a bar since its value does not need to be the same as the one used in eq. (3.7) and the same is true for the other evanescent operators (in the following we use $\bar a_i = a_i$ and $\bar b = b$ for simplicity). Finally when evaluating loop diagrams with the insertion of QCD counterterms we will need the following evanescent operator:

$$\gamma_\rho\gamma_\nu\gamma_\mu P_L\otimes\gamma^\rho\gamma^\nu\gamma^\mu P_L = (16+a_2\epsilon)\gamma_\mu P_L\otimes\gamma^\mu P_L + E_2[O]\,.\tag{3.9}$$

In order to check our results we have thus performed the calculation for arbitrary values of a_i and b (clearly no Fierz transformations have been used since they are only valid for a special choice of values). However, unless specified and for simplicity, we will quote our results for

$$a_5 = 4,\qquad a_3 = 4,\qquad b = 96,\qquad a_2 = -4\,.\tag{3.10}$$

JHEP08(2016)128

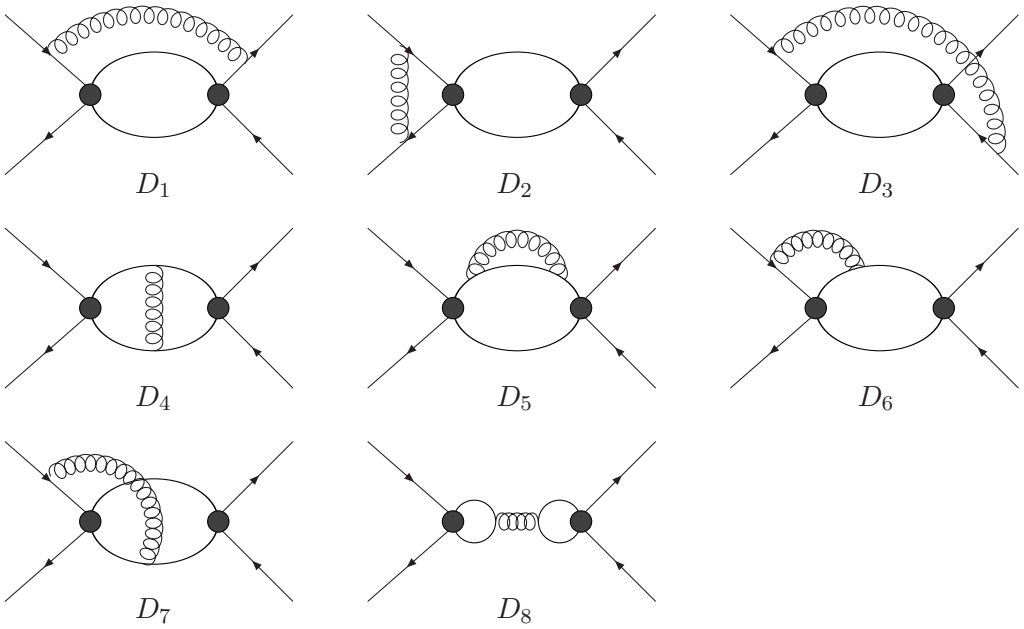

Figure 4. Diagrams D_i contributing at $\mathcal{O}(\alpha_s)$ to the operators O_{ij} in the effective four flavour theory. The curly lines denote gluons and the black circles the insertions of $|\Delta S| = 1$ current-current operators.

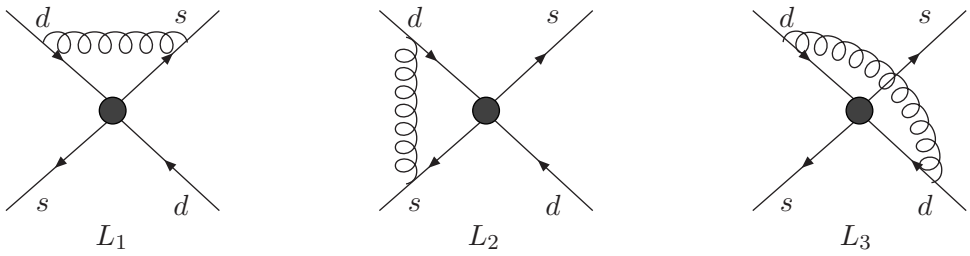

Figure 5. Diagrams L_i contributing at $\mathcal{O}(\alpha_s)$ in the effective four flavour theory. The curly lines denote gluons and the black circles the insertions of $|\Delta S| = 2$ local operators.

Indeed, these values have been used in the determination of the anomalous dimensions [39] which were relevant for the renormalisation group calculations of the Wilson coefficients recalled in appendix C, and choosing different a_i would require us to recompute these anomalous dimensions with the corresponding set of evanescent operators. Moreover, Fierz transformation can be applied in D dimensions with the choice $a_5 = a_3 = 4$.

The NLO QCD corrections will correspond to two different kinds of diagrams: first, the one-loop diagram involving two $|\Delta S| = 1$ operators and leading to the operators O_{ij} can be dressed with a gluon (figure 4), then the $|\Delta S| = 2$ local operators (counterterms or evanescent operators) can also be dressed (figure 5). We will consider both types of contributions in the following.

JHEP08(2016)128

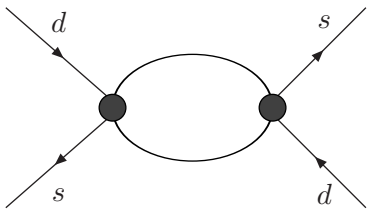

Figure 6. Diagram D_0 in the effective four-flavour theory. Black circles denote the insertions of $|\Delta S| = 1$ current-current operators.

3.2 Matching at the high scale

We will start by determining the value of the Wilson coefficients at the high scale. The coefficients C_{ij} for the bilocal operators are the product of C_i Wilson coefficients, known from the matching of $O_\pm$ operators onto the underlying theory, and they are given in appendix C.1. On the other hand, we have to determine the value of the Wilson coefficients for $C^r_{1,2}$ for the $|\Delta S| = 2$ local operators.

Let us consider the LO diagram in figure 6, giving in D dimensions:

$$\begin{aligned} D_0 = & \, i\frac{m_c^2}{16\pi^2}\left(\frac{1}{\epsilon} - \log\left(\frac{m_c^2}{\mu^2}\right) - 1 - \frac{a_5}{4}\right)\left(P_R \otimes P_L + \tau_{rl}\gamma_\mu P_R \otimes \gamma^\mu P_L\right) \\ & - i\frac{m_c^2}{64\pi^2}\frac{1}{\epsilon}\left(E_5 + 2\tau_{rl}(-E_6 + 8E_1)\right) \end{aligned} \tag{3.11}$$

τ_{rl} is defined in eq. (2.18) as

$$\tau_1^{rl} = \tau_{rl}/4\,, \qquad \tau_2^{rl} = 1/4\,, \qquad \tau_{rl} = -(r + l + Nrl)/2\,, \tag{3.12}$$

where r, l are equal to ± 1 depending on the operator O_{rl} considered. The two antisinglets evanescent operator E_1 and E_6 are needed to translate the antisinglet operators into $\gamma_\mu P_R \otimes \gamma^\mu, P_L$ while E_5 appears in the calculation of D_0 as can be seen from the presence of the term a_5 in eq. (3.11). As already noted it is important to keep track of these operators: they contribute at two loops even in four dimensions, since their one-loop matrix element yield contributions proportional to the physical operators Q_i^{LR} (see below).

The LO contribution to the part of the amplitude proportional to the Wilson coefficient C_{ij} in the effective four-quark theory eq. (3.4) thus reads:

$$A^{(WW')}(\mu) = 8G_F^2\beta h^2 \lambda_c^{LR}\lambda_c^{RL} \sum_{i,j=\pm} C_{ij}(\mu)\langle O_{ij}(\mu)\rangle^{(0)}\,, \tag{3.13}$$

with

$$\langle O_{ij}(\mu)\rangle^{(0)} = \frac{m_c^2(\mu)}{4\pi^2}\left(2 + \log\left(\frac{m_c^2}{\mu^2}\right)\right) \sum_{k=1,2} \tau_k^{ij}\langle Q_k^{LR}(\mu)\rangle^{(0)}\,, \tag{3.14}$$

where from now on we use the value $a_5 = 4$. The $1/\epsilon$ contribution in eq. (3.11) determines the renormalisation tensor

$$Z^{-1,(1)}_{ij,k} = \frac{\alpha_s}{4\pi}\frac{1}{\epsilon} 4\tau_k^{ij} \tag{3.15}$$

see appendix A for the notation of renormalisation quantities.

We can match eq. (3.13) to eq. (2.6) at the high scale μ_W (the precise value to be chosen for the high scale μ_W will be discussed in section 3.5), which leads to the following values of the Wilson coefficients C_i^r for the local $|\Delta S| = 2$ operators:

$$\begin{aligned} C_1^r(\mu_W) &= \mathcal{O}(\alpha_s^2)\,, \\ C_2^r(\mu_W) &= -\frac{\alpha_s(\mu_W)}{4\pi} \times 4\left[1 + \log\left(\frac{M_W^2}{\mu_W^2}\right) - \frac{1}{4}(\log\beta + F(\omega))\right] + \mathcal{O}(\alpha_s^2)\,, \end{aligned} \tag{3.16}$$

with $F(\omega)$ given in eq. (3.3) (using the fact that $C_{ij}(\mu_W) = 1$ at LO and $\sum_{ij}\tau_{ij} = 0$). This calculation is in fact sufficient to obtain $\bar{\eta}_{cc}$ at NLO. At NNLO which we will also briefly consider, the corrections to these equations will be very small since of $O(\alpha_s(\mu_W))^2$ and we will not consider them further.

3.3 RG evolution from the high scale down to $\mu = m_c$

The next step consists in determining the Wilson coefficients at a scale below μ_W. This can be achieved once we know the anomalous dimensions of all the operators involved. Most of them have been determined in ref. [39]. However, in the case of $\bar{\eta}_{cc}$, we need to determine the anomalous dimension tensor $\gamma_{rl,i}$ which enters the renormalisation group equations for the C_i coefficients and governs the mixing from double insertions into the C_i^r coefficients. Eq. (3.4) yields (see ref. [38] and appendix A for more detail)

$$\mu\frac{d}{d\mu}C_i^r(\mu) = \sum_j C_j^r(\mu)\gamma_{ji} + \sum_{r,l=\pm} C_r(\mu)C_l(\mu)\gamma_{rl,i}\,, \tag{3.17}$$

where

$$\gamma_{rl,i} = \frac{\alpha_s}{4\pi}\gamma_{rl,i}^{(0)} + \left(\frac{\alpha_s}{4\pi}\right)^2\gamma_{rl,i}^{(1)} + \cdots \tag{3.18}$$

Using the relations from appendix A and the result eq.(3.15), we get for the LO term $\gamma_{rl,i}^{(0)}$

$$\gamma_{rl,i}^{(0)} = 2[\tilde{Z}_1^{-1,(1)}]_{rl,i} = 8\tau_{rl,i}\,, \tag{3.19}$$

while the $\gamma_{rl,i}^{(1)}$ are obtained from the divergences stemming from the diagrams in figure 4 and figure 5. Some intermediate results for different classes of diagrams are given in appendix E while the final result is

$$\gamma_{rl,i}^{(1)} = -4h^{rl,i}(1/2) \tag{3.20}$$

with

$$\begin{aligned} -h^{rl,1}(\lambda) &= \frac{\lambda}{32N}\left((\bar{b}-96)\left(N^2-2\right)\beta_{rl} + \left(8(\bar{b}-48) - 6(\bar{b}-96)N^2\right)\tau_{rl} + 6N(\bar{b}-80)\right) \\ &\quad - (\bar{b}-280)\left(N^2-2\right)\frac{\beta_{rl}}{64N} + \left(3\bar{b}N^2 - 4\bar{b} - 152N^2 + 48\right)\frac{\tau_{rl}}{32N} + \frac{1}{32}(376-3\bar{b}), \\ -h^{rl,2}(\lambda) &= \frac{\lambda}{8N}\left(3\left(\bar{b} - 16\left(N^2+4\right)\right) + \left(48 - \frac{\bar{b}}{2}\right)N\beta_{rl} + \left(\bar{b}+96\right)N\tau_{rl}\right) \\ &\quad + \frac{1}{16N}\left(-3\bar{b} + 72N^2 + 304\right) + (\bar{b}-280)\frac{\beta_{rl}}{32} - \left(\frac{\bar{b}}{8} + 13\right)\frac{\tau_{rl}}{2}\,, \end{aligned} \tag{3.21}$$

JHEP08(2016)128

where $\beta_{rl} = r + l$ and the contribution from the evanescent operators is multiplied by a factor λ which is set to $\lambda = 1/2$ in eq. (3.20). Indeed as discussed in ref. [57], exploited in ref. [37], and recalled in appendix A, the contribution of evanescent operators to the NLO physical anomalous dimension corresponds to $1/\epsilon$ terms originating from $1/\epsilon^2$ poles in the tensor integrals multiplying a factor proportional to ϵ coming from the evanescent Dirac algebra. In each two-loop diagram the former are related to the corresponding one-loop counterterm diagrams by a factor of 1/2, because the non-local $1/\epsilon$-poles cancel in their sum in the expression for $\gamma^{(1)}_{rl,i}$. Therefore, the correct contribution of the evanescent operators is obtained by inserting the evanescent counterterms with a factor of 1/2 into the one-loop diagrams.

It is easy to check that these anomalous dimensions are independent of $\bar{b}$ as demonstrated in ref. [37]. This provides an important check of our calculation. In the case $N = 3$ one obtains:

$$\begin{aligned} &\gamma^{(1)}_{++,1} = -251/6\,, && \gamma^{(1)}_{+-,1} = \gamma^{(1)}_{-+,1} = 169/2\,, && \gamma^{(1)}_{--,1} = -355/6\,, \\ &\gamma^{(1)}_{++,2} = -41/3\,, && \gamma^{(1)}_{+-,1} = \gamma^{(1)}_{-+,2} = 73/3\,, && \gamma^{(1)}_{--,2} = 223/3\,. \end{aligned} \tag{3.22}$$

In order to solve eq. (3.17) we can rewrite the problem as a 6×6 homogeneous renormalisation group equation

$$\mu \frac{d}{d\mu} \vec{D} = \tilde{\gamma}^T \cdot \vec{D}\,, \qquad\qquad \vec{D} = \begin{pmatrix} C_r C_l \\ C_1 \\ C_2 \end{pmatrix}, \tag{3.23}$$

with

$$\tilde{\gamma}^T = \begin{pmatrix} (\gamma_r + \gamma_l) \cdot \mathbf{1}_{4\times 4} & 0 \\ \gamma_{rl} & \gamma^T \end{pmatrix}, \qquad\qquad \gamma_{rl} = \begin{pmatrix} \gamma_{++,1} & \gamma_{+-,1} & \gamma_{-+,1} & \gamma_{--,1} \\ \gamma_{++,2} & \gamma_{+-,2} & \gamma_{-+,2} & \gamma_{--,2} \end{pmatrix}, \tag{3.24}$$

and

$$\gamma^{(i)} = \begin{pmatrix} \hat{\gamma}^{(i)}_{LR,11} - 2(\gamma^{(i)}_m - \beta_i) & \hat{\gamma}^{(i)}_{LR,12} \\ \hat{\gamma}^{(i)}_{LR,21} & \hat{\gamma}^{(i)}_{LR,22} - 2(\gamma^{(i)}_m - \beta_i) \end{pmatrix}, \tag{3.25}$$

with $\hat{\gamma}^{(i)}_{LR}$ the anomalous dimension at LO ($i = 0$) or NLO ($i = 1$) of the two $|\Delta S| = 2$ operators Q^{LR}_j given in eq. (C.25) and β_i the β functions which govern the evolution of the QCD coupling constant. β_0 is given below eq. (1.15) and $\beta_1 = 102 - 38/3f$. The solution for $\vec{D}$ can be straightforwardly obtained and will be given below at the scale μ_c in eq. (3.44).

3.4 Matching between the four- and the three-quark effective theories

3.4.1 Expression in the four-quark theory

After running the Wilson coefficients from the high scale μ_W to the scale m_c, we have to match this theory onto a three-flavour effective theory with no charm. In order to perform this matching and determine the value of the Wilson coefficients in the three-flavour theory, we must compute $\langle H^{cc} \rangle$ in both theories. We will thus consider the computation in the four-flavour theory, which requires the finite part of the previous diagrams, given in appendix E.

JHEP08(2016)128

Adding up the two-loop calculation of the diagrams D_i and the contribution from the (evanescent and physical) counterterms, one obtains finally for the matrix element in the effective four-quark theory

$$\langle H^{cc}\rangle = \frac{2G_F^2}{\pi^2}\beta h^2 m_c^2 \lambda_c^{LR}\lambda_c^{RL}\sum_i\left[\sum_{rl} C_r C_l\left[\left(2+\log\frac{m_c^2}{\mu^2}\right)\tau_i^{rl}+\frac{\alpha_s}{4\pi}c_i^{rl}\right]+C_i^r\right]\langle Q_i^{LR}\rangle^{(0)}+\cdots \tag{3.26}$$

with

$$\begin{aligned}
4c_1^{rl} = &-\frac{3}{2}\log^2\left(\frac{m_c^2}{\mu^2}\right)\left(\frac{\left(N^2-2\right)\beta_{rl}}{2N}+N\tau_{rl}+1\right)\\
&-4\log\left(\frac{m_c^2}{\mu^2}\right)\left(-\frac{11\left(N^2-2\right)\beta_{rl}}{16N}+\left(\frac{N}{2}+\frac{1}{N}-\frac{3}{8}\right)\tau_{rl}-\frac{3}{16N}-1\right)\\
&+\frac{3}{N}\tau_{rl}\,R\left(2+\log\left(\frac{m_c^2}{\mu^2}\right)\right)\\
&-\frac{3\left(N^2-2\right)\beta_{rl}}{16N}-\frac{1}{8}\left(-71N+\frac{114}{N}-24\right)\tau_{rl}+\frac{3}{2N}-\frac{41}{8}\,,
\end{aligned} \tag{3.27}$$

$$\begin{aligned}
4c_2^{rl} = &-\frac{3}{N}R\left(\left(N^2-1\right)-2N\tau_{rl}\right)\left(2+\log\left(\frac{m_c^2}{\mu^2}\right)\right)-3\log^2\left(\frac{m_c^2}{\mu^2}\right)\left(\frac{1}{N}-\frac{\beta_{rl}}{2}+\tau_{rl}\right)\\
&-4\log\left(\frac{m_c^2}{\mu^2}\right)\left(3\left(1-\frac{1}{4N}\right)\tau_{rl}+\frac{1}{8}\left(-2N-\frac{14}{N}-3\right)+\frac{11\beta_{rl}}{8}\right)\\
&-4\left(\frac{43}{16}-\frac{3}{2N}\right)\tau_{rl}-\frac{1}{4}\left(-19N+\frac{60}{N}-12\right)+\frac{3\beta_{rl}}{8}\,,
\end{aligned} \tag{3.28}$$

and the values for C_i^r are given in eq. (3.16). These gauge-independent terms have a remaining dependence on the regularisation through the R infrared-regularising terms defined as

$$R=\frac{1}{m_s^2-m_d^2}\left(m_s^2\log(m_s^2/\mu^2)-m_d^2\log(m_d^2/\mu^2)\right). \tag{3.29}$$

The gauge-dependent terms are

$$\begin{aligned}
4c_{(1,\xi)}^{rl} = &-\left[\left(\log\left(\frac{m_d^2m_s^2}{\mu^4}\right)\left(\frac{1}{2}+\frac{\tau_{rl}}{N}\right)+\left(1-\frac{1}{2N}\right)+R\left(-1+2\tau_{rl}\left(N-\frac{2}{N}\right)\right)\right.\right.\\
&\left.\left.+\tau_{rl}\left(-2N+\frac{4}{N}-1\right)\right)\left(1+\frac{1}{2}\log\left(\frac{m_c^2}{\mu^2}\right)\right)\right],\\
4c_{(2,\xi)}^{rl} = &-\left[\left(\log\left(\frac{m_d^2m_s^2}{\mu^4}\right)\left(2\tau_{rl}+\frac{1}{N}\right)+2R\left(N-\frac{2}{N}-2\tau_{rl}\right)\right.\right.\\
&\left.\left.+\left(2(2-\frac{1}{N})\tau_{rl}-2N-1+\frac{4}{N}\right)\right)\left(1+\frac{1}{2}\log\left(\frac{m_c^2}{\mu^2}\right)\right)\right].
\end{aligned} \tag{3.30}$$

It is interesting to notice that all the regularisation and gauge-dependent terms in equations (3.27)–(3.30) are multiplied by the same quantity $2+\log(m_c^2/\mu^2)$ which is up to a constant the LO amplitude in the four-quark theory, eq. (3.14). We will come back to this

JHEP08(2016)128

point while discussing the matching but it already indicates that these terms will cancel against similar terms from the effective three-quark theory in the final result, which is an important test of our calculation.

3.4.2 Matching onto the effective three-quark theory

Below the scale $\mu_c \sim m_c$ the effective Hamiltonian is much simpler

$$H^{cc} = \frac{2G_F^2}{\pi^2}\beta h^2 m_c^2(\mu)\lambda_c^{LR}\lambda_c^{RL}\sum_{i=1,2}\tilde{C}_i(\mu)\tilde{Q}_i^{LR}(\mu)\,, \tag{3.31}$$

where the $|\Delta S| = 2$ local operators $\tilde{Q}_i^{LR}$ are defined as

$$\tilde{Q}_1^{LR} = (\bar{s}\gamma_\mu P_R d)(\bar{s}\gamma^\mu P_R d)\,, \qquad \tilde{Q}_2^{LR} = (\bar{s}P_L d)(\bar{s}P_R d)\,. \tag{3.32}$$

They differ from the corresponding ones in the effective four-quark theory only through a normalisation.

The matrix element of these operators can be written in the following way:

$$\langle\tilde{Q}_i^{LR}(\mu)\rangle^{(1)} = \langle\tilde{Q}_i^{LR}(\mu)\rangle^{(0)} + \frac{\alpha_s(\mu)}{4\pi}\left(\sum_j a(\mu)_{ji}\langle\tilde{Q}_j^{LR}(\mu)\rangle^{(0)} + \cdots\right)\,, \tag{3.33}$$

where the ellipsis represents possible contributions from other operators. The determination of $\langle\tilde{Q}_i^{LR}(\mu)\rangle^{(1)}$ is sketched in appendix E. Adding up the contributions detailed there and taking into account the colour factors (and the other members of each class obtained by left-right and up-down reflections), we obtain:

$$a(\mu) = \begin{pmatrix} -\frac{3N^2-3N-4}{2N} + \frac{3}{N}R - \xi a_g & \frac{3(2N+1)}{4N} + \xi\frac{b_g}{4} \\ \frac{N+3}{N} + 6R + \xi b_g & \frac{2N^2+3N+4}{2N} - \frac{3(N^2-1)}{N}R - \xi a_g \end{pmatrix}, \tag{3.34}$$

with the gauge-dependent parts given by

$$\begin{aligned} a_g &= \frac{N^2-2}{N}R - \frac{2N^2+N-4}{2N} + \frac{1}{2N}\log\left(\frac{m_s^2 m_d^2}{\mu^4}\right)\,, \\ b_g &= 2R - \frac{2N-1}{N} - \log\left(\frac{m_s^2 m_d^2}{\mu^4}\right)\,. \end{aligned} \tag{3.35}$$

At NLO the matching of the effective four-quark theory, eq. (3.26), to the three-quark theory, eq. (3.31), at the scale μ_c leads to

$$\tilde{C}_i(\mu_c) = \sum_{rl} C_r(\mu_c)C_l(\mu_c)\left(2 + \log\left(\frac{m_c^2}{\mu_c^2}\right)\right)\tau_i^{rl} + C_i^r(\mu_c)\frac{\pi}{\alpha_s(\mu_c)}, \tag{3.36}$$

which we will use in the following. The running of the Wilson coefficients below the scale μ_c is provided in appendix C.2.

JHEP08(2016)128

3.4.3 Estimate of NNLO corrections

In addition, our results also provide an estimate of the size of NNLO corrections. Indeed, at NNLO several new contributions appear, one of them coming from the $\mathcal{O}(\alpha_s)$ corrections to the operators discussed previously. In particular, the previous equation is modified as follows:

$$\tilde{C}_i^{\rm NNLO}(\mu_c) = \sum_{rl} C_r(\mu_c) C_l(\mu_c) \left[\left(2 + \log\left(\frac{m_c^2}{\mu_c^2}\right)\right) \tau_{rl}^i + \frac{\alpha_s(\mu_c)}{4\pi} C_i^{\rm op} \right] + \frac{\pi}{\alpha_s(\mu_c)} C_i^r(\mu_c) + \cdots \tag{3.37}$$

with

$$C_i^{\rm op} = c_i^{rl} - \frac{1}{8}\left(2 + \log\left(\frac{m_c^2}{\mu_c^2}\right)\right) a_i^{rl}\,, \quad a_i^{rl} = \sum_{k=1,2} \tau_k^{rl} a_{ki}(\mu)\,, \tag{3.38}$$

and the dots stand for all other NNLO contributions. Using the expressions from eq. (3.34) the a_i^{rl} read

$$\begin{aligned}
a_1^{rl} &= \frac{6}{N} R\tau_{rl} - \left(3N - \frac{4}{N} - 3\right)\tau_{rl} + \frac{3}{2N} + 3 + \xi\Bigg[-\left(\frac{1}{N}\tau_{rl} + \frac{1}{2}\right)\log\left(\frac{m_d^2 m_s^2}{\mu^4}\right) \\
&\quad + R\left(2\tau_{rl}\left(\frac{2}{N} - N\right) + 1\right) + \tau_{rl}\left(2N - \frac{4}{N} + 1\right) + \frac{1}{2N} - 1\Bigg]\,, \\
a_2^{rl} &= -6R\left(\frac{(N^2-1)}{N} - 2\tau_{rl}\right) + \frac{2(N+3)}{N}\tau_{rl} + 2N + \frac{4}{N} + 3 \\
&\quad + \xi\Bigg[-\left(\frac{1}{N} + 2\tau_{rl}\right)\log\left(\frac{m_d^2 m_s^2}{\mu^4}\right) + 2R\left(-N + \frac{2}{N} + 2\tau_{rl}\right) \\
&\quad + 2\left(\frac{1}{N} - 2\right)\tau_{rl} + 2N - \frac{4}{N} + 1\Bigg]\,.
\end{aligned} \tag{3.39}$$

It is easy to check that the gauge-dependent terms as well as the terms involving small quark masses m_s and m_d are canceled at the matching scale μ_c for any choice of the coefficients a_i in the definition of the evanescent operators. This provides additional powerful checks of the calculation and shows that our results are indeed independent of the choice of the QCD gauge and the infrared regularisation.

For completeness we give the final results in terms of $a_2 = -4 + \epsilon_2$, $a_3 = 4 + \epsilon_3$, $a_5 = 4 + \epsilon_5$, $\bar{b} = 96 + \epsilon_b$, where $\epsilon_i = 0$ corresponds to the most widely used definitions of the evanescent operators

$$\begin{aligned}
8C_1^{\rm op} &= \log\left(\frac{m_c^2}{\mu^2}\right)\Bigg[\epsilon_2\left(\frac{(N^2-2)\,\beta_{rl}}{4N} + \left(\frac{1}{N} - N\right)\tau_{rl} + 1\right) - \frac{\epsilon_3\tau_{rl}}{N} - \frac{\epsilon_5}{2} \\
&\quad + \frac{11\,(N^2-2)\,\beta_{rl}}{2N} - \frac{(N^2+12)\,\tau_{rl}}{N} + 5\Bigg] \\
&\quad + \log^2\left(\frac{m_c^2}{\mu^2}\right)\left(\left(\frac{3}{N} - \frac{3N}{2}\right)\beta_{rl} - 3N\tau_{rl} - 3\right) \\
&\quad + \epsilon_5^2\left(-\frac{(N^2-2)\,\beta_{rl}}{32N} + \left(\frac{3N}{16} - \frac{1}{4N}\right)\tau_{rl} - \frac{3}{16}\right)
\end{aligned}$$

JHEP08(2016)128

$$
\begin{aligned}
&+\epsilon_b\left(\frac{3\left(N^2-2\right)\beta_{rl}}{64N}-\frac{\left(N^2-2\right)\tau_{rl}}{32N}+\frac{1}{8}\right)\\
&+\epsilon_5\left(\epsilon_2\left(\frac{\left(N^2-2\right)\beta_{rl}}{16N}-\frac{\left(N^2-1\right)\tau_{rl}}{4N}+\frac{1}{4}\right)\right.\\
&\left.+\left(\frac{2}{N}-N\right)\beta_{rl}+\left(\frac{21N}{4}-\frac{11}{2N}\right)\tau_{rl}-\frac{45}{8}\right)\\
&+\epsilon_2\left(\left(\frac{N}{2}-\frac{1}{N}\right)\beta_{rl}+\left(\frac{2}{N}-2N\right)\tau_{rl}+2\right)-\frac{\epsilon_3\tau_{rl}}{N}\\
&-\frac{3\left(N^2-2\right)\beta_{rl}}{8N}+\left(\frac{95N}{4}-\frac{73}{2N}\right)\tau_{rl}-\frac{65}{4}\,,
\end{aligned}
\tag{3.40}
$$

$$
\begin{aligned}
8C_2^{\mathrm{op}} &= \log^2\left(\frac{m_c^2}{\mu^2}\right)\left(-\frac{6}{N}+3\beta_{rl}-6\tau_{rl}\right)\\
&+\log\left(\frac{m_c^2}{\mu^2}\right)\left(\epsilon_2\left(\frac{2}{N}-\frac{\beta_{rl}}{2}\right)-\frac{\epsilon_5}{N}-2\epsilon_3\tau_{rl}+\frac{10}{N}-11\beta_{rl}-26\tau_{rl}\right)-2\epsilon_3\tau_{rl}\\
&+\epsilon_5\left(-\frac{3\left(N^2+14\right)}{4N}+2\beta_{rl}-\frac{\tau_{rl}}{2}\right)+\epsilon_5^2\left(-\frac{3}{8N}+\frac{\beta_{rl}}{16}-\frac{\tau_{rl}}{8}\right)\\
&+\epsilon_b\left(\frac{1}{4N}-\frac{3\beta_{rl}}{32}+\frac{\tau_{rl}}{16}\right)\\
&+\epsilon_2\left(\epsilon_5\left(\frac{1}{2N}-\frac{\beta_{rl}}{8}\right)+\frac{4}{N}-\beta_{rl}\right)+\frac{11N}{2}-\frac{38}{N}+\frac{3\beta_{rl}}{4}-\frac{51\tau_{rl}}{2}\,.
\end{aligned}
\tag{3.41}
$$

The physical observables should not depend on the values chosen for ϵ_i. In the following, we will set $\epsilon_i = 0$ since this is consistent with the values used for the anomalous dimensions.

3.5 Short-distance corrections in EFT

Combining eq. (3.36) with the renormalisation equation for $\vec{D}$ down to the low scale μ below m_c, we obtain the final result for $\bar{\eta}_{a,cc}^{(LR)}$ at NLO in the EFT approach, corresponding to the gauge-invariant combination of diagrams shown in the first row of figure 2:

$$
\begin{aligned}
\bar{\eta}_{a,cc}^{(LR)} &= \frac{1}{S^{LR}(x_c(\mu_c),\beta,\omega)}\\
&\sum_{j=1,2}\left(\left(1+\frac{\alpha_s(\mu)}{4\pi}K^{[3]}\right)\exp\left[d^{[3]}\cdot\log\frac{\alpha_s(\mu_c)}{\alpha_s(\mu)}\right]\left(1-\frac{\alpha_s(\mu_c)}{4\pi}K^{[3]}\right)\right)_{aj}F_j(\mu_c)\,,
\end{aligned}
\tag{3.42}
$$

with $S^{LR}(x_c,\beta,\omega)$ given in eq. (3.2) and

$$
\begin{aligned}
F_a(\mu_c) &= \left(\frac{\pi}{\alpha_s(\mu_c)}C_a^r(\mu_c)+\sum_{r,l=\pm}\left(r_{rl,a}(\mu_c)+\frac{\alpha_s(\mu_c)}{4\pi}C_a^{\mathrm{op}}(\mu_c)\right)C_r(\mu_c)C_l(\mu_c)\right),\\
r_{rl,a}(\mu_c) &= \left(2+\log(m_c^2/\mu_c^2)\right)\tau_a^{rl}\,, \qquad a=1,2\,,
\end{aligned}
\tag{3.43}
$$

JHEP08(2016)128

where the values of $C_a^r(\mu_c)$, $C_r(\mu_c)$ and $C_l(\mu_c)$ are given by the evolution of $\vec{D}$ down to μ_c

$$\vec{D}(\mu_c) = \left(1 + \frac{\alpha_s(\mu_c)}{4\pi}\tilde{J}^{[4]}\right) \cdot \exp\left[\tilde{d}^{[4]} \cdot \log\frac{\alpha_s(\mu_b)}{\alpha_s(\mu_c)}\right] \cdot \left(1 + \frac{\alpha_s(\mu_b)}{4\pi}\left(\delta\tilde{r}^T(\mu_b) + \tilde{J}^{[5]} - \tilde{J}^{[4]}\right)\right)$$
$$\cdot \exp\left[\tilde{d}^{[5]} \cdot \log\frac{\alpha_s(\mu_W)}{\alpha_s(\mu_b)}\right] \cdot \left(1 - \frac{\alpha_s(\mu_W)}{4\pi}\tilde{J}^{[5]}\right) \cdot \vec{D}(\mu_W)\,. \tag{3.44}$$

In order to get an estimate of the error due to neglected higher-order contributions, we have added in eq. (3.43) the contribution $C_a^{\rm op}$ which first appears at the next order. The $C_i^r(\mu_W)$ are defined in eq. (3.16) while $C_\pm(\mu_W)$ is defined in eq. (C.7). The contribution $\delta\tilde{r}^T(\mu_b)$ cancels in the absence of penguin operators, which is the case here.

Finally the matrices $\tilde{d} = \tilde{d}^{[f]}$, $\tilde{J} = \tilde{J}^{[f]}$ and $d = d^{[3]}$, $K = K^{[3]}$ encode respectively the 6×6 anomalous dimension matrix $\tilde{\gamma}$ defined in section 3.3 and the 2×2 one $\hat{\gamma}_{LR}$ defined in appendix C.2, with the additional definition

$$\tilde{d} = \frac{(\tilde{\gamma}^{(0)})^T}{2\beta_0}\,, \qquad \tilde{J} + [\tilde{d}, \tilde{J}] = -\frac{(\tilde{\gamma}^{(1)})^T}{2\beta_0} + \frac{\beta_1}{\beta_0}\tilde{d}\,. \tag{3.45}$$

Simplified expressions for $D_i(\mu_c)$ where effects from the five-flavour theory have been neglected and which are extremely good approximations to the complete results read

$$\begin{aligned}
F_1 = {} & \frac{3}{104}\frac{\pi}{\alpha_s}\left(2A^{--} - 39A^{+-} - 26A^{++} + 63A_1\right) \\
& - \frac{1}{8}\left(\log\left(\frac{{m_c}^2(\mu_c)}{{\mu_c}^2}\right) + 2\right)\left(A^{--} - 6A^{+-} + 5A^{++}\right) \\
& + \frac{1}{4}\Bigg(-\frac{1761281}{390000}A^{--} + \frac{587029}{220000}A^{+-} + \frac{16120889}{1110000}A^{++} - \frac{4789827}{260000}A_1 + \frac{1737}{296}A_2 \\
& + A\left(A^{--}\left(-\frac{12}{13}\log\left(\frac{\mu_W}{M_W}\right) - \frac{10181}{16250}\right) + A^{+-}\left(\frac{9}{2}\log\left(\frac{\mu_W}{M_W}\right) + \frac{39993}{10000}\right)\right. \\
& \left. + A^{++}\left(-6\log\left(\frac{\mu_W}{M_W}\right) - \frac{7031}{2500}\right) + A_1\left(\frac{63}{26}\log\left(\frac{\mu_W}{M_W}\right) - \frac{974889}{1430000}\right)\right)\Bigg)\,,
\end{aligned} \tag{3.46}$$

$$\begin{aligned}
F_2 = {} & \frac{3}{1924}\frac{\pi}{\alpha_s}\left(2590A^{--} - 481A^{+-} - 182A^{++} + 777A_1 - 2704A_2\right) \\
& + \frac{1}{4}\left(\log\left(\frac{{m_c}^2(\mu_c)}{{\mu_c}^2}\right) + 2\right)\left(A^{--} + 2A^{+-} + A^{++}\right) \\
& + \frac{1}{4}\Bigg(-\frac{101273A^{--}}{9750} + \frac{3969529A^{+-}}{330000} + \frac{6590729A^{++}}{555000} - \frac{5219109A_1}{130000} + \frac{21963A_2}{3700} \\
& + A\left(-\frac{7}{1625}A^{--}\left(15000\log\left(\frac{\mu_W}{M_W}\right) + 10181\right) + A^{+-}\left(3\log\left(\frac{\mu_W}{M_W}\right) + \frac{13331}{5000}\right)\right. \\
& - \frac{7}{46250}\left(15000\log\left(\frac{\mu_W}{M_W}\right) + 7031\right)A^{++} \\
& + A_2\left(2\log\left(\frac{M_W}{M_{W'}}\right) + F(\omega) + \frac{2600}{37}\log\left(\frac{\mu_W}{M_W}\right) + \frac{1318747}{22200}\right) \\
& \left. + A_1\left(\frac{21}{13}\log\left(\frac{\mu_W}{M_W}\right) - \frac{324963}{715000}\right)\right)\Bigg)\,,
\end{aligned} \tag{3.47}$$

JHEP08(2016)128

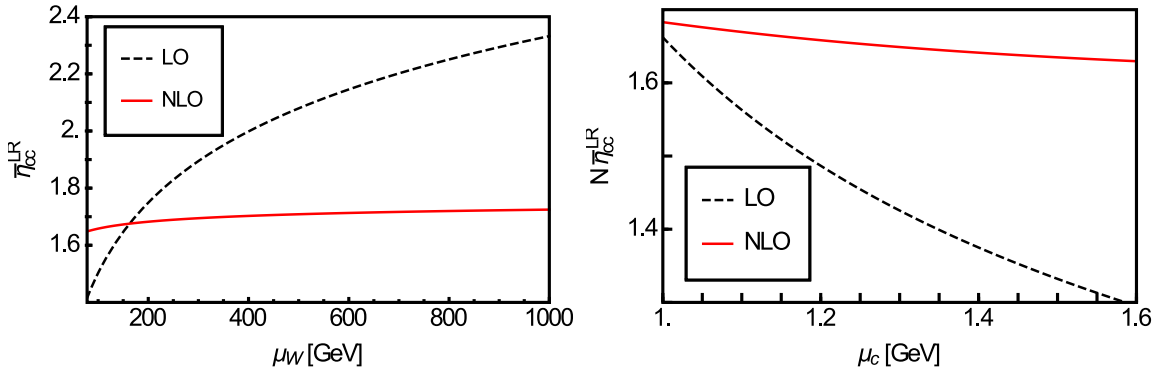

Figure 7. Dependence of $\bar{\eta}_{cc}$ on the high (left panel) and on the low (right panel) scale in the EFT approach for $M_{W_R} = 1\,\text{TeV}$ and respectively for $\mu_c = m_c$ and $\mu_W = M_W$. The other parameters are given in the text. The relevant quantity when $\mu_c \neq m_c$ is $N\bar{\eta}_{cc}$ with N defined in eq. (3.50).

with

$$A = \frac{\alpha_s(\mu_W)}{\alpha_s(\mu_c)}\,, \qquad A_1 = \left(\frac{\alpha_s(\mu_W)}{\alpha_s(\mu_c)}\right)^{\frac{2}{25}}, \qquad A_2 = \left(\frac{\alpha_s(\mu_W)}{\alpha_s(\mu_c)}\right)^{-1}, \tag{3.48}$$
$$A^{++} = \left(\frac{\alpha_s(\mu_W)}{\alpha_s(\mu_c)}\right)^{\frac{12}{25}}, \qquad A^{+-} = \left(\frac{\alpha_s(\mu_W)}{\alpha_s(\mu_c)}\right)^{-\frac{6}{25}}, \qquad A^{--} = \left(\frac{\alpha_s(\mu_W)}{\alpha_s(\mu_c)}\right)^{-\frac{24}{25}}.$$

The value of $\bar{\eta}_{cc}^{(LR)} \equiv \bar{\eta}_{2,cc}^{(LR)}$ at the scale $\mu = 1\,\text{GeV}$ is

$$\bar{\eta}_{cc}^{(LR)}\Big|_{EFT} = \frac{1}{1 - 0.0294\,F(\omega)}[1.562 + (0.604 - 0.037F(\omega)) - 0.473]\,, \tag{3.49}$$

where $F(\omega)$ is defined in eq. (3.3) and we have taken $M_{W'} = 1\,\text{TeV}$ (for $M_{W'} = \mathcal{O}(1-10)\,\text{TeV}$, the dependence on this parameter is very weak). The first and second terms in the brackets are the LO and NLO contributions stemming from the first term in eq. (3.43), whereas the last term comes from the $r_{rl,a}$ term in the same equation (the term C_a^{op} in eq. (3.43) being higher order).

The dependence on the matching scales μ_W and μ_c is illustrated on figure 7. This illustrates the strong dependence of the LO result on the matching scales and the much milder dependence at NLO. This behaviour is similar to what is observed in the SM [32, 36, 38] and it constitutes another significant check of our computation. In the case of the dependence on μ_c, the relevant quantity is $N\bar{\eta}_{cc}$ with the normalisation factor given by

$$N = S^{LR}(x_c(\mu_c), \beta, \omega)/S^{LR}(x_c(m_c), \beta, \omega)\,, \tag{3.50}$$

considering that $S^{LR}(x_c(m_c))$ is the quantity multiplied by $\bar{\eta}_{cc}^{(LR)}$. We also show the dependence on the choice of the hadronic scale μ_h on the right panel of figure 8 for typical values between $1 < \mu_h < 2\,\text{GeV}$. As can be seen on the left panel of the same figure, there is a very mild dependence on the ratio of the masses of the W' and H bosons at NLO.

JHEP08(2016)128

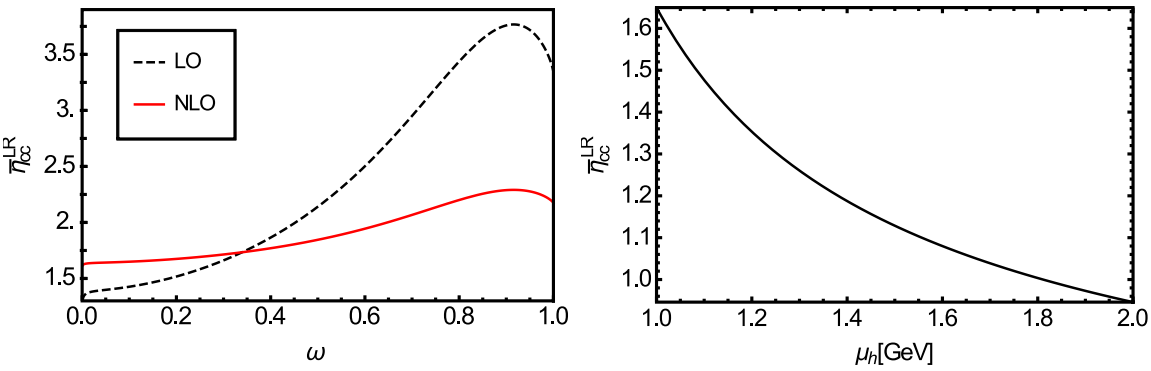

Figure 8. Dependence of $\bar{\eta}_{cc}$ on $\omega = M_{W'}^2/M_H^2$ (left panel) and on the hadronic scale μ_h (right panel) in the EFT approach.

4 Discussion of the results

We are now in a position to give our final results for the short-distance QCD corrections to $K\bar{K}$ mixing at NLO in LRM. Adding up our results from the previous sections yields the effective Hamiltonian:

$$\begin{aligned} H = H^{SM} &+ \frac{G_F^2 M_W^2}{4\pi^2} 8\beta h^2 Q_2^{LR} \sum_{U,V=c,t} \lambda_U^{LR}\lambda_V^{RL}\bar{\eta}_{UV}^{(LR)}\sqrt{x_U x_V}\, S^{LR}(x_U, x_V, \beta, \omega) \\ &- \frac{4G_F}{\sqrt{2}} u\beta\omega Q_2^{LR} \sum_{U,V=c,t} \lambda_U^{LR}\lambda_V^{RL}\bar{\eta}_{UV}^{(H)}\sqrt{x_U x_V} \\ &+ \frac{G_F^2 M_W^2}{4\pi^2} Q_2^{LR} \sum_{U,V=c,t} \lambda_U^{LR}\lambda_V^{RL}\bar{\eta}_{UV}^{(H^\pm \text{box})} S_{LR}^H(x_U, x_V, \beta\omega) + h.c., \end{aligned} \tag{4.1}$$

where H^{SM} is given in eq. (1.1), and

$$\begin{aligned} S^{LR}(x_c, x_t, \beta, \omega) &= \frac{1}{4}\left[\frac{x_t - 4}{x_t - 1}\log(x_t) + \log(\beta) + F(\omega)\right], \\ S^{LR}(x_t, \beta, \omega) &= \frac{1}{4}\left(\frac{x_t^2 - 2x_t + 4}{(x_t - 1)^2}\log(x_t) + \frac{x_t - 4}{x_t - 1} + \log(\beta) + F(\omega)\right). \end{aligned} \tag{4.2}$$

$S^{LR}(x_c, \beta, \omega)$ and $S_{LR}^H(x_U, x_V, \beta\omega)$ are given in eqs. (2.14) and (3.2), respectively.

In the MR model we add the contributions given in table 2 for the three diagrams 2(a), (b), (c) with the relevant weights and we normalise the result to $S^{LR}(x_U, x_V, \beta, \omega)$ in order to get the result in the appropriate form (the same applies to the charged Higgs in the box which corresponds to the third line in eq. (4.1)).

JHEP08(2016)128

4.1 Short-range contributions for the *cc* box

Since we computed $\bar{\eta}_{cc}^{(LR)}$ in both approaches, we can compare the EFT result with the MR calculation. We get from eq. (3.49) and table 2 for $\omega = 0.1$ ($\omega = 0.8$)

$$\bar{\eta}_{cc}^{(LR)}\Big|_{EFT} = 1.41 + 0.67 - 0.43 = 1.65 \qquad (3.41 - 0.17 - 1.03 = 2.21)\,, \tag{4.3}$$

$$\bar{\eta}_{cc}^{(LR)}\Big|_{MR} = 1.16 + 0.13 + 0.03 = 1.32 \qquad (2.46 + 0.27 - 1.32 = 1.41)\,. \tag{4.4}$$

For consistency, the MR result is obtained by applying the same counting for LO, NLO and NNLO contributions as in the EFT approach, which means that the non-logarithmic NLO contributions shown in table 2 are counted as NNLO and are not included in eq. (4.4). As in the SM case, we see that the central values from the MR are only in broad agreement (around 30%) with the EFT approach in the presence of large logarithms, and in this sense we could quote a 30% uncertainty in eq. (4.4). Including this uncertainty in our result and considering the values obtained with resummation of $\log\beta$, we have

$$\bar{\eta}_{cc}^{(LR)}\Big|_{MR} = 1.35 \pm 0.41 \pm 0.08 \qquad (1.48 \pm 0.44 \pm 0.10), \tag{4.5}$$

where the first error comes from the comparison of MR and EFT, and the second error is obtained by considering the values obtained with and without the resummation of $\log\beta$.

The EFT NLO central value will be taken as our final result. At the scale $\mu = 1\,\text{GeV}$ and for $\omega = 0.1$ ($\omega = 0.8$), we have:

$$\bar{\eta}_{cc}^{(LR)} = 1.65 \pm 0.50 \qquad (2.21 \pm 0.66)\,, \tag{4.6}$$

where the conservative 30% error bar includes our estimate of higher-order terms, namely: the contribution from C_a^{op} (which turns out to be very small), contributions from the expansion of eq. (3.43) up to NNLO, an estimate of the NNLO term assuming a geometrical growth from LO to NLO, the arbitrariness in the choice of μ_W when integrating out the W and W' bosons to match onto the four-flavour theory (we vary μ_W between the two high scales M_W and $M_{W'}$), the dependence on the choice of the matching scales for the matching onto the three-flavour theory. Each of these uncertainties are of the order of a few percent. Furthermore we have not resummed the contributions $\log\beta$. This last error is clearly difficult to determine without an explicit calculation, however this logarithm $\log\beta$ is multiplied by a suppressing factor $\alpha_s(\mu_W)$, suggesting that the error should be smaller than our conservative estimate of 30%.

4.2 Short-range contributions for the *ct* and *tt* boxes

The short-distance contributions from the ct and tt boxes in the MR are:

$$\bar{\eta}_{ct}^{(LR)} = 2.74 \pm 0.82 \pm 0.05 \qquad (2.67 \pm 0.80 \pm 0.03)\,, \tag{4.7}$$

$$\bar{\eta}_{tt}^{(LR)} = 5.88 \pm 1.76 \pm 0.23 \qquad (5.55 \pm 1.67 \pm 0.11)\,, \tag{4.8}$$

where the central value and the second uncertainty are obtained by considering the values obtained with or without a resummation of $\log\beta$. The first uncertainty is a conservative

JHEP08(2016)128

30% estimate of the uncertainty of the MR coming from our previous experience in the SM, in relation with the fact that the top quark is not treated on the same footing as other heavy degrees of freedom in this approach. As indicated earlier, resumming or not $\log\beta$ yields a small uncertainty from a few percent in both cases (as expected, since the potentially large logarithm $\log\beta$ is multiplied by a suppressing factor $\alpha_s(\mu_W)$). Moreover, we can see that our result is very stable with respect to ω, which will allow us to neglect the dependence of QCD short-distance corrections on ω when discussing constraints on LRM coming from $K\bar{K}$ mixing [54].

4.3 Short range contribution from neutral and charged Higgs exchange

The values of the QCD short-distance corrections for the box containing a charged heavy Higgs (see figure 2) are

$$\bar{\eta}_{ct}^{(H^\pm\text{box})} = 2.76 \pm 0.83 \pm 0.07 \qquad (2.79 \pm 0.84 \pm 0.10), \tag{4.9}$$

$$\bar{\eta}_{tt}^{(H^\pm\text{box})} = 5.85 \pm 1.76 \pm 0.20 \qquad (5.90 \pm 1.77 \pm 0.25), \tag{4.10}$$

$$\bar{\eta}_{cc}^{(H^\pm\text{box})} = 1.29 \pm 0.39 \pm 0.01, \tag{4.11}$$

where the first uncertainty corresponds to a conservative 30% error related to the MR method,[3] and the second uncertainty corresponds to an average of the results with and without a resummation of $\log\beta$. For the tree-level neutral Higgs exchange we have

$$\bar{\eta}_{ct}^{(H)} = 2.70 \pm 0.09, \tag{4.12}$$

$$\bar{\eta}_{tt}^{(H)} = 5.66 \pm 0.30, \tag{4.13}$$

$$\bar{\eta}_{cc}^{(H)} = 1.28 \pm 0.04, \tag{4.14}$$

where the quoted uncertainty assesses conservatively the neglected NLO corrections coming from the matching at μ_H and the NNLO corrections based on a geometrical progression of the perturbative series.

5 Conclusion

Among the extensions of the Standard Model, Left-Right models provide an interesting solution to the violation of parity coming from the weak interaction. These models exhibit both additional W' and Z' gauge bosons and an extended Higgs sector needed to trigger the breakdown of the left-right symmetry. They are significantly constrained by several kinds of observables, and in particular kaon mixing which is accurately measured and which gets contributions from tree-level neutral Higgs inducing flavour-changing neutral currents.

Kaon mixing can be analysed in the framework of the effective Hamiltonian, separating short- and long-distance contributions. The latter yield matrix elements that can be evaluated at a hadronic scale of a few GeV using lattice QCD simulations. The short-distance contributions can be determined thanks to a matching onto the fundamental theory (SM or Left-Right model) at a high scale corresponding to the mass of the heavy degrees of

[3] Note that we provide only one $\bar{\eta}_{cc}^{(H^\pm\text{box})}$ since the dependence on ω is negligible.

JHEP08(2016)128

freedom. The bridge between the two scales is provided by RGE, which allows one to perform a resummation of large logarithms stemming from QCD corrections.

These short-distance QCD corrections are relevant to compute kaon mixing accurately in the Standard Model. They have been computed in the SM using a rigorous EFT approach where heavy degrees of freedom are progressively integrated out as the scale is lowered, showing the importance of NLO corrections. Another, approximate, method has been devised in earlier times to compute these QCD corrections at LO, consisting in determining the range of loop momenta responsible for the large logarithms and introducing the relevant anomalous dimensions to resum these logarithms. This method of regions is admittedly approximate but is far less demanding in terms of computation, compared to the EFT approach (once the relevant anomalous dimensions have been computed).

We first recalled basic features of these two methods, before proposing an extension of the method of regions to include NLO corrections. We compared the results of the two methods in the case of the Standard Model, finding a good agreement for SM diagrams dominated by a single mass, but a 30% discrepancy between our extension of the method of regions and the EFT computation in the case of large logarithm. We then considered the corrections for the Left-Right models using the method of regions. For some of the contributions, the computation has a different structure, depending on whether $\log \beta$ is treated as a large logarithm or not.

Since the cc box exhibits a large logarithm $\log x_c$ at LO and thus might suffer from a large uncertainty in the method of regions, we decided to compute the short-distance QCD correction within the EFT approach, following closely refs. [36–39]. We matched the LRM onto a four-flavour theory, which was run down to m_c and matched onto a three-flavour theory, before reaching a low hadronic scale μ_h. A large number of cross-checks have been performed on our results (independence of the QCD gauge, independence of the definition of the evanescent operators, independence of the infrared regulators). Our result for $\bar{\eta}_{cc}^{(LR)}$ at NLO in the EFT approach showed again a 30% discrepancy with the method of regions. We finally provided an estimate of the uncertainty to attach to our EFT computation at NLO.

We considered also the case of ct and tt boxes, where another logarithm, namely $\log \beta$, may or may not be considered as large. Within the method of regions, both cases led to very similar results. We then provided estimates for $\bar{\eta}_{ct}^{(LR)}$ and $\bar{\eta}_{tt}^{(LR)}$ at NLO, using conservative error estimates based on our previous comparisons between the two approaches.

These results can be extended to the mixing for B_d and B_s meson, and they can be used in order to constrain Left-Right models. Other constraints, such as electroweak precision observables, flavour-changing charged currents and direct searches, have also proven important and call for a global analysis of these models within an appropriate statistical framework. This will be the object of future work to determine the viability of Left-Right models in the doublet case, their ability to solve the violation of parity occurring in the Standard Model and the possibility to find part of their spectrum in the next run of the LHC [54].

JHEP08(2016)128

Acknowledgments

We would like to thank A. Buras, M. Knecht, H. Sadzjian and G. Senjanović for interesting and useful discussions. LVS acknowledges funding by the P2IO LabEx (ANR-10-LABX-0038) in the framework "Investissements d'Avenir" (ANR-11-IDEX-0003-01) managed by the French National Research Agency (ANR).

A $|\Delta S| = 2$ effective Hamiltonian in the SM

We outline the main steps of the derivation of the $|\Delta S| = 2$ Hamiltonian in the Standard Model, borrowing heavily from ref. [38] (which should be consulted for any further detail) and neglecting penguin contributions for simplicity.

A.1 Minimal operator basis

One has the following Hamiltonian for $|\Delta S| = 1$ transitions

$$H_{\text{eff}}^{|\Delta S|=1} = -\frac{G_F}{\sqrt{2}} \sum_{i=1}^{2} \sum_{U,V=u,c} V_{ks}^* V_{ld} C_i Q_i^{UV} \tag{A.1}$$

with the two operators

$$Q_1^{UV} = (\bar{s}\gamma_\mu LU) \cdot \left(\bar{V}\gamma^\mu Ld\right) \cdot \widetilde{\mathbf{1}} \qquad Q_2^{UV} = (\bar{s}\gamma_\mu LU) \cdot \left(\bar{V}\gamma^\mu Ld\right) \cdot \mathbf{1} \tag{A.2}$$

where $\mathbf{1}$ and $\widetilde{\mathbf{1}}$ denote colour singlet and antisinglet and $L = (1 - \gamma_5)$. The 2×2 renormalization matrix Z_{ij}^{-1} is diagonal in the basis

$$Q_\pm^{UV} = \frac{1}{2}\left(Q_2^{UV} \pm Q_1^{UV}\right), \tag{A.3}$$

provided one preserves Fierz symmetry in the renormalization process

The Hamiltonian for $|\Delta S| = 2$ transitions reads

$$\begin{aligned} H_{\text{eff}}^{|\Delta S|=2} = &-\frac{G_F}{\sqrt{2}} \sum_{i=\pm} C_i \left[\sum_{j=\pm} Z_{ij}^{-1} \sum_{U,V=u,c} V_{Us}^* V_{Vd} Q_j^{UV,\,\text{bare}} \right] \\ &- \frac{G_F^2}{16\pi^2} \lambda_t^2 \tilde{C}_{S2}^{(t)} \tilde{Z}_{S2}^{-1} \tilde{Q}_{S2}^{\text{bare}} - \frac{G_F^2}{2} \lambda_c \lambda_t \left[\sum_{k,l=\pm} C_k C_l \tilde{Z}_{kl,7}^{-1} + \tilde{C}_7 \tilde{Z}_{77}^{-1} \right] \tilde{Q}_7^{\text{bare}} \end{aligned} \tag{A.4}$$

where counterterms proportional to evanescent operators are not displayed and local operators absorb the divergences arising from the charm-top and top-top boxes:

$$\tilde{Q}_7 = \frac{m_c^2}{g^2 \mu^{2\epsilon}} \tilde{Q}_{S2} = \frac{m_c^2}{g^2 \mu^{2\epsilon}} \cdot \bar{s}\gamma_\mu Ld \cdot \bar{s}\gamma^\mu Ld\,. \tag{A.5}$$

Since the charm is still dynamical, the $\tilde{Q}_7$ operator gets two types of divergences, corresponding to graphs with two insertions of $|\Delta S| = 1$ operators with charm quarks, or to the

JHEP08(2016)128

single insertion of the local operator $\tilde{Q}_7$. Due to the GIM mechanism, there are no divergences in the SM for boxes with identical internal flavours, so that for top-top boxes, only the second type of contribution arises for $\tilde{Q}_{S2}$ whereas there are no such local operators for charm-charm boxes.

Evanescent operators must be introduced as counterterms above in order to make the one-loop diagrams with the insertion of Q_j finite:

$$E_1[Q_j] = [\gamma_\mu\gamma_\nu\gamma_\eta L \otimes \gamma^\eta\gamma^\nu\gamma^\mu L - (4+a_1\epsilon)\,\gamma_\mu L \otimes \gamma^\mu L]\,K_{1j}, \quad j = 1,\dots 2 \tag{A.6}$$

$$E_1[\tilde{Q}_7] = \frac{m_c^2}{g^2}\,[\gamma_\mu\gamma_\nu\gamma_\eta L \otimes \gamma^\eta\gamma^\nu\gamma^\mu L - (4+\hat{a}_1\epsilon)\,\gamma_\mu L \otimes \gamma^\mu L]\,K_{12}, \tag{A.7}$$

$$E_2[\tilde{Q}_7] = \frac{m_c^2}{g^2}\left[\gamma_\mu\gamma_\nu\gamma_\eta\gamma_\sigma\gamma_\tau L \otimes \gamma^\tau\gamma^\sigma\gamma^\eta\gamma^\nu\gamma^\mu L - \left[(4+\hat{a}_1\epsilon)^2 + \hat{b}_1\epsilon\right]\gamma_\mu L \otimes \gamma^\mu L\right] K_{22}\,, \tag{A.8}$$

with colour factors K_{ij} being linear combinations of $\widetilde{\mathbf{1}}$ and $\mathbf{1}$ and arbitrary constants $a_{1,2}, \hat{a}_1, \hat{b}_1$ defining these evanescent operators.

A.2 Matching at the high scale

The determination of the $|\Delta S| = 1$ Wilson coefficients can be done at the high scale as

$$C_\pm(\mu_{tW}) = 1 + \frac{\alpha_s(\mu_{tW})}{4\pi}\left[\ln\frac{\mu_{tW}}{M_W}\gamma_\pm^{(0)} + B_\pm\right] + \mathcal{O}(\alpha_s^2) \tag{A.9}$$

with the anomalous dimensions $\gamma_\pm^{(0)}$ of the $|\Delta S = 1|$ operators defined in appendix C. For $|\Delta S| = 2$ Wilson coefficients, we must perform the matching of a $|\Delta S| = 2$ Green function at the high scale in the full and the effective theory

$$\left\langle T\exp\left[i\int d^Dx H_{\text{eff}}^{|\Delta S|=2}(x)\right]\right\rangle_{|\Delta S|=2} = -i\left\langle H^c + H^t + H^{ct}\right\rangle + \mathcal{O}\left(G_F^3\right), \tag{A.10}$$

where

$$H^c(x) = \lambda_c^2\frac{G_F^2}{2}\sum_{i,i',j,j'=\pm} C_iC_j\underbrace{Z_{ii'}^{-1}Z_{jj'}^{-1}\mathcal{O}_{i'j'}^{\text{bare}}(x)}_{\equiv\,\mathcal{O}_{ij}(x)}, \tag{A.11a}$$

$$H^t(x) = \lambda_t^2\frac{G_F^2}{16\pi^2}\tilde{C}_{S2}^{(t)}\tilde{Z}_{S2}^{-1}\tilde{Q}_{S2}^{\text{bare}}(x)\,, \tag{A.11b}$$

$$H^{ct}(x) = \lambda_c\lambda_t\frac{G_F^2}{2}\left[\sum_{i,j=\pm}C_iC_j\underbrace{\left(\sum_{i',j'=\pm}Z_{ii'}^{-1}Z_{jj'}^{-1}\mathcal{R}_{i'j'}^{\text{bare}}(x) + \tilde{Z}_{ij,7}^{-1}\tilde{Q}_7^{\text{bare}}(x)\right)}_{\equiv\,\mathcal{R}_{ij}(x)} + \tilde{C}_7\tilde{Z}_{77}^{-1}\tilde{Q}_7^{\text{bare}}(x)\right]. \tag{A.11c}$$

JHEP08(2016)128

Here, the bare $\mathcal{O}_{ij}$ and $\mathcal{R}_{ij}$ combinations denote the bilocal structures composed of two $|\Delta S| = 1$ operators. In each case (charm-charm, charm-top, or top-top box), the computation of the above Green function allows one to determine the values of the Wilson coefficients for the $|\Delta S| = 2$ operators.

A.3 RG evolution of the Wilson coefficients from the high scale down to $\mu = m_c$

The renormalisation is again discussed in a different manner for single and double insertions. In the first case, the derivation can be obtained from the RG equation

$$\sum_{j=\pm}\left[\delta_{jk}\frac{d}{d\mu}-\gamma_{jk}\right]C_j=0 \qquad \gamma_{ij}\left(g\left(\mu\right)\right)=\sum_{k=\pm}Z_{ik}^{-1}\mu\frac{d}{d\mu}Z_{kj} \tag{A.12}$$

for the Wilson coefficient functions C_j, where γ is the anomalous dimension matrix of the $|\Delta S| = 1$ operators Q_k (we recall that we neglect penguin operators). In the case of $Q_\pm$, $\tilde{Q}_7$ or $\tilde{Q}_{S2}$ which do not mix with other operators, this matrix reduces to simple numbers. Attention should be paid for the crossing of thresholds (such as $\mu = m_b$).

We expand the renormalization matrix Z^{-1} as

$$Z^{-1}=1+\frac{\alpha_s}{4\pi}Z^{-1,(1)}+\left(\frac{\alpha_s}{4\pi}\right)^2Z^{-1,(2)}+\ldots, \qquad Z^{-1,(n)}=\sum_{r=0}^{n}\frac{1}{\epsilon^r}Z_r^{-1,(n)}\,. \tag{A.13}$$

To deal with the evanescent operators, Z^{-1} contains a finite renormalization piece. The coefficients of the perturbative expansion of

$$\gamma=\frac{\alpha_s}{4\pi}\gamma^{(0)}+\left(\frac{\alpha_s}{4\pi}\right)^2\gamma^{(1)}+\ldots, \tag{A.14}$$

are obtained as

$$\gamma^{(0)}=2Z_1^{-1,(1)}+2\epsilon Z_0^{-1,(1)} \tag{A.15}$$

$$\gamma^{(1)}=4Z_1^{-1,(2)}+2\left\{Z_0^{-1,(1)},Z_1^{-1,(1)}\right\}+2\beta_0Z_0^{-1,(1)}\,. \tag{A.16}$$

The local operator counterterms proportional to $\widetilde{Z}_{kl,7}^{-1}\left(\mu\right)$ do not influence the RG evolution of the coefficients C_l, but they modify the running of $\tilde{Q}_7$. The independence of the $|\Delta S| = 2$ effective Hamiltonian on μ yields the following RG equation

$$\frac{d}{d\mu}\tilde{C}_7\left(\mu\right)=\tilde{C}_7\left(\mu\right)\tilde{\gamma}_{77}+\sum_{k,k'=\pm}C_k\left(\mu\right)C_{k'}\left(\mu\right)\tilde{\gamma}_{kk',7} \tag{A.17}$$

with the anomalous dimension tensor

$$\begin{aligned}\tilde{\gamma}_{kn,7}&=\frac{\alpha_s}{4\pi}\tilde{\gamma}_{kn,7}^{(0)}+\left(\frac{\alpha_s}{4\pi}\right)^2\tilde{\gamma}_{kn,7}^{(1)}+\ldots\\&=-\sum_{k',n'=\pm}\left[\gamma_{kk'}\delta_{nn'}+\delta_{kk'}\gamma_{nn'}\right]\tilde{Z}_{k'n',7}^{-1}\tilde{Z}_{77}-\left[\mu\frac{d}{d\mu}\tilde{Z}_{kn,7}^{-1}\right]\tilde{Z}_{77}.\end{aligned} \tag{A.18}$$

JHEP08(2016)128

Its first perturbative coefficients are

$$\tilde{\gamma}^{(0)}_{kn,7} = 2\left[\tilde{Z}_1^{-1,(1)}\right]_{kn,7} + 2\epsilon\left[\tilde{Z}_0^{-1,(1)}\right]_{kn,7} \tag{A.19}$$

$$\begin{aligned}\tilde{\gamma}^{(1)}_{kn,7} = {} & 4\left[\tilde{Z}_1^{-1,(2)}\right]_{kn,7} + 2\beta_0\left[\tilde{Z}_0^{-1,(1)}\right]_{kn,7} \\ & - 2\left[\tilde{Z}_0^{-1,(1)}\right]_{kn,7}\left[\tilde{Z}_1^{-1,(1)}\right]_{77} - 2\left[\tilde{Z}_1^{-1,(1)}\right]_{kn,7}\left[\tilde{Z}_0^{-1,(1)}\right]_{77} \\ & - 2\sum_{k',n'=1}^{2}\left\{\left(\left[Z_0^{-1,(1)}\right]_{kk'}\delta_{nn'} + \delta_{kk'}\left[Z_0^{-1,(1)}\right]_{nn'}\right)\left[\tilde{Z}_1^{-1,(1)}\right]_{k'n',7}\right. \\ & \left. + \left(\left[Z_1^{-1,(1)}\right]_{kk'}\delta_{nn'} + \delta_{kk'}\left[Z_1^{-1,(1)}\right]_{nn'}\right)\left[\tilde{Z}_0^{-1,(1)}\right]_{k'n',7}\right\}.\end{aligned} \tag{A.20}$$

The above equations include finite renormalisation constants (subscript 0), which appear when counterterms proportional to evanescent operators must be included. The extra terms involving the finite renormalisation constants can be simply included into the calculation by multiplying all one-loop diagrams containing a finite counterterm by a factor of 1/2.

The value of the anomalous dimension tensor $\tilde{\gamma}_{\pm j,7}$ governs the mixing from double insertions to $\tilde{C}_7$. This tensor is determined from the renormalization factor $\tilde{Z}^{-1}_{ij,7}$, which can be determined from the finiteness of the Green function $-i\langle H^{ct}\rangle$

$$\left[\tilde{Z}^{-1,(1)}\right]_{ij,7}\left\langle\tilde{Q}_7\right\rangle^{(0)} = -\left\langle\mathcal{R}_{ij}\right\rangle^{(0),\text{bare}}, \tag{A.21}$$

and similarly for higher orders, requiring the evaluation of $\langle\mathcal{R}_{ij}\rangle^{\text{bare}}$ and $\langle\tilde{Q}_7\rangle^{\text{bare}}$ up to the relevant order. Standard methods can then be used to solve the differential equation eq. (A.17) (especially when $i, j = \pm$ leading to diagonal expressions).

A.4 Matching at $\mu = m_c$

At the scale $\mu = m_c$, one can then match this theory to the effective three-quark theory

$$H = -\frac{G_F^2}{16\pi^2}\left[\lambda_c^2\tilde{C}^{(cc)}_{S2}(\mu) + \lambda_t^2\tilde{C}^{(tt)}_{S2}(\mu) + \lambda_c\lambda_t\tilde{C}^{(ct)}_{S2}(\mu)\right]\tilde{Z}^{-1}_{S2}(\mu)\,\tilde{Q}^{\text{bare}}_{S2}. \tag{A.22}$$

Equating the Green function eq. (A.10) in both four-quark and three-quark theories yields the values of the Wilson coefficients in this theory at the scale $\mu = \mu_c$. In the charm-top case, one gets

$$\sum_{i,j=\pm} C_i(\mu_c)C_j(\mu_c)\langle\mathcal{R}_{ij}\rangle(\mu_c) + \tilde{C}_7(\mu_c)\langle\tilde{Q}_7\rangle(\mu_c) = \frac{1}{8\pi^2}\tilde{C}^{(ct)}_{S2}(\mu_c)\langle\tilde{Q}_{S2}\rangle(\mu_c). \tag{A.23}$$

$\tilde{C}_7(\mu_c)$ is already nonzero in the LO due to its mixing with C_2, whereas the two insertion contribution starts at NLO only

$$\langle\mathcal{R}_{ij}(\mu)\rangle^{(0)} = \frac{m_c^2(\mu)}{16\pi^2}\,2\,r_{ij,S2}(\mu)\left\langle\tilde{Q}_{S2}\right\rangle^{(0)}, \tag{A.24}$$

JHEP08(2016)128

with $r_{ij,S2}$ given by the finite part of the diagrams D_i and L_i leading to

$$\tilde{C}_{S2}^{(ct)}(\mu_c) = m_c^2(\mu_c)\left[\frac{1}{2}\frac{4\pi}{\alpha_s(\mu_c)}\tilde{C}_7(\mu_c) + \sum_{i=\pm}\sum_{j=1}^{6} r_{ij,S2}(\mu_c)\, C_i(\mu_c)\, C_j(\mu_c)\right]. \tag{A.25}$$

In the top-top case, the three-quark and four-quark theories are completely identical up to the running of the strong coupling constant, making the determination of the Wilson coefficient $\tilde{C}_{S2}(\mu)$ very simple. In the charm-charm case, only two insertions of $|\Delta S| = 1$ operators contribute in the four-quark theory, leading to a simple parametrisation of the matching

$$\langle \mathcal{O}_{ij}(\mu)\rangle = \frac{m_c^2(\mu)}{16\pi^2}\, 2\, d_{ij,S2}(\mu)\left\langle \tilde{Q}_{S2}(\mu)\right\rangle. \tag{A.26}$$

A.5 RG evolution of the Wilson coefficients from $\mu = m_c$ down to the low scale

The running of the Wilson coefficients according to the RG equation in the three-flavour theory is then trivial, limited to the single operator $\tilde{Q}_{S2}$, with the expression

$$\tilde{C}_{S2}^{(j)}(\mu) = \tilde{C}_{S2}^{(j)}(\mu_c)\left[\frac{\alpha_s(\mu_c)}{\alpha_s(\mu)}\right]^{d_+^{[3]}}\left(1 - J_+^{[3]}\frac{\alpha_s(\mu_c) - \alpha_s(\mu)}{4\pi}\right), \tag{A.27}$$

where $d_+^{[3]}$ and $J_+^{[3]}$ are the RG quantities for three active flavours which can be determined from the results in appendix C.2.

The results at the low scale allow then to determine the expression of the short-distance QCD corrections for the three different boxes in the SM case.

B SM case at NLO with the method of regions

We want to apply the method of regions as explained in section 1.3 in order to determine the short-distance corrections $\bar{\eta}$ at NLO. We start with the behaviour of the one-loop integrals. In the SM these integrals are given by the following functions

$$\begin{aligned}
S^{LL}(x_t) &= x_t\left(\frac{1}{4} + \frac{9}{4}\frac{1}{1-x_t} - \frac{3}{2}\frac{1}{(1-x_t)^2}\right) - \frac{3}{2}\left[\frac{x_t}{(1-x_t)}\right]^3 \log x_t\,,\\
S^{LL}(x_c) &= x_c + \mathcal{O}(x_c^2)\,,\\
S^{LL}(x_c, x_t) &= -x_c \log x_c + x_c F(x_t) + \mathcal{O}(x_c^2 \log x_c)\,,\\
F(x_t) &= \frac{x_t^2 - 8x_t + 4}{4(1-x_t)^2}\log x_t + \frac{3}{4}\frac{x_t}{(x_t-1)}\,.
\end{aligned} \tag{B.1}$$

Clearly the leading behaviour of the one-loop integral for $\bar{\eta}_{tt}$ is $\mathcal{O}(1)$, for $\bar{\eta}_{cc}$ $\mathcal{O}(x_c)$ and for $\bar{\eta}_{ct}$ $\mathcal{O}(x_c \log(x_c))$. Following the method of regions, the remaining integration over the momentum k leads to m_t^2 in the first case, and m_c^2 in the second, as already discussed in section 1.3. For ct one has to introduce the function $R(\gamma, m_1, m_2)$ defined in eq. (1.23) at LO. At NLO the quantity $x_c F(x_t)$ contributes to $\bar{\eta}_{ct}$, so that the result of the integration is m_c^2, similarly to $\bar{\eta}_{cc}$.

JHEP08(2016)128

One has then to determine the anomalous dimensions of the operators which appear in the calculation of the box diagrams. These anomalous dimensions are well known up to NLO, for instance see ref. [39]. We have to combine the contributions of the $|\Delta S| = 1$ operators (hence the presence of d_r and d_l) between μ_W^2 and k^2 with the term from the $|\Delta S| = 2$ operator between k^2 and μ_h (leading to d_V). Setting $k^2 = m_t^2$, we obtain the following formula for the scale-independent correction η_{tt}

$$\eta_{tt} = \frac{\left(\eta_{tt}^{(WW)} + \eta_{tt}^{(GG)} x_t^2/4\right) I_2(x_t, x_t, 1) - \eta_{tt}^{(WG)} 2x_t^2 I_1(x_t, x_t, 1)}{(1 + x_t^2/4) I_2(x_t, x_t, 1) - 2x_t^2 I_1(x_t, x_t, 1)} \tag{B.2}$$

where $I_{1,2}$ are the Inami-Lim functions of eq. (2.2). The superscripts $(WW), (WG)$, and (GG) indicate respectively the contributions from a box containing two W bosons, one W boson and one Goldstone G, and two Goldstones G in the 't Hooft-Feynman gauge (the last two come at higher order on m_c/M_W in the ct and cc cases). The corresponding short-distance corrections are given by

$$\begin{aligned}
\eta_{tt}^{(WW)} = & \sum_{r,l=\pm} (\alpha_s(m_c))^{d_V^{(3)}} \left(\frac{\alpha_s(m_t)}{\alpha_s(\mu_5)}\right)^{d_V^{(5)}} \left(\frac{\alpha_s(\mu_5)}{\alpha_s(m_c)}\right)^{d_V^{(4)}} \left(\frac{\alpha_s(\mu_W)}{\alpha_s(m_t)}\right)^{d_r^{(5)}+d_l^{(5)}} a_{rl}^{(WW)} \\
& \left(1 - \frac{\alpha_s(m_c)}{4\pi}\left(J_V^{(3)} - J_V^{(4)}\right) - \frac{\alpha_s(\mu_5)}{4\pi}\left(J_V^{(4)} - J_V^{(5)}\right) + \frac{\alpha_s(m_t)}{4\pi}\left(J_r^{(5)} + J_l^{(5)} - J_V^{(5)}\right)\right. \\
& \left. - \frac{\alpha_s(\mu_W)}{4\pi}\left(J_l^{(5)} + J_r^{(5)} - B_r - B_l\right)\right),
\end{aligned} \tag{B.3}$$

$$\begin{aligned}
\eta_{tt}^{(WG)} = & \sum_{i,j,k,p,q=1}^{2} \sum_{r=\pm} (\alpha_s(m_c))^{d_V^{(3)}} \left(\frac{\alpha_s(m_t)}{\alpha_s(\mu_5)}\right)^{d_V^{(5)}} \left(\frac{\alpha_s(\mu_5)}{\alpha_s(m_c)}\right)^{d_V^{(4)}} \\
& \left(\frac{\alpha_s(\mu_W)}{\alpha_s(m_t)}\right)^{d_r^{(5)}+2d_m^{(5)}+d_j^{(5)}} \left(\hat{a}_r^{(WG)}\right)_i \delta_{ip} \hat{V}_{pj} \hat{V}_{jq}^{-1} \delta_{qk} (C_0)_k \\
& \left(1 - \frac{\alpha_s(m_c)}{4\pi}\left(J_V^{(3)} - J_V^{(4)}\right) - \frac{\alpha_s(\mu_5)}{4\pi}\left(J_V^{(4)} - J_V^{(5)}\right)\right. \\
& + \frac{\alpha_s(m_t)}{4\pi}\left(J_r^{(5)} + 2J_m^{(5)} - J_V^{(5)} + \left(\hat{J}^{(5)}\right)_{ip}\right) \\
& \left. - \frac{\alpha_s(\mu_W)}{4\pi}\left(J_r^{(5)} - B_r + 2J_m^{(5)} + \left(\hat{J}^{(5)}\right)_{qk}\right)\right),
\end{aligned} \tag{B.4}$$

$$\begin{aligned}
\eta_{tt}^{(GG)} = & \sum_{i,j,k,p,q=1}^{2} \sum_{i',j',k',p',q'=1}^{2} (\alpha_s(m_c))^{d_V^{(3)}} \left(\frac{\alpha_s(m_t)}{\alpha_s(\mu_5)}\right)^{d_V^{(5)}} \left(\frac{\alpha_s(\mu_5)}{\alpha_s(m_c)}\right)^{d_V^{(4)}} \\
& \left(\frac{\alpha_s(\mu_W)}{\alpha_s(m_t)}\right)^{4d_m^{(5)}+d_j^{(5)}+d_{j'}^{(5)}} \left(\hat{a}^{(GG)}\right)_{ii'} \delta_{ip} \hat{V}_{pj} \hat{V}_{jq}^{-1} \delta_{qk} (C_0)_k \delta_{i'p'} \hat{V}_{p'j'} \hat{V}_{j'q'}^{-1} \delta_{q'k'} (C_0)_{k'} \\
& \left(1 - \frac{\alpha_s(m_c)}{4\pi}\left(J_V^{(3)} - J_V^{(4)}\right) - \frac{\alpha_s(\mu_5)}{4\pi}\left(J_V^{(4)} - J_V^{(5)}\right)\right.
\end{aligned} \tag{B.5}$$

JHEP08(2016)128

$$+\frac{\alpha_s(m_t)}{4\pi}\left(4J_m^{(5)}-J_V^{(5)}+\left(\hat{J}^{(5)}\right)_{ip}+\left(\hat{J}^{(5)}\right)_{i'p'}\right)$$
$$-\frac{\alpha_s(\mu_W)}{4\pi}\left(4J_m^{(5)}+\left(\hat{J}^{(5)}\right)_{qk}+\left(\hat{J}^{(5)}\right)_{q'k'}\right)\Bigg)\,,$$

where

$$a_{rl}^{(WW)}=t_{rl}\,,\quad \hat{a}_r^{(WG)}=\begin{pmatrix}-(1+Nr)\\-(1+r)\end{pmatrix}\,,\quad \hat{a}^{(GG)}=4\begin{pmatrix}N&1\\1&1\end{pmatrix}\,,\quad C_0=\begin{pmatrix}0\\-1/2\end{pmatrix}\,, \tag{B.6}$$

with t_{rl} defined in eq. (1.15). Above, the J's arise from the RGE evolution as described in appendix C, where the definition of all the quantities appearing here are given and the exponents denote the number of active flavours. The thresholds are explicitly shown: μ_5 is the threshold for the integration of the b quark, and $\mu_4 = m_c$ for the c quark. Since the formulae become rather large once including the thresholds explicitely we will not give their expressions in the following, but it is rather straightforward to implement them and their effect is included in our final results.

It is interesting to compare the MR result, eq. (B.2), with the one obtained at NLO in EFT [34]. There, contrary to what is done in the Method of Regions where one keeps explicitely the top quark degree of freedom, one ignores the difference between the two scales $\mu_t \equiv m_t$ and μ_W, and integrates at the same time both the top and the W. The EFT approach leads to a much simpler expression since in this case only the $|\Delta S| = 2$ operator survives

$$\eta_{tt}^{EFT,NLO}=(\alpha_s(m_c))^{d_V^{(3)}}\left(\frac{\alpha_s(\mu_W)}{\alpha_s(\mu_5)}\right)^{d_V^{(5)}}\left(\frac{\alpha_s(\mu_5)}{\alpha_s(m_c)}\right)^{d_V^{(4)}} \tag{B.7}$$
$$\left(1-\frac{\alpha_s(m_c)}{4\pi}\left(J_V^{(3)}-J_V^{(4)}\right)-\frac{\alpha_s(\mu_5)}{4\pi}\left(J_V^{(4)}-J_V^{(5)}\right)-\frac{\alpha_s(\mu_W)}{4\pi}\left(J_V^{(5)}-Y(x_t)-R\right)\right)\,.$$

The last two terms in this equation stem from the NLO matching on the full theory at the high scale $\mu_W = \mathcal{O}(m_t, M_W)$ ($5.8 < Y(x_t) + R < 13.4$ for $1 \le x_t \le 4.6$). We refer the reader to [34] for more details. At LO, taking $m_t = \mu_W$ in the MR expressions above, it is easy to show that $\eta_{tt}^{(WW)} = \eta_{tt}^{(WG)} = \eta_{tt}^{(GG)} = \eta_{tt}^{EFT,NLO}$. At NLO, one would have to replace the contributions from $B_{l,r}$, which come from the matching onto two $|\Delta S| = 1$ local operators, by $Y(x_t) + R$. Clearly the difference between the two approaches involves the ratio $\alpha_s(m_t)/\alpha_s(\mu_W)$ and terms of $\mathcal{O}(\alpha_s(\mu_W)/(4\pi))$, which are effects of a few percent, as detailed in section 1.4.

For η_{ct}, we have two different types of contributions: a large logarithm $\log x_c$ and a constant term. Since we want to resum contributions of the form $\alpha_s \log x_c$, the first can be formally counted as coming one order earlier than the latter in the power counting. We can take this into account by treating differently the resummation of the large logarithm and the constant term

$$\eta_{ct}=\frac{1}{-\log x_c+F(x_t)}\alpha_s(m_c)^{d_V}\sum_{r,l=\pm}a_{rl}\left(\frac{\alpha_s(\mu_W)}{\alpha_s(m_c)}\right)^{d_l+d_r} \tag{B.8}$$
$$\times\left(-\log x_c R_{\log}^{NLO}\left[-d_l-d_r+d_V+2d_m,u_{rl},j_{rl};m_c,\mu_W\right]+F(x_t)\right)\,,$$

JHEP08(2016)128

with

$$\begin{aligned} a_{rl} &= [1 + r + l + 3rl]/4 \\ u_{rl} &= 1 + 2\frac{\alpha_s(m_c)}{4\pi} J_m - \frac{\alpha_s(\mu_W)}{4\pi}(J_l + J_r - B_l - B_r), \\ j_{rl} &= J_l + J_r - J_V - 2J_m \,, \end{aligned} \tag{B.9}$$

and

$$R_{\log}^{NLO}(\gamma, U, J; m_1, m_2) = \log^{-1}\frac{m_2^2}{m_1^2}\left(\frac{\alpha_s(m_1)}{\alpha_s(\mu)}\right)^{-\gamma}\int_{m_1^2}^{m_2^2}\frac{dk^2}{k^2}\left(\frac{\alpha_s(k)}{\alpha_s(\mu)}\right)^{\gamma}\left[U + \frac{\alpha_s(k)}{4\pi}J\right], \tag{B.10}$$

where U does not depend on k, yielding for $\gamma \neq 0, 1$

$$\begin{aligned} R_{\log}^{NLO}(\gamma, U, J; m_1, m_2) &= \frac{1}{\log(m_2^2/m_1^2)}\frac{4\pi}{\beta_0\alpha_s(m_1)} \\ &\times \left[\frac{1}{1-\gamma}\left\{\left(\frac{\alpha_s(m_2)}{\alpha_s(m_1)}\right)^{\gamma-1} - 1\right\}U + \frac{\alpha_s(m_1)}{4\pi}\frac{1}{\gamma}\left[\frac{\beta_1}{\beta_0}U - J\right]\left\{\left(\frac{\alpha_s(m_2)}{\alpha_s(m_1)}\right)^{\gamma} - 1\right\}\right]. \end{aligned} \tag{B.11}$$

An analytic comparison with the EFT result in this case would be much more difficult due to the complexity of the expressions. We refer to section 1.4 for a numerical comparison. The previous cases, where a single mass scale m_1 dominates the integral, can be described using the averaging function

$$R_1^{NLO}(\gamma, U, J; m_1, m_2) = \left[U + \frac{\alpha_s(m_1)}{4\pi}J\right]. \tag{B.12}$$

C Operators and anomalous dimensions

C.1 $|\Delta S| = 1$ operators

We have the $|\Delta S| = 1$ vector operators for the SM case [38, 39]

$$O_1^{VLL} = (\bar{d}^\alpha\gamma_\mu P_L s^\beta)(\bar{V}^\beta\gamma^\mu P_L U^\alpha)\,, \qquad O_2^{VLL} = (\bar{d}\gamma_\mu P_L s)(\bar{V}\gamma^\mu P_L U)\,, \tag{C.1}$$

$$O_1^{VLR} = (\bar{d}\gamma_\mu P_L s)(\bar{V}\gamma^\mu P_R U)\,, \qquad O_2^{VLR} = (\bar{d}^\alpha\gamma_\mu P_L s^\beta)(\bar{V}^\beta\gamma^\mu P_R U^\alpha)\,, \tag{C.2}$$

where U and V can be any up-type fermions. The anomalous dimensions for the vector-vector operators is simpler for [39]

$$O_\pm = \frac{O_1 \pm O_2}{2}\,, \tag{C.3}$$

which are the following

$$\begin{aligned} \gamma_\pm^{(0)} &= \pm 6\frac{N \mp 1}{N}\,, & \gamma_\pm^{(1)} &= \frac{N \mp 1}{2N}\left(-21 \pm \frac{57}{N} \mp 19\frac{N}{3} \pm \frac{4}{3}f\right), \\ \gamma_m^{(0)} &= 6C_F\,, & \gamma_m^{(1)} &= C_F\left(3\,C_F + \frac{97}{3}N - \frac{10}{3}f\right), \end{aligned} \tag{C.4}$$

JHEP08(2016)128

where the second line corresponds to the anomalous dimensions for masses with $C_F = (N^2-1)/2N$, and for $N=3$, $\gamma_+^{(0)} = 4, \gamma_-^{(0)} = -8, \gamma_m^{(0)} = 8$.

We introduce the correction of the anomalous dimensions

$$J_\pm = \frac{d_\pm \beta_1}{\beta_0} - \frac{\gamma_\pm^{(1)}}{2\beta_0}\,, \qquad d_\pm = \frac{\gamma_\pm^{(0)}}{2\beta_0}\,, \tag{C.5}$$

$$J_m = \frac{d_m \beta_1}{\beta_0} - \frac{\gamma_m^{(1)}}{2\beta_0}\,, \qquad d_m = \frac{\gamma_m^{(0)}}{2\beta_0}\,, \tag{C.6}$$

and the value of the Wilson coefficients at the high scale $C_\pm(\mu_W)$ defined in ref. [32]

$$C_\pm(\mu_W) = 1 + \frac{\alpha_s(\mu_W)}{4\pi}\left(\log\frac{\mu_W}{M_W}\gamma_\pm^{(0)} + B_\pm\right) + \mathcal{O}(\alpha_s^2)\,, \tag{C.7}$$

with

$$B_\pm = -\frac{11}{2N} \pm \frac{11}{2}\,, \tag{C.8}$$

leading to the evolution

$$C_\pm^{NLO}(\mu;\mu_0) = \left(1 + \frac{\alpha_s(\mu)}{4\pi}J_\pm\right)\left(\frac{\alpha_s(\mu_0)}{\alpha_s(\mu)}\right)^{d_\pm}\left(1 - \frac{\alpha_s(\mu_0)}{4\pi}[J_\pm - B_\pm]\right)\,, \tag{C.9}$$

$$C_m^{NLO}(\mu;\mu_0) = \left(1 + \frac{\alpha_s(\mu)}{4\pi}J_m\right)\left(\frac{\alpha_s(\mu_0)}{\alpha_s(\mu)}\right)^{d_m}\left(1 - \frac{\alpha_s(\mu_0)}{4\pi}J_m\right)\,. \tag{C.10}$$

We have

$$d_m = 4/\beta_0 \qquad d_+ = 2/\beta_0 \qquad d_- = -4/\beta_0\,. \tag{C.11}$$

The same equations can be written for O_i^{VRR} which will be useful for the discussion of the LRM, with identical results for the anomalous dimensions.

One may also consider the running of the $|\Delta S| = 1$ local operators VLR. In the basis O_1^{VLR}, O_2^{VLR}, the anomalous dimensions are

$$\hat\gamma_{VLR}^{(0)} = \begin{bmatrix} 6/N & -6 \\ 0 & -6N + 6/N \end{bmatrix}\,, \tag{C.12}$$

$$\hat\gamma_{VLR}^{(1)} = \begin{bmatrix} \frac{137}{6} + \frac{15}{2N^2} - \frac{22}{3N}f & -\frac{100N}{3} + \frac{3}{N} + \frac{22}{3}f \\ -\frac{71}{2}N - \frac{18}{N} + 4f & -\frac{203}{6}N^2 + \frac{479}{6} + \frac{15}{2N^2} + \frac{10}{3}Nf - \frac{22}{3N}f \end{bmatrix}\,.$$

Introducing

$$\hat V = \begin{pmatrix} 3/2 & 0 \\ -1/2 & -1/2 \end{pmatrix}\,, \tag{C.13}$$

$$\hat\gamma_D^{(0)} = \hat V^{-1}\hat\gamma_{VLR}^{(0)T}\hat V = \begin{pmatrix} 6/N & 0 \\ 0 & -6N + 6/N \end{pmatrix}\,, \qquad \gamma_1^{(0)} = 2\,, \qquad \gamma_2^{(0)} = -16\,, \tag{C.14}$$

$$\hat G = \hat V^{-1}\hat\gamma_{VLR}^{(1)T}\hat V\,, \tag{C.15}$$

$$\hat H_{ij} = \delta_{ij}\gamma_i^{(0)}\frac{\beta_1}{2\beta_0^2} - \frac{\hat G_{ij}}{2\beta_0 + \gamma_i^{(0)} - \gamma_j^{(0)}} \qquad \left(2\beta_0 + \gamma_i^{(0)} - \gamma_j^{(0)} \neq 0\right)\,, \tag{C.16}$$

$$\hat J = \hat V \hat H \hat V^{-1}\,, \tag{C.17}$$

JHEP08(2016)128

one can write down the evolution

$$\vec{C}^{LR}(\mu;\mu_0) = \left(1+\frac{\alpha_s(\mu)}{4\pi}\hat{J}\right)\hat{V}D(\mu;\mu_0)\hat{V}^{-1}\left(1-\frac{\alpha_s(\mu_0)}{4\pi}\hat{J}\right)\vec{C}^{LR}(\mu_0)\,, \tag{C.18}$$

$$D(\mu;\mu_0) = \begin{pmatrix} (\alpha_s(\mu_0)/\alpha_s(\mu))^{d_1} & 0 \\ 0 & (\alpha_s(\mu_0)/\alpha_s(\mu))^{d_2} \end{pmatrix}, \tag{C.19}$$

with $d_i = \gamma_i^{(0)}/(2\beta_0)$.

C.2 $|\Delta S| = 2$ operators

For $|\Delta S| = 2$ operators, we recall the anomalous dimensions associated with the operator Q_V

$$Q_V = (\bar{s}^\alpha \gamma_\mu P_L d^\alpha)(\bar{s}^\beta \gamma^\mu P_L d^\beta)\,, \tag{C.20}$$

with

$$\gamma_V^{(0)} = 6 - 6/N\,, \tag{C.21}$$

$$\gamma_V^{(1)} = -19/6N - 22/3 + 39/N - 57/(2N^2) + 2/3f - 2/(3N)f\,, \tag{C.22}$$

$$J_V = \frac{d_V\beta_1}{\beta_0} - \frac{\gamma_V^{(1)}}{2\beta_0}\,, \qquad d_V = \frac{\gamma_V^{(0)}}{2\beta_0}\,, \tag{C.23}$$

and we can write down a similar evolution for the $|\Delta S| = 2$ local operators Q_1^{LR}, Q_2^{LR}

$$Q_1^{LR} = (\bar{s}^\alpha \gamma_\mu P_L d^\alpha)(\bar{s}^\beta \gamma_\mu P_R d^\beta)\,, \qquad Q_2^{LR} = (\bar{s}^\alpha P_L d^\alpha)(\bar{s}^\beta P_R d^\beta)\,, \tag{C.24}$$

with the anomalous dimensions

$$\hat{\gamma}_{LR}^{(0)} = \begin{bmatrix} 6/N & 12 \\ 0 & -6N + 6/N \end{bmatrix}, \tag{C.25}$$

$$\hat{\gamma}_{LR}^{(1)} = \begin{bmatrix} \frac{137}{6} + \frac{15}{2N^2} - \frac{22}{3N}f & \frac{200N}{3} - \frac{6}{N} - \frac{44}{3}f \\ \frac{71}{4}N + \frac{9}{N} - 2f & -\frac{203}{6}N^2 + \frac{479}{6} + \frac{15}{2N^2} + \frac{10}{3}Nf - \frac{22}{3N}f \end{bmatrix}.$$

Introducing

$$\hat{W} = \begin{pmatrix} 3/2 & 0 \\ 1 & 1 \end{pmatrix}, \tag{C.26}$$

$$\hat{\gamma}_D^{(0)} = \hat{W}^{-1}\hat{\gamma}_{LR}^{(0)T}\hat{W} = \begin{pmatrix} 6/N & 0 \\ 0 & -6N + 6/N \end{pmatrix} \qquad \gamma_1^{(0)} = 2 \qquad \gamma_2^{(0)} = -16\,, \tag{C.27}$$

$$\hat{G} = \hat{W}^{-1}\hat{\gamma}_{LR}^{(1)T}\hat{W}\,, \tag{C.28}$$

$$\hat{H}_{ij} = \delta_{ij}\gamma_i^{(0)}\frac{\beta_1}{2\beta_0^2} - \frac{\hat{G}_{ij}}{2\beta_0 + \gamma_i^{(0)} - \gamma_j^{(0)}} \qquad \left(2\beta_0 + \gamma_i^{(0)} - \gamma_j^{(0)} \neq 0\right), \tag{C.29}$$

$$\hat{K} = \hat{W}\hat{H}\hat{W}^{-1}\,, \tag{C.30}$$

JHEP08(2016)128

one can write down the evolution

$$\vec{C}^{LR}(\mu;\mu_0) = \left(1+\frac{\alpha_s(\mu)}{4\pi}\hat{K}\right)\hat{W}D(\mu;\mu_0)\hat{W}^{-1}\left(1-\frac{\alpha_s(\mu_0)}{4\pi}\hat{K}\right)\vec{C}^{LR}(\mu_0)\,, \quad \text{(C.31)}$$

$$D(\mu;\mu_0) = \begin{pmatrix} (\alpha_s(\mu_0)/\alpha_s(\mu))^{d_1} & 0 \\ 0 & (\alpha_s(\mu_0)/\alpha_s(\mu))^{d_2} \end{pmatrix}, \quad \text{(C.32)}$$

with $d_i = \gamma_i^{(0)}/(2\beta_0)$. The associated LO anomalous dimensions are

$$\gamma_1^{(0)} = 2\,, \qquad \gamma_2^{(0)} = -16\,, \quad \text{(C.33)}$$

and we have

$$d_1 = 1/\beta_0\,, \qquad d_2 = -8/\beta_0\,, \qquad d_V = 2/\beta_0\,. \quad \text{(C.34)}$$

D LR case at NLO with the method of regions

D.1 Contributions with $\log\beta$

Following ref. [43], if we consider the box with the Goldstone boson associated to W together with W', the masses stem from the Goldstone boson coupling (evaluated at the scale μ_W), whereas the largest contribution to I_2 comes from the range between μ_W and μ_R. We obtain

$$\begin{aligned}
\xi^{(W'2)}_{a,UV}[R] = &\sum_{r=\pm,i,j=1,2}\left(\frac{\alpha_s(\mu_W)}{\alpha_s(\mu_h)}\right)^{-d_r+d_i+2d_m}\left(\frac{\alpha_s(m_U)}{\alpha_s(\mu_h)}\right)^{-d_m}\left(\frac{\alpha_s(m_V)}{\alpha_s(\mu_h)}\right)^{-d_m}\left(\frac{\alpha_s(\mu_R)}{\alpha_s(\mu_h)}\right)^{d_r}\\
&\times\left[\left(1+\frac{\alpha_s(\mu_h)}{4\pi}\hat{K}\right)\hat{W}\right]_{ai}\\
&\times R^{NLO}\Bigg(-d_r+d_i-d_j,\\
&\qquad\left[\hat{W}^{-1}\hat{a}_r^{(W'2)}\hat{V}\right]_{ij}[\hat{V}^{-1}\vec{C}_0]_j\\
&\qquad\quad\times\left(1-\frac{\alpha_s(\mu_R)}{4\pi}[J_r-B_r]-\frac{\alpha_s(\mu_W)}{4\pi}2J_m+\frac{\alpha_s(m_U)+\alpha_s(m_V)}{4\pi}J_m\right)\\
&\qquad\quad-\frac{\alpha_s(\mu_W)}{4\pi}\left[\hat{W}^{-1}\hat{a}_r^{(W'2)}\hat{V}\right]_{ij}[\hat{V}^{-1}\hat{J}\vec{C}_0]_j,\\
&\qquad\left[\hat{W}^{-1}[\hat{a}_r^{(W'2)}\hat{J}-\hat{K}\hat{a}_r^{(W'2)}]\hat{V}\right]_{ij}[\hat{V}^{-1}\vec{C}_0]_j+\left[\hat{W}^{-1}\hat{a}_r^{(W'2)}\hat{V}\right]_{ij}[\hat{V}^{-1}\vec{C}_0]_jJ_r,\\
&\qquad\mu_W,\mu_R\Bigg)\,,
\end{aligned} \quad \text{(D.1)}$$

with the initial conditions for the evolution of the operators $O^{VLR}_{1,2}$ and the coefficients for the matching from the two-point function of $O^{VRR}_{\pm}$ and $O^{VLR}_{1,2}$ to the local operators $Q^{LR}_{1,2}$ at $\mu = k^2$.

$$\vec{C}_0 = \begin{pmatrix} 0 \\ -1/2 \end{pmatrix}, \qquad C_a^{LR} \leftrightarrow \sum_{r,i}(\hat{a}_r^{(W'2)})_{ai}C_i^{VLR}C_r^{VRR}\,, \qquad \hat{a}_r^{(W'2)} = \begin{pmatrix} (3r+1)/2 & r/2 \\ 0 & -1 \end{pmatrix}. \quad \text{(D.2)}$$

If we consider the box with W and a charged Higgs boson H, the masses stem from the Higgs couplings (to be evaluated at a high scale μ_H), whereas the largest contribution to I_2 comes from the range between μ_W and M_H. We obtain

$$\begin{aligned}
\xi^{(H2)}_{a,UV}[R] = & \sum_{l=\pm,i,j=1,2} \left(\frac{\alpha_s(\mu_W)}{\alpha_s(\mu_h)}\right)^{d_i-d_j} \left(\frac{\alpha_s(m_U)}{\alpha_s(\mu_h)}\right)^{-d_m} \left(\frac{\alpha_s(m_V)}{\alpha_s(\mu_h)}\right)^{-d_m} \left(\frac{\alpha_s(\mu_H)}{\alpha_s(\mu_h)}\right)^{d_j+2d_m} \\
& \times \left[\left(1+\frac{\alpha_s(\mu_h)}{4\pi}\hat{K}\right)\hat{W}\right]_{ai} \\
& \times R^{NLO}\Bigg(-d_l+d_i-d_j, \\
& \qquad \left[\hat{W}^{-1}\hat{a}^{(H2)}_l\hat{V}\right]_{ij}[\hat{V}^{-1}\vec{C}_0]_j \\
& \qquad \times\left(1-\frac{\alpha_s(\mu_W)}{4\pi}[J_l-B_l]-\frac{\alpha_s(\mu_H)}{4\pi}2J_m+\frac{\alpha_s(m_U)+\alpha_s(m_V)}{4\pi}J_m\right), \\
& \qquad \left[\hat{W}^{-1}\left[\hat{a}^{(H2)}_l\hat{J}-\hat{K}\hat{a}^{(H2)}_l\right]\hat{V}\right]_{ij}[\hat{V}^{-1}\vec{C}_0]_j - \left[\hat{W}^{-1}\hat{a}^{(H2)}_l\hat{V}\right]_{ij}[\hat{V}^{-1}\hat{J}\vec{C}_0]_j \\
& \qquad\quad + \left[\hat{W}^{-1}\hat{a}^{(H2)}_l\hat{V}\right]_{ij}[\hat{V}^{-1}\vec{C}_0]_j J_l, \mu_W, \mu_H\Bigg),
\end{aligned} \tag{D.3}$$

with the same initial conditions for the evolution of the operators $Q^{VLR}_{1,2}$ and the coefficients for the matching from the two-point function of $O^{VLL}_{\pm}$ and $O^{VRL}_{1,2}$ to the local operators $Q^{LR}_{1,2}$ at $\mu = k^2$.

$$C^{LR}_a \leftrightarrow \sum_{l,j}(\hat{a}^{(H2)}_l)_{ai}C^{VRL}_j C^{VLL}_l\,, \qquad \hat{a}^{(H2)}_l = \hat{a}^{(W'2)}_{r=l}\,. \tag{D.4}$$

One can check that the expressions from ref. [43] are recovered at leading order.

If we consider $\log\beta$ as small ("small $\log\beta$ approach"), we see that the diagrams are dominated by the region $k^2 = \mathcal{O}(m_t^2, \mu_W^2)$ in all cases: this is obvious for tt and ct boxes, whereas the cc box receives only suppressed contributions from the region $k^2 = \mathcal{O}(m_c^2)$. We obtain thus expressions involving the averaging weight for constant terms R_1^{NLO}

$$\bar{\eta}^{(W'2)}_{a,UV} = \xi^{(W'2)}_{a,UV}\left[R_1^{NLO}\right], \qquad \bar{\eta}^{(H2)}_{a,UV} = \xi^{(H2)}_{a,UV}\left[R_1^{NLO}\right], \tag{D.5}$$

where we have identified the two scales for the integration $\mu_W = \mu_R$ to a common average value (this is similar to the treatment of the region between m_t and M_W in the SM case).

In the case of a large $\log\beta$ ("large $\log\beta$ approach"), we want to perform the resummation of the large $\log\beta$ with $R^{NLO}_{\log}$ and consider the rest of the contribution as dominated

JHEP08(2016)128

by the region $k^2 = \mathcal{O}(m_t^2, \mu_W^2)$. In the case of $(W'2)$ we obtain

$$\bar{\eta}_{a,UV}^{(W'2)} = \Bigg[F_{UV}^{(W'2)} \times \sum_{r=\pm,\, i,j=1,2} \left(\frac{\alpha_s(\mu_W)}{\alpha_s(\mu_h)}\right)^{-d_r+d_i+2d_m} \left(\frac{\alpha_s(m_U)}{\alpha_s(\mu_h)}\right)^{-d_m} \left(\frac{\alpha_s(m_V)}{\alpha_s(\mu_h)}\right)^{-d_m} \left(\frac{\alpha_s(\mu_R)}{\alpha_s(\mu_h)}\right)^{d_r} \times \hat{W}_{ai} \left[\hat{W}^{-1} \hat{a}_r^{(W'2)} \hat{V}\right]_{ij} [\hat{V}^{-1} \vec{C}_0]_j + \log(\beta) \times \xi_{a,UV}^{(W'2)} \left[R_{\log}^{NLO}\right] \Bigg] \frac{1}{\log(\beta) + F_{UV}^{(W'2)}} \tag{D.6}$$

with the contributions from the constant term

$$F_{tt}^{(W'2)} = \frac{x_t^2 - 2x_t}{(x_t-1)^2} \log(x_t) + \frac{x_t}{x_t - 1}\,, \quad F_{ct}^{(W'2)} = \frac{x_t}{x_t-1} \log(x_t)\,, \quad F_{cc}^{(W'2)} = 0\,, \tag{D.7}$$

and similarly for $(H2)$

$$\bar{\eta}_{a,UV}^{(H2)} = \Bigg[F_{UV}^{(H2)} \times \sum_{l=\pm,\, i,j=1,2} \left(\frac{\alpha_s(\mu_W)}{\alpha_s(\mu_h)}\right)^{d_i-d_j} \left(\frac{\alpha_s(m_U)}{\alpha_s(\mu_h)}\right)^{-d_m} \left(\frac{\alpha_s(m_V)}{\alpha_s(\mu_h)}\right)^{-d_m} \left(\frac{\alpha_s(\mu_H)}{\alpha_s(\mu_h)}\right)^{d_j+2d_m} \times \hat{W}_{ai} \left[\hat{W}^{-1} \hat{a}_l^{(H2)} \hat{V}\right]_{ij} [\hat{V}^{-1} \vec{C}_0]_j + \log(\beta\omega) \times \xi_{a,UV}^{(H2)} \left[R_{\log}^{NLO}\right] \Bigg] \frac{1}{\log(\beta\omega) + F_{UV}^{(H2)}} \tag{D.8}$$

with the contributions from the constant term

$$F_{tt}^{(H2)} = x_t \frac{x_t + (x_t-2)\log(x_t) - 1}{(x_t-1)^2}\,, \qquad F_{ct}^{(H2)} = \frac{x_t}{x_t-1}\log(x_t)\,, \qquad F_{cc}^{(H2)} = 0\,. \tag{D.9}$$

D.2 Contributions without $\log\beta$

If we consider the box with the Goldstone associated with W and a charged Higgs boson H, the masses stem from the Higgs couplings, the Goldstone boson couplings and the propagator, whereas the largest contribution to I_1 comes from the range between m_V and μ_W. We obtain

$$\begin{aligned}
\bar{\eta}_{a,UV}^{(H1)} = \sum_{b,i,j,j',k,k'=1,2} & \left(\frac{\alpha_s(m_U)}{\alpha_s(\mu_h)}\right)^{-3d_m} \left(\frac{\alpha_s(m_V)}{\alpha_s(\mu_h)}\right)^{d_i-d_k-d_{k'}-d_m} \left(\frac{\alpha_s(\mu_W)}{\alpha_s(\mu_h)}\right)^{d_k+2dm} \left(\frac{\alpha_s(\mu_H)}{\alpha_s(\mu_h)}\right)^{d_{k'}+2d_m} \\
& \times \bar{a}_{b,jj'}^{(H1)} \left[\left(1 + \frac{\alpha_s(\mu_h)}{4\pi}\hat{K}\right)\hat{W}\right]_{ai} \left[\hat{V}^{-1}\left(1 - \frac{\alpha_s(\mu_W)}{4\pi}\hat{J}\right)\vec{C}_0\right]_k \left[\hat{V}^{-1}\left(1 - \frac{\alpha_s(\mu_H)}{4\pi}\hat{J}\right)\vec{C}_0\right]_{k'} \\
& \times R^{NLO}\Bigg(d_i - d_k - d_{k'} + 2d_m, \\
& \quad \hat{W}_{ib}^{-1}\hat{V}_{jk}\hat{V}_{j'k'} \times \left(1 - \frac{\alpha_s(\mu_W)}{4\pi}2J_m - \frac{\alpha_s(\mu_H)}{4\pi}2J_m + \frac{\alpha_s(m_U)+\alpha_s(m_V)}{4\pi}3J_m\right), \\
& \quad - 2J_m \hat{W}_{ib}^{-1}\hat{V}_{jk}\hat{V}_{j'k'} - (\hat{W}^{-1}\hat{K})_{ib}\hat{V}_{jk}\hat{V}_{j'k'} + \hat{W}_{ib}^{-1}(\hat{J}\hat{V})_{jk}\hat{V}_{j'k'} + \hat{W}_{ib}^{-1}\hat{V}_{jk}(\hat{J}\hat{V})_{j'k'}, \\
& \quad m_V, \mu_W \Bigg),
\end{aligned} \tag{D.10}$$

JHEP08(2016)128

where $\bar{a}^{(H1)}_{a,ij}$ provides the coefficients for the matching from the two-point function of $O^{VLR}_{1,2}$ to the local operators $Q^{LR}_{1,2}$ at $\mu = k^2$:

$$C^{LR}_a \leftrightarrow \sum_{ij} \bar{a}^{(H1)}_{a,ij} C^{VLR}_i C^{VRL}_j \,, \tag{D.11}$$

with the non-vanishing entries

$$\bar{a}^{(H1)}_{1,12} = -2\,, \qquad \bar{a}^{(H1)}_{1,21} = -2\,, \qquad \bar{a}^{(H1)}_{1,11} = -6\,, \qquad \bar{a}^{(H1)}_{2,22} = 4\,. \tag{D.12}$$

The only relevant case is tt, where R^{NLO} can be replaced by R^{NLO}_1.

If we consider tree-level H^0 exchanges, we have

$$\begin{aligned}\bar{\eta}^{(H)}_{a,UV} = &\left(\frac{\alpha_s(m_U)}{\alpha_s(\mu_h)}\right)^{-d_m} \left(\frac{\alpha_s(m_V)}{\alpha_s(\mu_h)}\right)^{-d_m} \left(\frac{\alpha_s(\mu_H)}{\alpha_s(\mu_h)}\right)^{2d_m} \\ &\times \left(1 - \frac{\alpha_s(\mu_H)}{4\pi} 2J_m + \frac{\alpha_s(m_U)+\alpha_s(m_V)}{4\pi} J_m\right) \\ &\times \left[\left(1 + \frac{\alpha_s(\mu_h)}{4\pi}\hat{K}\right) \hat{W} \left(\frac{\alpha_s(\mu_H)}{\alpha_s(\mu_h)}\right)^{\vec{d}} \hat{W}^{-1} \left(1 - \frac{\alpha_s(\mu_H)}{4\pi}\hat{K}\right) \vec{C}_0\right]_a ,\end{aligned} \tag{D.13}$$

where the matching yields the value of the Wilson coefficients for the $|\Delta S| = 2$ operators at the high scale. One can check that the expressions from ref. [43] are recovered at leading order.

E Result for the individual diagrams

In order to evaluate the diagrams necessary to determine the short-distance QCD corrections for meson mixing in Left-Right models we used the packages Feyncalc and TARCER [59].

E.1 Diagrams D_i

The two-loop diagrams in figure 4 have the following structure

$$\begin{aligned}D^{rl}_i = -i\frac{m_c^2}{64\pi^2}\frac{\alpha_s}{4\pi}\Bigg(&\left[-\frac{1}{\epsilon}\left(C^{rl}_i d_i - 2\widetilde{C}^{rl}_i \tilde{d}_i\right) + \left(C^{rl}_i A_i - 2\widetilde{C}^{rl}_i B_i\right)\right] P_R \otimes P_L \\ &+ \left[-\frac{1}{\epsilon}\left(\tilde{d}_i C^{rl}_i - \widetilde{C}^{rl}_i d_i/2\right) + \left(B_i C^{rl}_i - \widetilde{C}^{rl}_i A_i/2\right)\right] \gamma_\mu P_R \otimes \gamma_\mu P_L \cdots\Bigg)\end{aligned} \tag{E.1}$$

where the ellipsis stands for possible other operators (and $1/\epsilon^2$ poles) uninteresting for our purpose. The coefficients d_i and $\tilde{d}_i$ of the $1/\epsilon$ term are given in table 4 while the C^{rl}_i and $\widetilde{C}^{rl}_i$ are colour factors given in table 5. The diagram $D_8 = 0$ for zero external momenta. Other classes can be obtained through either a rotation of 90 or 180 degrees, or a left-right reflection (resulting in the exchange $r \leftrightarrow l$ in the colour factors in some cases, see table 5).

JHEP08(2016)128

	$1/\epsilon$
d_1	$-2(6R-7+\xi(2R-1))$
d_2	$\left(\left(24-\frac{\bar{b}}{4}\right)\lambda+\frac{\bar{b}}{4}+\xi(4-4R)-30\right)$
d_3	$\left(-3+\frac{\bar{b}}{8}+2\xi\left(2\log\left(\frac{m_s^2}{\mu^2}\right)+1\right)\right)$
$\tilde{d}_3$	$-(3+\xi)$
d_4	$\left(\left(48-\frac{\bar{b}}{2}\right)\lambda+\frac{\bar{b}-72}{4}+4\xi\right)$
d_5	$2(7-\xi)$
d_6	$(-3+2\xi)$
d_7	$\left(\left(24-\frac{\bar{b}}{4}\right)\lambda+\frac{\bar{b}}{8}-2\xi-32\right)$

Table 4. Divergences $d_i, \tilde{d}_i$ of the two-loop diagrams D_i leading to Q_i. λ multiplies the contribution from the evanescent operators which vanish for the standard value $\bar{b}=b=96$, see eq. (3.10). The exact definition of the divergences can be found in eq. (E.1).

	D_0	D_1	D_2	D_3
C^{rl}	1	$\frac{N^2-1}{2N}-\tau_{rl}$	$-\frac{1}{2N}$	$-\frac{1}{2N}-\tau_{rl}$
$\widetilde{C}^{rl}$	$-2\tau_{rl}$	$\frac{\tau_{rl}}{N}$	$\frac{1}{2}-\frac{N^2-1}{N}\tau_{rl}$	$\frac{1}{2}+\frac{1}{N}\tau_{rl}$
	D_4	D_5	D_6	D_7
C^{rl}	$-\frac{1}{2N}$	$\frac{N^2-1}{2N}$	$\frac{N^2+rN-1}{2N}$	$\frac{rN-1}{2N}$
$\widetilde{C}^{rl}$	$\frac{1}{2}-\frac{N^2-1}{N}\tau_{rl}$	$-\frac{(N^2-1)}{N}\tau_{rl}$	$\frac{(N^2-1)l-r}{2N}$	$\frac{l(N^2-1)+N-r}{2N}$

Table 5. Colour factors for the diagrams D_i. r, l can have the values ± 1 and τ_{rl} is defined in eq. (2.18).

The finite gauge-independent part is given by

$$
\begin{aligned}
A_1 &= 6\big(-2(R-2)\log\left(m_c^2/\mu^2\right)+\log^2\left(m_c^2/\mu^2\right)+2R/3-R_2-\pi^2/6+8/3\big)\,,\\
A_2 &= -6\big(\log\left(m_c^2/\mu^2\right)+R+1/2\big)\,,\\
A_3 &= \frac{3}{2}\left(12\log(m_s^2/\mu^2)-13\right)\,,\\
B_3 &= -3\big(\log(m_s^2/\mu^2)+\log\left(m_c^2/\mu^2\right)+7/6\big)\,,\\
A_4 &= 12\log\left(m_c^2/\mu^2\right)+59\,,\\
A_5 &= -2\big(3\log^2\left(m_c^2/\mu^2\right)+4\log\left(m_c^2/\mu^2\right)+3\big)\,,\\
A_6 &= -6\big(\log\left(m_c^2/\mu^2\right)+7/12\big)\,,\\
A_7 &= 6\log^2\left(m_c^2/\mu^2\right)-16\log\left(m_c^2/\mu^2\right)+5\,,
\end{aligned}
\tag{E.2}
$$

JHEP08(2016)128

while the gauge-dependent part

$$
\begin{aligned}
A_1^\xi &= 2\big(-2(R-2)\log\left(m_c^2/\mu^2\right)+\log^2\left(m_c^2/\mu^2\right)-2R-R_2+7-\pi^2/6\big)\,,\\
A_2^\xi &= -4\big((R-1)\log\left(m_c^2/\mu^2\right)+R+R_2/2-1+\pi^2/12\big)\,,\\
A_3^\xi &= 2\big(\log(m_s^2/\mu^2)^2+2(\log(m_s^2/\mu^2)-1)\log\left(m_c^2/\mu^2\right)+4\log(m_s^2/\mu^2)-\\
&\quad \log^2\left(m_c^2/\mu^2\right)+\pi^2/6-5\big),\\
B_3^\xi &= -\log(m_s^2/\mu^2)-\log\left(m_c^2/\mu^2\right)-1/2\,,\\
A_4^\xi &= -4\big(\log^2\left(m_c^2/\mu^2\right)+2\log\left(m_c^2/\mu^2\right)+5\big)\,,\\
A_5^\xi &= 2\big(\log^2\left(m_c^2/\mu^2\right)+2\log\left(m_c^2/\mu^2\right)+5\big)\,,\\
A_6^\xi &= -2\big(\log^2\left(m_c^2/\mu^2\right)+2\log\left(m_c^2/\mu^2\right)+5\big)\,,\\
A_7^\xi &= 2\big(\log^2\left(m_c^2/\mu^2\right)+2\log\left(m_c^2/\mu^2\right)+5\big)\,.
\end{aligned}
\tag{E.3}
$$

R and R_2 are defined as

$$
\begin{aligned}
R &= \frac{1}{m_s^2-m_d^2}\big(m_s^2\log(m_s^2/\mu^2)-m_d^2\log(m_d^2/\mu^2)\big)\,,\\
R_2 &= \frac{1}{m_s^2-m_d^2}\big(m_s^2\log^2(m_s^2/\mu^2)-m_d^2\log^2(m_d^2/\mu^2)\big)\,.
\end{aligned}
\tag{E.4}
$$

They add up to

$$
\langle O_{rl}(\mu)\rangle^{(1)} = \langle O_{rl}(\mu)\rangle^{(0)} - \frac{m_c^2(\mu)}{64\pi^2}\frac{\alpha_s(\mu)}{4\pi}\sum_{i=1}^{2}(\langle Q_i^{LR}(\mu)\rangle^{(0)} d_i^{rl}(\mu)+\cdots),
\tag{E.5}
$$

with

$$
\begin{aligned}
N d_1^{rl}(\mu) &= e_1^{rl}(\mu)+\xi\Bigg[\log\left(\frac{m_c^2}{\mu^2}\right)\\
&\quad\left((N+2\tau_{rl})\log\left(\frac{m_d^2m_s^2}{\mu^4}\right)+R\left(4\left(N^2-2\right)\tau_{rl}-2N\right)-2\left(2N^2+N-4\right)\tau_{rl}+2N-1\right)\\
&\quad+\left((4-N)\tau_{rl}+2N-\frac{1}{2}\right)\log\left(\frac{m_d^2m_s^2}{\mu^4}\right)+R_2\left(2\left(N^2-2\right)\tau_{rl}-N\right)\\
&\quad+R\left(4\left(N^2-2\right)\tau_{rl}-2N\right)\\
&\quad+\left(\frac{1}{3}\left(\pi^2-12\right)N^2-N-\frac{\pi^2}{3}+8\right)\tau_{rl}+T\left(\frac{N}{2}+\tau_{rl}\right)+2N-\frac{1}{2}\Bigg]\,,
\end{aligned}
\tag{E.6}
$$

$$
\begin{aligned}
N d_2^{rl}(\mu) &= e_2^{rl}(\mu)+\xi\Bigg[\log\left(\frac{m_c^2}{\mu^2}\right)\\
&\quad\left((4N\tau_{rl}+2)\log\left(\frac{m_d^2m_s^2}{\mu^4}\right)+R\left(4\left(N^2-2\right)-8N\tau_{rl}\right)-2\left(2N^2+N-4\right)+(8N-4)\tau_{rl}\right)\\
&\quad+((8N-2)\tau_{rl}-N+4)\log\left(\frac{m_d^2m_s^2}{\mu^4}\right)+R\left(4\left(N^2 2\right)-8N\tau_{rl}\right)\\
&\quad+R_2\left(2\left(N^2-2\right)-4N\tau_{rl}\right)+\frac{1}{3}\left(\pi^2-12\right)N^2+(2N(T+4)-2)\tau_{rl}-N+T-\frac{\pi^2}{3}+8\Bigg].
\end{aligned}
\tag{E.7}
$$

JHEP08(2016)128

$\xi = 0$ corresponds to the gauge-independent results, $T = \log^2(m_d^2/\mu^2) + \log^2(m_s^2/\mu^2)$ and $\beta_{rl} = l + r$. The gauge-independent parts $e_i^{rl}(\mu)$ are given by:

$$\begin{aligned} e_1^{rl}(\mu) = & \log\left(\frac{m_c^2}{\mu^2}\right)\left(-11\left(N^2-2\right)\beta_{rl} + \left(8N^2-6N+16\right)\tau_{rl} - 16N - 12R\tau_{rl} - 3\right) \\ & + \log^2\left(\frac{m_c^2}{\mu^2}\right)\left(3\left(N^2-2\right)\beta_{rl} + 6N^2\tau_{rl} + 6N\right) \\ & + \left((9-3N)\tau_{rl} + \frac{3}{2}(3N-1)\right)\log\left(\frac{m_d^2 m_s^2}{\mu^4}\right) + R\left(\left(6N^2-2\right)\tau_{rl} - 3N\right) - 6R_2\tau_{rl} \\ & + \frac{3}{4}\left(N^2-2\right)\beta_{rl} + \left(-\frac{41N^2}{2} - 7N - \pi^2 + 17\right)\tau_{rl} + \frac{1}{2}(17N-7)\,, \end{aligned} \tag{E.8}$$

$$\begin{aligned} e_2^{rl}(\mu) = & \log\left(\frac{m_c^2}{\mu^2}\right)\left(R\left(12\left(N^2-1\right) - 24N\tau_{rl}\right) + 22N\beta_{rl} + (48N-12)\tau_{rl}\right. \\ & \left. - 2(N(2N+3)+14)\right) \\ & + \log^2\left(\frac{m_c^2}{\mu^2}\right)(-6N\beta_{rl} + 12N\tau_{rl} + 12) + ((18N-6)\tau_{rl} - 3N + 9)\log\left(\frac{m_d^2 m_s^2}{\mu^4}\right) \\ & + R\left(-4N^2 + 8N\tau_{rl} - 2\right) + R_2\left(6\left(N^2-1\right) - 12N\tau_{rl}\right) \\ & - \frac{3N\beta_{rl}}{2} - \left(\left(7+2\pi^2\right)N + 14\right)\tau_{rl} + N\left(\left(\pi^2-3\right)N - 7\right) - \pi^2 + 20\,. \end{aligned} \tag{E.9}$$

E.1.1 Contributions of the diagrams L_i

The diagrams L_i have different types of contributions depending on the operators involved.

Contribution from the operators Q_i. The three diagrams of figure 5 have to be evaluated with insertions of the operators Q_i/ϵ $(i = 1, 2)$ defined in eq. (3.5). Considering also the other members of each class of diagrams obtained by left-right and up-down reflections, we get

$$\langle Q_i(\mu)\rangle^{(1)} = \langle Q_i(\mu)\rangle^{(0)} + \frac{\alpha_s(\mu)}{4\pi}\sum_j\left(\frac{h_{Q_i}}{\epsilon}\delta_{ij} + b_{ji}(\mu)\right)\langle Q_j(\mu)\rangle^{(0)}\,, \tag{E.10}$$

where the divergent parts are

$$\begin{aligned} h_{Q1} = & \frac{3R\tau_{rl}}{N} + \frac{1}{2}\left(\frac{4}{N} - 3N + 3\right)\tau_{rl} + \frac{3}{4N} + \frac{3}{2} - \frac{\xi}{2}\left(\left(\frac{\tau_{rl}}{N} + \frac{1}{2}\right)\log\left(\frac{m_d^2 m_s^2}{\mu^4}\right)\right. \\ & \left. + R\left(\left(2N - \frac{4}{N}\right)\tau_{rl} - 1\right) + \left(\frac{4}{N} - 2N - 1\right)\tau_{rl} - \frac{1}{2N} + 1\right), \\ h_{Q2} = & 3R\left(-N + \frac{1}{N} + 2\tau_{rl}\right) + N + \frac{2}{N} + \frac{3}{2} + \left(\frac{3}{N} + 1\right)\tau_{rl} - \frac{\xi}{2}\left(\left(\frac{1}{N} + 2\tau_{rl}\right)\log\left(\frac{m_d^2 m_s^2}{\mu^4}\right)\right. \\ & \left. + 2R\left(N - \frac{2}{N} - 2\tau_{rl}\right) - 2N + \frac{4}{N} - 1 + 2\left(2 - \frac{1}{N}\right)\tau_{rl}\right). \end{aligned} \tag{E.11}$$

JHEP08(2016)128

L_k	L_1	L_2	L_3
C^k	$\frac{N^2-1}{2N}$	$-\frac{1}{2N}$	$-\frac{1}{2N}$
$\widetilde{C}^k$	0	$\frac{1}{2}$	$\frac{1}{2}$

Table 6. Colour factors for the diagrams L_k.

The finite parts of the diagrams in figure 5 with insertions from the operators Q_i divided by ϵ can be written in the following way

$$Q_{ii}^{(1)} = \sum_{k=1}^{3} \left(\bar{A}_{ii}^k C_k + f_i \bar{A}_{ji}^k \widetilde{C_k} \right) Q_i \,, \quad Q_{ij}^{(1)} = \sum_{k=1}^{3} \left(\bar{A}_{ii}^k \widetilde{C_k}/f_i + \bar{A}_{ji}^k C_k \right) Q_j,$$
$$Q_i^{(1)} = Q_{ii}^{(1)} + Q_{ij}^{(1)} = \sum_m b_{mi} Q_m \,, \tag{E.12}$$

(no sum on repeated indices) where k denotes the diagram k and $j = 2, 1$. C_k and $\widetilde{C_k}$ are the colour factors given in table 6 and f_i are coefficients coming from the Fierz transformation, $f_1 = -1/2$ and $f_2 = -2$. The 2×2 matrices $\bar{A}^{1,2}$ turn out to be diagonal. One has:

$$\bar{A}^1 = \begin{pmatrix} \frac{3}{2}R - \frac{5}{4} + G_a\xi & 0 \\ 0 & G^{\text{ind}} + G_a\xi \end{pmatrix}, \tag{E.13}$$

$$\bar{A}^2 = \begin{pmatrix} G^{\text{ind}} + G_a\xi & 0 \\ 0 & \frac{3}{2}R - \frac{9}{4} + G_a\xi \end{pmatrix}, \tag{E.14}$$

and

$$\bar{A}^3 = \begin{pmatrix} \frac{3}{2}\left(\log\left(\frac{m_s^2}{\mu^2}\right) - \frac{1}{2}\right) + G_b\xi & \frac{1}{4}\left(3\log\left(\frac{m_s^2}{\mu^2}\right) - \frac{5}{2}\right) + \frac{1}{4}\xi\left[\log\left(\frac{m_s^2}{\mu^2}\right) - \frac{3}{2}\right] \\ 3\log\left(\frac{m_s^2}{\mu^2}\right) - \frac{11}{2} + \xi\left[\log\left(\frac{m_s^2}{\mu^2}\right) - \frac{5}{2}\right] & \frac{3}{2}\left(\log\left(\frac{m_s^2}{\mu^2}\right) - \frac{1}{2}\right) + G_b\xi \end{pmatrix} \tag{E.15}$$

with

$$G^{\text{ind}} = \frac{1}{2}\left(-2R + 3R_2 + \frac{\pi^2}{2} + 2\right), \quad G_a = \frac{1}{4}\left(-4R + 2R_2 + \frac{\pi^2}{3} + 4\right),$$
$$G_b = -\frac{1}{2}\left(\log^2\left(\frac{m_s^2}{\mu^2}\right) + \frac{\pi^2}{6}\right). \tag{E.16}$$

Note that the graph L_2 can be obtained from L_1 by a Fierz transformation. It is easy to check that this implies that $\bar{A}_1$ and $\bar{A}_2$ are obtained from one another by interchanging their diagonal elements. One can see that this is indeed the case for the gauge-dependent terms but not for the terms independent of the regularisation in the gauge-independent ones. This comes from the fact that the relations for the Fierz transformation are generally valid only in 4 dimensions. The corrections in D dimensions define the evanescent operators E_5 and E_6, eq. (3.7).

JHEP08(2016)128

One can perform a similar computation inserting Q_i (without additional $1/\epsilon$ contribution). We get the following finite parts for the first diagram L_1

$$A^1 = \begin{pmatrix} -\frac{3}{2} + \xi(1-R) & 0 \\ 0 & 1 - 3R + \xi(1-R) \end{pmatrix}. \tag{E.17}$$

A^2 can be obtained from A^1 by interchanging the diagonal elements. This can be understood easily, since L_2 can be obtained from L_1 by a Fierz transformation and the evanescent operators have been defined so as to conserve the Fierz relations. Evaluating L_3 one gets

$$A^3 = \begin{pmatrix} -\frac{3}{2} + \xi \log\left(\frac{m_s^2}{\mu^2}\right) & -(3+\xi)/4 \\ -3 - \xi & -\frac{3}{2} + \xi \log\left(\frac{m_s^2}{\mu^2}\right) \end{pmatrix}. \tag{E.18}$$

The infinite parts of these diagrams are related to the LO anomalous dimensions of the operators $\tilde{Q}_{1,2}^{LR}$ and $Q_{1,2}^{LR}$. We have checked that they agree with the ones obtained in ref. [39].

Adding up these contributions, the elements (ij) of the gauge-independent finite part of the matrix $4Nb(\mu)$ in eq. (E.10) are given by

$$\begin{aligned}
(11) &= -3(N+1)\log\left(\frac{m_d^2 m_s^2}{\mu^4}\right) + 2\left(3N^2-1\right)R - 6R_2 - 5N^2 + 11N - \pi^2 + 8\,, \\
(12) &= -\frac{3}{2}(N+1)\log\left(\frac{m_d^2 m_s^2}{\mu^4}\right) - 3NR + 6N + \frac{5}{2}\,, \\
(21) &= -6(N+1)\log\left(\frac{m_d^2 m_s^2}{\mu^4}\right) + 8NR - 12NR_2 + 2\left(\left(3-\pi^2\right)N + 11\right)\,, \\
(22) &= -3(N+1)\log\left(\frac{m_d^2 m_s^2}{\mu^4}\right) - 2\left(2N^2+1\right)R + 6\left(N^2-1\right)R_2 \\
&\quad + N(4N+5) + 8 + \pi^2\left(N^2-1\right)\,,
\end{aligned} \tag{E.19}$$

and the gauge-dependent ones by

$$\begin{aligned}
(11) &= \xi\Bigg(T - N\log\left(\frac{m_d^2 m_s^2}{\mu^4}\right) + 4\left(2-N^2\right)R + 2\left(N^2-2\right)R_2 \\
&\quad + N(4N+5) - 8 + \frac{\pi^2}{3}(N^2-1)\Bigg), \\
(12) &= \xi\left(\frac{N}{2}T - \frac{1}{2}\log\left(\frac{m_d^2 m_s^2}{\mu^4}\right) + 2NR - NR_2 - 2N + \frac{3}{2}\right), \\
(21) &= \xi\left(2NT - 2\log\left(\frac{m_d^2 m_s^2}{\mu^4}\right) + 8NR - 4NR_2 - 8N + 10\right), \\
(22) &= \xi\Bigg(T - N\log\left(\frac{m_d^2 m_s^2}{\mu^4}\right) + 4\left(2-N^2\right)R + 2\left(N^2-2\right)R_2 \\
&\quad + N(4N+3) - 8 + \frac{\pi^2}{3}(N^2-1)\Bigg).
\end{aligned} \tag{E.20}$$

JHEP08(2016)128

E.1.2 Insertion of E_i

The contribution of the evanescent operators $E_{1,3,5}$ have also to be evaluated. In principle, a finite contribution could be added to these evanescent operators in the same way as for the C_i. However, as indicated earlier, it has been shown in refs. [37, 58] that the result should not depend on the value of the constant coefficients and that one can choose a regularisation scheme where these contributions cancel. Summing all the diagrams L_i together with all the members of the same class (not shown, obtained by left-right and up-down reflections) one gets both finite and infinite parts, with a similar structure to eq. (E.10). The divergent pieces are

$$\begin{aligned} h_{E5,1} &= -12 + \frac{\bar{b}}{4}\,, & h_{E5,2} &= -24N + \frac{\bar{b}}{2N}\,, \\ h_{E1,1} &= 0\,, & h_{E1,2} &= 0\,, \\ h_{E6,1} &= -12N + \frac{\bar{b}\,(N^2-2)}{8N}\,, & h_{E6,2} &= -\frac{\bar{b}+96}{4}\,, \end{aligned} \tag{E.21}$$

while the finite parts read

$$\begin{aligned} b_{E1,1} &= \left(3+2N+\xi\right)\frac{1}{4}\,, \\ b_{E6,1} &= \left(\frac{6}{N}\log\left(\frac{m_d^2 m_s^2}{\mu^4}\right) + \frac{12}{N}R + 14N - \frac{24}{N} + 3 + \xi\right)\,, \\ b_{E5,1} &= -6\left(\log\left(\frac{m_d^2 m_s^2}{\mu^4}\right) - 3\right)\,, \\ b_{E1,2} &= \left(3+2N+\xi\right)\left(\frac{1}{2N}\right)\,, \\ b_{E6,2} &= 12\left(\log\left(\frac{m_d^2 m_s^2}{\mu^4}\right) + 2R + \frac{1}{2N} - \frac{5}{3} + \frac{1}{6N}\xi\right)\,, \\ b_{E5,2} &= \frac{12}{N}\left(-\log\left(\frac{m_d^2 m_s^2}{\mu^4}\right) + 2(N^2-1)R - N^2 + 4\right)\,. \end{aligned} \tag{E.22}$$

References

[1] J.C. Pati and A. Salam, *Lepton Number as the Fourth Color*, *Phys. Rev.* **D 10** (1974) 275 [*Erratum ibid.* **D 11** (1975) 703] [INSPIRE].

[2] R.N. Mohapatra and J.C. Pati, *Left-Right Gauge Symmetry and an Isoconjugate Model of CP-violation*, *Phys. Rev.* **D 11** (1975) 566 [INSPIRE].

[3] R.N. Mohapatra and J.C. Pati, *A Natural Left-Right Symmetry*, *Phys. Rev.* **D 11** (1975) 2558 [INSPIRE].

[4] G. Senjanović and R.N. Mohapatra, *Exact Left-Right Symmetry and Spontaneous Violation of Parity*, *Phys. Rev.* **D 12** (1975) 1502 [INSPIRE].

JHEP08(2016)128

[5] G. Senjanović, *Spontaneous Breakdown of Parity in a Class of Gauge Theories*, *Nucl. Phys.* **B 153** (1979) 334 [INSPIRE].

[6] D. Chang, *A Minimal Model of Spontaneous CP-violation with the Gauge Group* $\mathrm{SU}(2) - L \times \mathrm{SU}(2) - R \times U(1) - (B - L)$, *Nucl. Phys.* **B 214** (1983) 435 [INSPIRE].

[7] Y. Zhang, H. An, X. Ji and R.N. Mohapatra, *General CP-violation in Minimal Left-Right Symmetric Model and Constraints on the Right-Handed Scale*, *Nucl. Phys.* **B 802** (2008) 247 [arXiv:0712.4218] [INSPIRE].

[8] A. Maiezza, M. Nemevšek, F. Nesti and G. Senjanović, *Left-Right Symmetry at LHC*, *Phys. Rev.* **D 82** (2010) 055022 [arXiv:1005.5160] [INSPIRE].

[9] D. Guadagnoli and R.N. Mohapatra, *TeV Scale Left Right Symmetry and Flavor Changing Neutral Higgs Effects*, *Phys. Lett.* **B 694** (2011) 386 [arXiv:1008.1074] [INSPIRE].

[10] R.N. Mohapatra and G. Senjanović, *Neutrino Masses and Mixings in Gauge Models with Spontaneous Parity Violation*, *Phys. Rev.* **D 23** (1981) 165 [INSPIRE].

[11] N.G. Deshpande, J.F. Gunion, B. Kayser and F.I. Olness, *Left-right symmetric electroweak models with triplet Higgs*, *Phys. Rev.* **D 44** (1991) 837 [INSPIRE].

[12] S. Descotes-Genon, J. Matias and J. Virto, *Understanding the* $B \to K^* \mu^+ \mu^-$ *Anomaly*, *Phys. Rev.* **D 88** (2013) 074002 [arXiv:1307.5683] [INSPIRE].

[13] S. Descotes-Genon, L. Hofer, J. Matias and J. Virto, *On the impact of power corrections in the prediction of* $B \to K^* \mu^+ \mu^-$ *observables*, *JHEP* **12** (2014) 125 [arXiv:1407.8526] [INSPIRE].

[14] S. Descotes-Genon, L. Hofer, J. Matias and J. Virto, *Global analysis of* $b \to s\ell\ell$ *anomalies*, *JHEP* **06** (2016) 092 [arXiv:1510.04239] [INSPIRE].

[15] K. Hsieh, K. Schmitz, J.-H. Yu and C.P. Yuan, *Global Analysis of General* $\mathrm{SU}(2) \times \mathrm{SU}(2) \times \mathrm{U}(1)$ *Models with Precision Data*, *Phys. Rev.* **D 82** (2010) 035011 [arXiv:1003.3482] [INSPIRE].

[16] ATLAS collaboration, *Search for heavy neutrinos and right-handed W bosons in events with two leptons and jets in pp collisions at* $\sqrt{s} = 7$ *TeV with the ATLAS detector*, *Eur. Phys. J.* **C 72** (2012) 2056 [arXiv:1203.5420] [INSPIRE].

[17] CMS collaboration, *Search for heavy neutrinos and* W *bosons with right-handed couplings in proton-proton collisions at* $\sqrt{s} = 8$ *TeV*, *Eur. Phys. J.* **C 74** (2014) 3149 [arXiv:1407.3683] [INSPIRE].

[18] C.-Y. Chen, P.S.B. Dev and R.N. Mohapatra, *Probing Heavy-Light Neutrino Mixing in Left-Right Seesaw Models at the LHC*, *Phys. Rev.* **D 88** (2013) 033014 [arXiv:1306.2342] [INSPIRE].

[19] P.S.B. Dev, D. Kim and R.N. Mohapatra, *Disambiguating Seesaw Models using Invariant Mass Variables at Hadron Colliders*, *JHEP* **01** (2016) 118 [arXiv:1510.04328] [INSPIRE].

[20] S. Patra, F.S. Queiroz and W. Rodejohann, *Stringent Dilepton Bounds on Left-Right Models using LHC data*, *Phys. Lett.* **B 752** (2016) 186 [arXiv:1506.03456] [INSPIRE].

[21] H. Harari and M. Leurer, *Left-Right Symmetry and the Mass Scale of a Possible Right-Handed Weak Boson*, *Nucl. Phys.* **B 233** (1984) 221 [INSPIRE].

JHEP08(2016)128

[22] G. Beall, M. Bander and A. Soni, *Constraint on the Mass Scale of a Left-Right Symmetric Electroweak Theory from the $K_L - K_S$ Mass Difference*, *Phys. Rev. Lett.* **48** (1982) 848 [INSPIRE].

[23] P. Langacker and S.U. Sankar, *Bounds on the Mass of W_R and the $W_L - W_R$ Mixing Angle ξ in General* SU(2) $-$ $L \times$ SU(2) $-$ $R \times$ U(1) *Models*, *Phys. Rev.* **D 40** (1989) 1569 [INSPIRE].

[24] G. Barenboim, J. Bernabeu, J. Prades and M. Raidal, *Constraints on the W_R mass and CP-violation in left-right models*, *Phys. Rev.* **D 55** (1997) 4213 [hep-ph/9611347] [INSPIRE].

[25] G. Barenboim, M. Gorbahn, U. Nierste and M. Raidal, *Higgs sector of the minimal left-right symmetric model*, *Phys. Rev.* **D 65** (2002) 095003 [hep-ph/0107121] [INSPIRE].

[26] R.N. Mohapatra, F.E. Paige and D.P. Sidhu, *Symmetry Breaking and Naturalness of Parity Conservation in Weak Neutral Currents in Left-Right Symmetric Gauge Theories*, *Phys. Rev.* **D 17** (1978) 2462 [INSPIRE].

[27] R.N. Mohapatra, G. Senjanović and M.D. Tran, *Strangeness Changing Processes and the Limit on the Right-handed Gauge Boson Mass*, *Phys. Rev.* **D 28** (1983) 546 [INSPIRE].

[28] G. Barenboim, J. Bernabeu and M. Raidal, *Spontaneous CP-violation in the left-right model and the kaon system*, *Nucl. Phys.* **B 478** (1996) 527 [hep-ph/9608450] [INSPIRE].

[29] M. Blanke, A.J. Buras, K. Gemmler and T. Heidsieck, *$\Delta F = 2$ observables and $B \to X_q$ gamma decays in the Left-Right Model: Higgs particles striking back*, *JHEP* **03** (2012) 024 [arXiv:1111.5014] [INSPIRE].

[30] S. Bertolini, A. Maiezza and F. Nesti, *Present and Future K and B Meson Mixing Constraints on TeV Scale Left-Right Symmetry*, *Phys. Rev.* **D 89** (2014) 095028 [arXiv:1403.7112] [INSPIRE].

[31] ETM collaboration, N. Carrasco et al., *$\Delta S = 2$ and $\Delta C = 2$ bag parameters in the standard model and beyond from $N_f = 2 + 1 + 1$ twisted-mass lattice QCD*, *Phys. Rev.* **D 92** (2015) 034516 [arXiv:1505.06639] [INSPIRE].

[32] G. Buchalla, A.J. Buras and M.E. Lautenbacher, *Weak decays beyond leading logarithms*, *Rev. Mod. Phys.* **68** (1996) 1125 [hep-ph/9512380] [INSPIRE].

[33] F.J. Gilman and M.B. Wise, *K0 anti-K0 Mixing in the Six Quark Model*, *Phys. Rev.* **D 27** (1983) 1128 [INSPIRE].

[34] A.J. Buras, M. Jamin and P.H. Weisz, *Leading and Next-to-leading QCD Corrections to ϵ Parameter and $B^0 - \bar{B}^0$ Mixing in the Presence of a Heavy Top Quark*, *Nucl. Phys.* **B 347** (1990) 491 [INSPIRE].

[35] A.J. Buras, M. Jamin, M.E. Lautenbacher and P.H. Weisz, *Effective Hamiltonians for $\Delta S = 1$ and $\Delta B = 1$ nonleptonic decays beyond the leading logarithmic approximation*, *Nucl. Phys.* **B 370** (1992) 69 [INSPIRE].

[36] S. Herrlich and U. Nierste, *Enhancement of the $K_L - K_S$ mass difference by short distance QCD corrections beyond leading logarithms*, *Nucl. Phys.* **B 419** (1994) 292 [hep-ph/9310311] [INSPIRE].

[37] S. Herrlich and U. Nierste, *Evanescent operators, scheme dependences and double insertions*, *Nucl. Phys.* **B 455** (1995) 39 [hep-ph/9412375] [INSPIRE].

[38] S. Herrlich and U. Nierste, *The Complete $|\Delta S| = 2$ — Hamiltonian in the next-to-leading order*, *Nucl. Phys.* **B 476** (1996) 27 [hep-ph/9604330] [INSPIRE].

JHEP08(2016)128

[39] A.J. Buras, M. Misiak and J. Urban, *Two loop QCD anomalous dimensions of flavor changing four quark operators within and beyond the standard model*, *Nucl. Phys.* **B 586** (2000) 397 [hep-ph/0005183] [INSPIRE].

[40] A.I. Vainshtein, V.I. Zakharov, V.A. Novikov and M.A. Shifman, *Processes of the Second Order in the Weak Interaction in Asymptotically Free Strong Interaction Theories*, *Sov. J. Nucl. Phys.* **23** (1977) 540 [*Yad. Fiz.* **23** (1976) 1024] [INSPIRE].

[41] A.I. Vainshtein, V.I. Zakharov, V.A. Novikov and M.A. Shifman, *On the Strong Interaction Effects on the $K_L \to 2\mu$ Decay and $K_L - K_s$ Mass Difference. A Reply*, *Phys. Rev.* **D 16** (1977) 223 [INSPIRE].

[42] M.I. Vysotsky, *K0 anti-K0 transition in the standard* $\mathrm{SU}(3) \times \mathrm{SU}(2) \times U(1)$ *model*, *Sov. J. Nucl. Phys.* **31** (1980) 797 [INSPIRE].

[43] G. Ecker and W. Grimus, *CP Violation and Left-Right Symmetry*, *Nucl. Phys.* **B 258** (1985) 328 [INSPIRE].

[44] I.I.Y. Bigi and J.M. Frere, *Strong Radiative Corrections to Strangeness Changing Processes in the Presence of Right-handed Currents*, *Phys. Lett.* **B 129** (1983) 469 [*Erratum ibid.* **B 154** (1985) 457] [INSPIRE].

[45] J. Brod and M. Gorbahn, *ϵ_K at Next-to-Next-to-Leading Order: The Charm-Top-Quark Contribution*, *Phys. Rev.* **D 82** (2010) 094026 [arXiv:1007.0684] [INSPIRE].

[46] J. Brod and M. Gorbahn, *Next-to-Next-to-Leading-Order Charm-Quark Contribution to the CP-violation Parameter ϵ_K and ΔM_K*, *Phys. Rev. Lett.* **108** (2012) 121801 [arXiv:1108.2036] [INSPIRE].

[47] M.K. Gaillard and B.W. Lee, *Rare Decay Modes of the K-Mesons in Gauge Theories*, *Phys. Rev.* **D 10** (1974) 897 [INSPIRE].

[48] A. Datta, E.A. Paschos, J.M. Schwarz and M.N. Sinha Roy, *QCD corrections for the $K^0 - \bar{K}^0$ and $B^0 - \bar{B}^0$ system*, hep-ph/9509420 [INSPIRE].

[49] D. Chang, J. Basecq, L.-F. Li and P.B. Pal, *Comment on the $K_L - K_S$ Mass Difference in Left-right Model*, *Phys. Rev.* **D 30** (1984) 1601 [INSPIRE].

[50] J. Basecq, L.-F. Li and P.B. Pal, *Gauge Invariant Calculation of the $K_L - K_S$ Mass Difference in the Left-right Model*, *Phys. Rev.* **D 32** (1985) 175 [INSPIRE].

[51] Z. Gagyi-Palffy, A. Pilaftsis and K. Schilcher, *Gauge independent analysis of $K_L \to e\mu$ in left-right models*, *Nucl. Phys.* **B 513** (1998) 517 [hep-ph/9707517] [INSPIRE].

[52] M. Kenmoku, Y. Miyazaki and E. Takasugi, *Gauge Invariant Sets of Diagrams for the P0 anti-P0 Mixing*, *Phys. Rev.* **D 37** (1988) 812 [INSPIRE].

[53] W.-S. Hou and A. Soni, *Gauge Invariance of the $K_L - K_S$ Mass Difference in Left-right Symmetric Model*, *Phys. Rev.* **D 32** (1985) 163 [INSPIRE].

[54] V. Bernard, S. Descotes-Genon and L. Vale Silva, *Phenomenological analysis of doublet left-right models*, in preparation.

[55] E. Witten, *Short Distance Analysis of Weak Interactions*, *Nucl. Phys.* **B 122** (1977) 109 [INSPIRE].

[56] C.-k. Lee, *General Theory of Virtual Heavy Particle Effects in Renormalizable Field Theories*, *Nucl. Phys.* **B 161** (1979) 171 [INSPIRE].

JHEP08(2016)128

[57] A.J. Buras and P.H. Weisz, *QCD Nonleading Corrections to Weak Decays in Dimensional Regularization and 't Hooft-Veltman Schemes*, *Nucl. Phys.* **B 333** (1990) 66 [INSPIRE].

[58] M.J. Dugan and B. Grinstein, *On the vanishing of evanescent operators*, *Phys. Lett.* **B 256** (1991) 239 [INSPIRE].

[59] R. Mertig and R. Scharf, *TARCER: A Mathematica program for the reduction of two loop propagator integrals*, *Comput. Phys. Commun.* **111** (1998) 265 [hep-ph/9801383] [INSPIRE].

JHEP08(2016)128